DECKBLATT

The role of negative regulators in coordination of the *Myxococcus xanthus* developmental program

D I S S E R T A T I O N

zur Erlangung des Doktorgrades der Naturwissenschaften
(Dr. rer. nat.)

dem
Fachbereich Biologie
der Philipps-Universität Marburg

vorgelegt von

Bongsoo Lee

aus Suwon, Republic of Korea

Marburg/Lahn im Oktober 2009

Die Untersuchungen zur vorliegenden Arbeit wurden von Oktober 2006 bis Oktober 2008 am Max-Planck-Institut für Terrestrische Mikrobiologie unter der Leitung von Dr. Penelope I. Higgs durchgeführt.

Vom Fachbereich Biologie der Philipps-Universität Marburg als Dissertation am

_____ angenommen.

Erstgutachter:	Prof. Dr. MD Lotte Søgaard-Andersen
Zweitgutachter:	Prof. Dr. Erhard Bremer

Tag der mündlichen Prüfung: _____

Die während der Promotion erzielten Ergebnisse wurden und werden in folgenden Originalpublikationen veröffentlicht:

Lee, B., A. Treuner-Lange and P. I. Higgs. Analysis of developmental marker proteins in the developing subpopulations of *Myxococcus xanthus*. In preparation.

Lee, B. and P. I. Higgs. Progression through the developmental program is controlled by several orphan two component histidine kinase proteins in *Myxococcus xanthus*. In preparation.

Lee, B., A. Schramm, B. Mensch and P. I. Higgs. Two component systems controlling cell differentiation in *Myxococcus xanthus*. *In Methods in Enzymology*. Submitted.

KURZFASSUNG

Myxococcus xanthus ist ein Mikroorganismus mit einem komplexen Lebenszyklus, welcher sich durch mutizelluläres Verhalten und Zelldifferenzierung auszeichnet. Durch Nahrungsmangel initiiert durchlaufen die *M. xanthus* zellen ein Entwicklungsprogramm worin sie unterschiedliche Entwicklungsschicksale haben: Der Großteil der Zellen unterliegt programmiertem Zelltod (PCD), die übrigen Zellen wandern entweder in Fruchtkörper wo sie sich zu Sporen differenzieren oder aggregieren nicht und verbleiben als periphere Zellen. Dieses Entwicklungsprogramm ist von einer Kaskade positiver Entwicklungs-regulatoren kontrolliert, deren Expression positiver Autoregulation unterliegt. Die Untersuchungen diverser Histidinkinasenhomologe (HK) (*espA, espC, red* und *todK)* zeigte, dass sie für eine adäquate Progression durch dieses Entwicklungsprogramm erforderlich sind. Mutanten dieser Gene weisen verfrühte Aggregation sowie Sporulation verglichen mit dem Wildtyp auf, bilden unorganisierte Fruchtkörper und weisen Sporen außerhalb dieser Fruchtkörper auf. Diese Beobachtungen legen nahe, dass diese Kinasen als negative Regulatoren (NR) zur Hemmung des Entwicklungsprogrammes wirken. Es ist jedoch unklar ob sie in einem oder mehreren Signaltransduktionswegen wirken und welchen Vorteil sie für das Entwicklungsprogramm darstellen.

Mit der Hilfe von epistatischen Analysen zeigten wir, dass diese NRs in drei eigenständigen Signalsystemen organisiert sind, zusammengesetzt aus 1) EspA/EspC, 2) TodK and 3) Red. Übereinstimmend zu diesen Beobachtungen weist die Proteinexpression diverser Entwicklungsregulatorproteine in den NR Mutanten drei unterschiedliche Muster auf: 1) in *espA* und *espC* Mutanten akkumulieren die meisten dieser Entwicklungsregulatorproteine früher als im Wildtyp, die Reihenfolge ihrer Produktion bleibt erhalten, 2) in *red* Mutanten sind die meisten Markerproteine unter representiert ihre Reighenfolge wird jedoch verändert, 3) in *todK* Mutanten werden gewisse Markerproteine früher produziert und die Reihenfolge der Produktion ist gestört. Phenotypische Analysen von Einfach, Doppelter, Dreifach und Vierfach Mutanten dieser NRs zeigen dass eine stark gegensätzliche Beziehung zwischen der Progressionsgeschwindigkeit durch das Entwicklungsprogramm und der koordinierten Bildung der Fruchtkörper besteht. Der Verlust der koordinierten Fruchtkörperbildung scheint das Resultat von Unkoordiniertheit der Subpopulationen während der Entwicklung zu sein.

Um zu verstehen ob die Störung der geordneten Kaskade der Entwicklungs-regulatoren in den *red* und *todK* Mutanten durch eine Missregulation der sich entwickelnden Subpopulationen hervorgerufen wird, definierten wir die Proportionen der sich entwickelnden Zell-Subpopulationen sowie die Akkumulation der Haupt-entwicklungsregulatorproteine in diesen. Unsere Analysen zeigen, dass die Zellpopulation sich während der ersten 24 Stunden verdoppelt, dann jedoch einem schlagartigen programmierten Zelltod (PCD) unterliegt. Die aggregierenden- sowie die nicht aggregierenden Subpopulationen weisen unterschiedliche Akkumulationsmuster von Komponenten der Typ IV Pili vermittelten Zellbewegung, sowie Sporen spezifischer Strukturproteine auf. Die meisten der Haupt-entwicklungsregulatorproteine zeigen erst eine allmähliche Akkumulation in der nicht aggregierenden Zellfraktion, wiesen später aber eine schnelle Akkumulation in der aggregierenden Zellfraktion auf.

Mittels einer ähnlichen Herangehensweise zeigten wir, dass beide Mutanten nicht in der Lage sind ihre Zellzahl in ähnlicher Weise wie der Wildtyp zu erhöhen, wahrscheinlich weil der PCD früher induziert wird als im Wildtyp. Darüber hinaus, in beiden Mutanten, werden die Entwicklungsregulatorproteine verfrüht in den nicht aggregierenden Zellen induziert und scheitern anschließend daran in den aggregierenden Zellen angemessen zu akkumulieren. Folglich werden viele dieser Zellen sporulieren bevor sie mit der Aggregation abgeschlossen haben, wodurch eine koordinierte Bildung von Fruchtkörpern verhindert wird. Diese Resultate legen nahe, dass TodK, sowie Red die stufenweise Akkumulation von einem oder mehreren Entwicklungskoordinatoren während der Aggregationsphase des Entwicklungs-programmes vermitteln. Zusätzlich legen sie nahe, dass die Koordinierung der Subpopulationen negative regulatorischer Signalsysteme benötigt, die positive autoregulatorische Schleifen dämpfen um eine Kopplung von Sporulation und Aggregation zu erzielen.

ABSTRACT

Myxococcus xanthus is a prokaryote that has a complex life cycle distinguished by multicellular behaviors and cell differentiation. Upon starvation, *Myxococcus xanthus* cells enter a developmental program wherein cells have different developmental fates: the majority of cells undergo programmed cell death (PCD), and the remaining cells either migrate into fruiting bodies and then differentiate into spores or do not aggregate and remain as peripheral rods. This developmental program is controlled by a cascade of positive developmental regulators whose expression is subject to positive autoregulation. Several histidine kinase (HK) homologs (*espA*, *espC*, *red* and *todK*) have been described that are necessary for appropriate progression through the developmental program. Mutants in these genes aggregate and sporulate earlier than wild type, producing disorganized fruiting bodies and spores outside of the fruiting bodies. These observations suggest that these kinases act as negative regulators (NRs) to repress the developmental program, but it is not clear if they function in one or more signaling pathways, how they mediate repression of the developmental program, and what ultimate advantage they provide to the developmental program.

Using genetic epistasis analysis, we demonstrate that these NRs are organized into three distinct signaling systems comprised of 1) EspA/EspC, 2) TodK and 3) Red. Consistently, analysis of the accumulation patterns of several developmental regulatory proteins in each NR mutant demonstrated three distinct patterns: 1) in *espA* and *espC* mutants most developmental regulators accumulate earlier than in wild type, but the ordered cascade of production is maintained, 2) in *red* mutants most developmental marker proteins are under accumulated and the ordered cascade of production is not maintained, 3) in *todK* mutants certain developmental marker proteins are produced earlier than in wild type and the ordered cascade of production is perturbed. Phenotypic analysis of single, double, triple and quadruple NR mutants demonstrated that there is a strong negative correlation between the rate of progression through the developmental program and coordinated fruiting body formation. Loss of coordinated fruiting body formation appeared to be the result of uncoordinated developmental subpopulations.

To determine whether the perturbation in the ordered cascade of developmental regulators in the *red* and *todK* mutants was due to misregulation of the developmental subpopulations, we first set out to define the temporal proportion of the different cell subpopulations and then examined the accumulation of key developmental regulator proteins in the two developmental subpopulations. Our analyses indicate that the cell population doubles over

the course of 24 hours followed by a sudden burst programmed cell death (PCD). The aggregating and non-aggregating subpopulations displayed distinct accumulation patterns of components involved in Type IV pilus-mediated motility, and spore structural proteins. Most key developmental regulator proteins were shown to first gradually accumulate in the non-aggregating cell fraction and then to rapidly accumulate in the aggregating cell fraction.

Using a similar approach to analyze the *red* and *todK* NR mutants, we demonstrate that both mutants do not increase their population to the same extent as wild type, likely because PCD is induced earlier than wild type. Furthermore, in both mutants, developmental regulatory proteins are induced inappropriately rapidly in the non-aggregating cell fraction, and subsequently fail to accumulate appropriately in the aggregating cell fraction. Consequently, many cells are induced to sporulate before they have completed aggregation, and coordinated fruiting body formation is perturbed. These results strongly suggest that TodK and Red mediate the gradual accumulation of one or more developmental coordinators during the aggregation phase of the developmental program. These results suggest that coordination of developmental subpopulations requires negative regulatory signaling systems that quench the positive autoregulatory loops that ensure coupling of sporulation and aggregation.

TABLE OF CONTENTS

ABBREVIATIONS

APS	Ammonium persulfate
bp	Base pairs
CYE	Casitone Yeast Extract medium
cDNA	single stranded complementary DNA
CF agar	Clone Fruiting agar
DTT	Dithiothreitol
DMSO	Dimethyl sulfoxide
EDTA	Ethylendiamine tetraacetic acid
FPLC	Fast performance liquid chromatography
HEPES	4-(2-hydroxyethyl)-1-piperazineethanesulfonic acid
h	Hours
IPTG	Isopropyl β-D-1-thiogalactopyranoside
kb	Kilo base pairs
kDa	Kilo Dalton
LB	Luria-Bertani medium
MOPS	Morpholinepropanesulfonic acid
min	Minute
rpm	rounds per minute
SDS	Sodium dodecylsulfate
SDS-PAGE	Sodium dodecyl sulfate polyacrylamide gel electrophoresis
TE	Tris-EDTA
TEMED	*N,N,N',N'*-Tetramethylethylendiamine
Tris	Tris-(hydroxymethyl)-aminomethane
TAE	Tris-acetate-EDTA
wt	wild type
X-Gal	5-bromo-4-chloro-3-indolyl- β -D-galactopyranoside

1 INTRODUCTION

1.1 Myxobacteria

The Myxobacteria are gram-negative, rod-shaped bacteria that have a complex life cycle and social behaviors, including fruiting body development. The Myxobacteria were initially thought to be fungi because of their mutilcellular behavior. In the nineteenth century, the Myxobacteria first described by Roland Thaxter, were distinguished from each other based on the shape of their fruiting bodies. Later, based on 16S rRNA analysis, the Myoxbacteria were classified as δ-proteobacterium (Shimkets & Woese, 1992). In addition to their mutilcellular behavior, one major feature of the Myxobacteria is that they produce a number of biomedically and industrially useful chemicals. So far, approximately 80 different basic structures and 450 structural variants have been isolated and characterized as antimicrobial agents (Reichenbach, 2001)

1.1.1 Life cycle of *Myxococcus xanthus*

Myxococcus xanthus is a model organism for studying prokaryotic multicellular development and differentiation. *M. xanthus* mainly inhabits the soil or herbivore dung and obtains nutrients by degrading organic matter or preying on other microorganisms (Reichenbach, 1999). Under nutrient-replete conditions, the cells swarm in groups by gliding motility and obtain nutrients cooperatively. This group feeding mechanism (known as wolf pack feeding) is advantageous, because groups of cells can secrete sufficient quantities of hydrolytic enzymes to digest organic compounds or other microorganisms (Rosenberg *et al.*, 1977). In contrast, in a nutrient-depleted environment, swarms of about 100,000 cells move into aggregation centers and form multicellular fruiting bodies inside which cells differentiate into spherical spores (Shimkets, 1990b, Dworkin & Kaiser, 1993). Some cells, known as peripheral rods, do not enter aggregates and remain as rod-shaped cells outside of the fruiting body structure (O'Connor & Zusman, 1991c). When spores are exposed to a nutrient-rich environment, they germinate and re-enter vegetative growth phase (Figure1. 1A). It is presumed that formation of fruiting bodies facilitates dispersal of groups of spores to nutrient replete environments which then facilitates group feeding. Under laboratory

conditions, *M. xanthus* wild-type strain DZ2 development occurs over at least 72 h (Figure1. 1B).

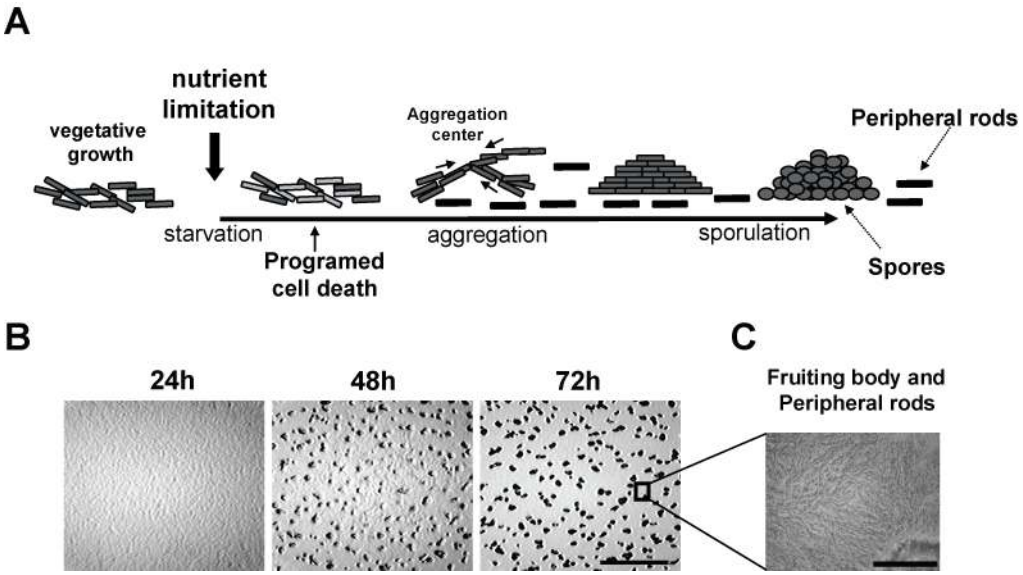

Figure 1.1 The life cycle of *Myxococcus xanthus* and the developmental phenotype of the wild-type strain, DZ2. (A) Scheme of vegetative and developmental cycle of *M. xanthus*. (B) 10 ul spots (4 X 10^9 cells ml^{-1}) of wild-type, DZ2 were placed on nutrient limited (CF) plates and incubated at 32 °C. Pictures were recorded by a stereo microscope at the indicated time points. Scale bar, 1.0 mm. (C) 500 ul of cell culture (2 X 10^7 cells ml^{-1}) of wild-type were placed in starvation media (MMC) and incubated at 32 °C. Pictures were recorded by inverted microscope at 72 hours development. Scale bar, 50 μm.

1.1.2 Gliding motility of *Myxococcus xanthus*

M. xanthus gliding motility is requried in both vegetative and developmental phases of the life cycle (Rosenberg et al., 1977, Shimkets, 1990a). Gliding motility involves two mechanisms, called adventurous (A) and social (S) motility. Two models have been proposed to explain the mechanism of A-motility. One model is that nozzle-like structures secrete slime and extrusion of slime might generate the force for A-motility (Wolgemuth *et al.*, 2002). Another model is that multiple force-generating adhesion complexes moving on cytoskeleton filaments act as the engine and generate the force for A-motility (Mignot, 2007). However, the exact mechanisms of A-motility are mysterious so far.

In contrast, the S-motility system is well-known. *M. xanthus* cell possess type IV pili, and type IV pili are now widely accepted as the motor for S-motility of *M. xanthus* and twitching motility in other species (Mattick *et al.*, 1996, Wall & Kaiser, 1999). It has been first observed that there is a tight association between pili and S-motility (Kaiser,

1979) and this observation was confirmed by the evidence that mechanically removed type IV pili result in loss of S-motility (Rosenbluh & Eisenbach, 1992). The pilus filament comprises a single protein, PilA (Wu & Kaiser, 1997) (Figure 1. 2D). PilC is an inner membrane protein (Figure 1. 2D) and mutation in this gene causes both pilus and S-motility defects. This result suggests that *M. xanthus* PilC is required for pilus bioynthesis (Wu & Kaiser, 1997). PilQ provides a channel through the outer membrane (Figure 1. 2D). Mutations in this gene also result in defective pilus synthesis and S-motility (Wall *et al.*, 1999). Recently, Yoderian and coworkers (2006) revisited their random mutagenesis screen by screening a *magellan4* insertion library for mutants deficient in S-motility. Type IV pilin biosynthesis genes containing 15 ORFs were mapped to 27-kb region on the *M. xanthus* genome. Mutations of these ORFs caused deficiencies in production of type IV pili, suggesting that type IV pilin biosythesis genes clearly play important roles in S-motility of *M. xanthus* (Whitworth, 2008). Moreover, experimental evidence suggests that type IV pili retraction provides the force for S-motility and bacterial twitching (Nudleman & Kaiser, 2004).

It has been demonstrated that exopolysaccharide (EPS) is required for S-motility. *M. xanthus* cells are covered by an extracellular matrix (ECM) which consists of approximately equal amounts of protein and polysaccharide (EPS) (Kim *et al.*, 1999, Merroun *et al.*, 2003). *dsp* mutants, which fail to produce EPS, have defects in cellular cohesion, S-motility, and fruiting body formation (Shimkets, 1986a, Shimkets, 1986b). SEM (Scanning Electron Microscopy) analysis demonstrated that *dsp* mutants are altered in their surface properties and lack ECM (Arnold & Shimkets, 1988, Behmlander & Dworkin, 1991).

It has been revealed that all mutants lacking the ECM are defective in S-motility (Shimkets, 1986b, Dana & Shimkets, 1993, Yang *et al.*, 2000). These all results not only suggest that *M. xanthus* ECM is required for cellular cohesion, social (S-) motility, and fruiting body formation, but also indicate that there are correlations between EPS and Type IV pili which are required for S-motility. The relationship between EPS and type IV pili has been elucidated by phenotypic analysis of mutants lacking EPS in *M. xanthus*. The EPS defective mutant produced hyperpiliated cells and failed to move by S-motility. However, addition of fibril material resulted in pilus retraction and rescued S-motility suggesting that EPS triggers Type IV pilus retraction by providing anchor for attachment (Li et al., 2003) (Figure 1. 2).

FibA, which is a zinc metalloprotease of the elastase family, was characterized as protein associated with ECM (Kearns *et al.*, 2002, Bonner *et al.*, 2006). It has been

shown that FibA is required for lipid chemotaxis, but not S-motility (Kearns et al., 2002). *fibA* mutants formed elongated and irregular fruiting bodies, but a *fibA pilA* double mutant results in defect of fruiting body formation suggesting that FibA and PilA act cooperatively during fruiting body formation (Bonner et al., 2006).

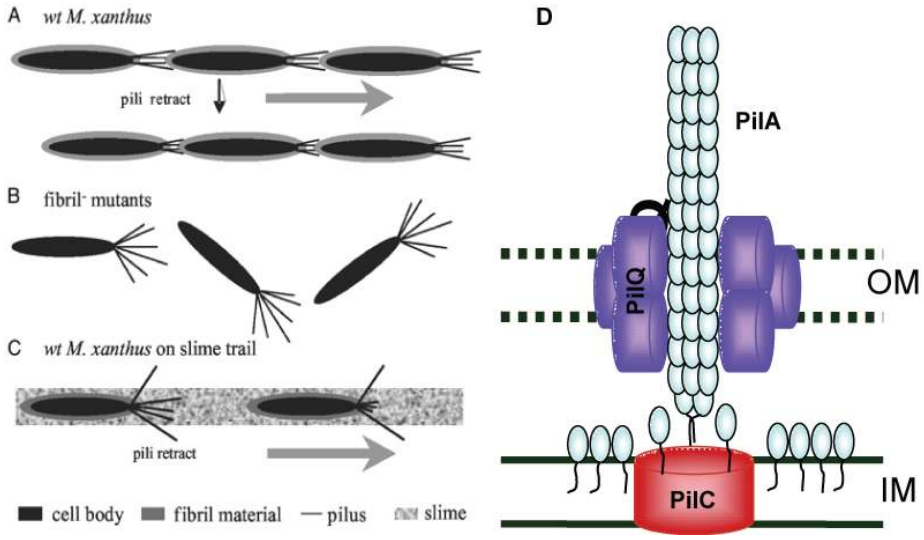

Figure 1.2 A model for the pili–fibril material interaction and some subunit proteins of Type IV pili. (A) The interaction between TFP and fibril material on the surface of wild-type cells allows TFP retraction and S-motility. (B) The absence of fibril material in fibril$^-$ mutants abolishes fibril–TFP interaction, resulting in their overpiliation phenotype and defects in S-motility. (C) The interaction between TFP and fibril material present in slime trails guides *M. xanthus* cells along these trails. This figure is adapted from (Li et al., 2003). (D) Some subunit proteins of Type IV pili. This cartoon is taken from Iryna Bulyha.

1.1.3 Development of *Myxococcus xanthus*

The *M. xanthus* development program is induced by starvarion and controlled by a series of temporally regulated extracellular and intracellular signals that must be coordinated and integrated to ensure proper fruiting body formation and sporulation (Kaiser, 2004). Starvation of nutrients such as amino acids, carbon, or phosphorus, which are all requried to make a complete set of amino-acylated tRNAs, induces the development program (Dworkin, 1962, Manoil & Kaiser, 1980b, Shimkets, 1987). It has been shown that in *E. coli,* RelA, a ribosomal-associated protein, is triggered by an uncharged tRNA in acceptor site of ribosome and catalyzes the synthesis of (p)ppGpp (Haseltine & Block, 1973, Pedersen *et al.*, 1973, Cochran & Byrne, 1974).

As in *E. coli*, uncharged tRNAs stimulate production of guanosine-5′-(tri)di-3′-diphosphate [(p)ppGpp] in *relA*-dependent mechanism, and rising levels of (p)ppGpp

induce development in *M. xanthus* (Manoil & Kaiser, 1980a, Manoil & Kaiser, 1980b, Singer & Kaiser, 1995, Harris *et al.*, 1998). Accumulation of (p)ppGp induces production of the A-signal which is a proposed mechanism for population-sensing (quorum sensing). A-signal, a mixture of amino acids and small peptides, is produced in proportion to the density of *M. xanthus*, and only if cells are present at a threshold density, genes necessary for development are induced and the developmental program continues (Figure 1. 3).

One of the genes upregulated in response to the A-signal is the *mrpAB* locus encoding a cytoplasmic histidine protein kinase and an enhancer biding protein of the NtrC type family (Sun & Shi, 2001a, Sun & Shi, 2001b). The MrpAB proteins are neceaasry for *mrpC* transcription (Sun & Shi, 2001a, Sun & Shi, 2001b, Nariya & Inouye, 2006). MrpC is a transcriptional activator of the cyclic AMP receptor family which is required for aggregation and sporulation (Sun & Shi, 2001a). Moreover, MrpC has recently proposed to be an anti-toxin for MazF which mediates programmed cell death (see Figure 1. 4) (Nariya & Inouye, 2008).

It has been shown that MrpC is phosphorylated by the Pkn14/Pkn8 Ser/Thr kinase cascade (Nariya & Inouye, 2005). Phosphorylation of MrpC results in decreased *mrpC* transcription. Moreover, MrpC seems to be proteolytically processed into MrpC2 in a manner that depends on LonD ATP-dependent protease. *pkn14* and *pkn8* mutants induce earlier accumulation of MrpC2 and FruA leading to earlier development suggesting that Pkn14 and Pkn8 kinases negatively regulate production of MrpC2 protein by phosphorylation of MrpC (Nariya & Inouye, 2006).

MrpC2 binds with high affinity to the *fruA* and *mrpC* promoters indicating that MrpC2 induces *fruA* gene transcription and positively autoregulates its own expression (Ueki & Inouye, 2003) (Figure 1. 3). FruA is an orphan two component DNA-binding response regulator containing N-terminal receiver and C-terminal DNA binding domains and is essential for aggregation and sporulation (Ogawa *et al.*, 1996, Ellehauge *et al.*, 1998, Horiuchi *et al.*, 2002). Recently, it also has been shown that MrpC, together with FruA, is required for control of transcription of several genes expressed late during the developmental program near the onset of sporulation (Mittal & Kroos, 2009a, Mittal & Kroos, 2009b). It has been proposed that FruA is likely activated by phosphorylation, and genetic evidence suggests that FruA activation occurs in response to the C-signal pathway (Sogaard-Andersen & Kaiser, 1996, Ellehauge et al., 1998). Cell-surface-associated CsgA protein (p25), encoded by *csgA* gene, is cleaved into C-signal protein (p17) by PopC protease (Rolbetzki *et al.*, 2008). In response to end-to-end contact

between cells, C-signal is produced and sensed by an unidentified receptor on a neighbor cell and then C-signal production is further amplified by cell to cell contact leading to increased FruA activation (Gronewold & Kaiser, 2001).

A current model suggests that FruA protein that has been activated by the C-signal induces two branches of *M. xanthus* development: aggregation and sporulation (Sogaard-Andersen *et al.*, 1996). Low level of phosphorylated FruA are though to induce the aggregation branch by stimulating methylation of FrzCD, a methyl-accepting chemosensory-protein which controls cell reversal frequency leading to aggregation during development. It has been shown that FrzCD methylation during development results in decreased cell reversal frequency which directs cells to aggregate into fruiting bodies (Blackhart & Zusman, 1985, McBride *et al.*, 1992, McBride & Zusman, 1993, Shi *et al.*, 1996, Sogaard-Andersen & Kaiser, 1996).

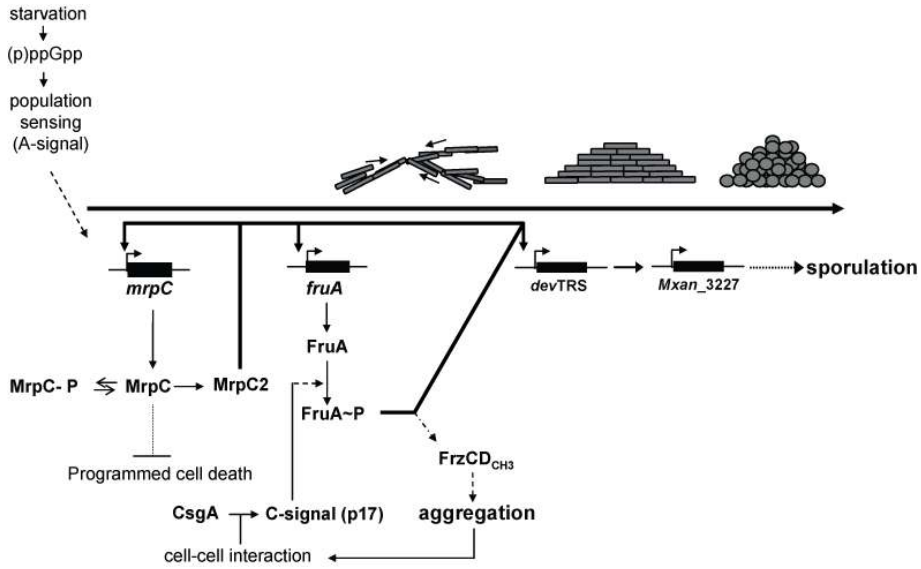

Figure 1.3 Molecular events during the *M. xanthus* developmental program (bottom) in relation to aggregation and sporulation (top). The *M. xanthus* developmental program is induced by starvation and controlled by temporally ordered cascade of gene expression. See text for details.

In the sporulation branch, higher levels of activated FruA, thought to be induced by increased cell-cell contact during aggregation, induce the sporulation branch (Sogaard-Andersen et al., 1996, Ellehauge et al., 1998). It has been demonstrated that FruA induces transcription of the *dev* locus which is necessary for induction of sporulation (Viswanathan *et al.*, 2007). FruA and MrpC both bind to the *dev* promoter (Mittal & Kroos, 2009a, Mittal & Kroos, 2009b). One of the products of the *dev* locus (DevT) is also required for stimulation of *fruA* transcription providing a positive feedback loop

on *fruA* expression (Boysen *et al.*, 2002). The *dev* locus is necessary for *Mxan_3227* (*exo*) expression (Licking *et al.*, 2000). Mutants in *dev* and *Mxan_3227* (*exo*) form mounds, but fail to form spores suggesting that both *dev* and *Mxan_3227* (*exo*) are required for sporulation (Thony-Meyer & Kaiser, 1993, Licking *et al.*, 2000).

1.1.4 Positive feedback loops of *Myxococcus xanthus*

Positive and negative feedback (autoregulatory) loops are frequently found in transcription regulatory networks and signaling pathways (Banerjee & Bose, 2008, Mitrophanov & Groisman, 2008) and maintain homostasis during regulation of cell growth and differentiation in response to external stimuli (Kim *et al.*, 2007). The feedback loop normally consists of genes, proteins and other molecules which are connected by regulatory interaction. Depending on the components and their interaction, feedback loops have distinct roles in diverse regulatory systems. A regulatory interaction is positive, when an increase of the amount or activity of one component increases the amount or activity of its interaction paterner (Banerjee & Bose, 2008). In contrast, a regulatory interaction is negative, when one component decreases the activity of its partner. In general, it is known that positive feedback induce a swich-like behavior and biastability (Ferrell, 2002, Tyson *et al.*, 2003) and that negative feedback represses noise effects (Tyson et al., 2003, Loewer & Lahav, 2006).

In the *M. xanthus* development program, three major positive regulatory loops have been shown to play important roles in control of development program. First, MrpC, which is major developmental protein, acts as transcriptional regulator inducing own gene transcription (Sun & Shi, 2001b, Sun & Shi, 2001a, Nariya & Inouye, 2006). Second, C-signaling (CsgA p17) acummulated by increased cell-cell contact during development, activates *csgA* transcription which results in CsgA p25 accumulation (Kim & Kaiser, 1990, Kim & Kaiser, 1991, Li & Shimkets, 1993, Gronewold & Kaiser, 2001). Fianlly, one of the products of the *dev* locus (DevT) activated by FruA protein directly or indirectly stimulates *fruA* transcription providing a positive feedback loop on *fruA* expression (Boysen *et al.*, 2002) (see details in section 1.1.3). It has been shown that overexpression of C-signal during early development results in uncoupling of aggregation and sporulation, forming spores outside of fruiting bodies, while reduced synthesis of CsgA protein causes delayed aggregation forming large fruiting bodies and reduced sporulation (Kruse *et al.*, 2001). Since aggregation and sporulation are induced at distinct low and higher threshold levels of C-signal respectively, sporulation is though to be coupled to completion of aggregation by C-signaling loop coupled to the positive feedback loop on FruA expression.

1.1.5 Cell fate during development

In addition to the cells that aggregate and then sporulate, two other distinct cell fates have been observed. It was first observed that the majority of cells (approximately 80 to 90 %) undergo obligatory cell lysis (Wireman & Dworkin, 1977). It was later demonstrated that some developing cells do not aggregate and becomes peripheral rods which remain as rod-shaped cells (O'Connor & Zusman, 1991c).

It currently has been proposed that programmed cell death (PCD) is mediated by a toxin/antitoxin system composed of MazF/MrpC. MazF is an endoribonuclease and MrpC is a transcriptional regulator described above. A current model suggests that under vegetative conditions, non-phosphorylated MrpC forms a complex with MazF to prevent MazF activity. In nutrient depleted conditions, the Pkn8 and Pkn14 Ser/Thr kinase cascade is inactivated and MrpC is cleaved into MrpC2. MrpC2 activates both transcription of *mazF* and *mrpC*. Later during development, MrpC does not form a complex with MazF so that MazF can act as an endoribonuclease inducing programmed cell death (Figure 1. 4). Mutants in *mazF* display a delayed developmental phenotype compared to wild-type suggesting programmed cell death plays an important role for developmental progression (Nariya & Inouye, 2008, Sogaard-Andersen & Yang, 2008).

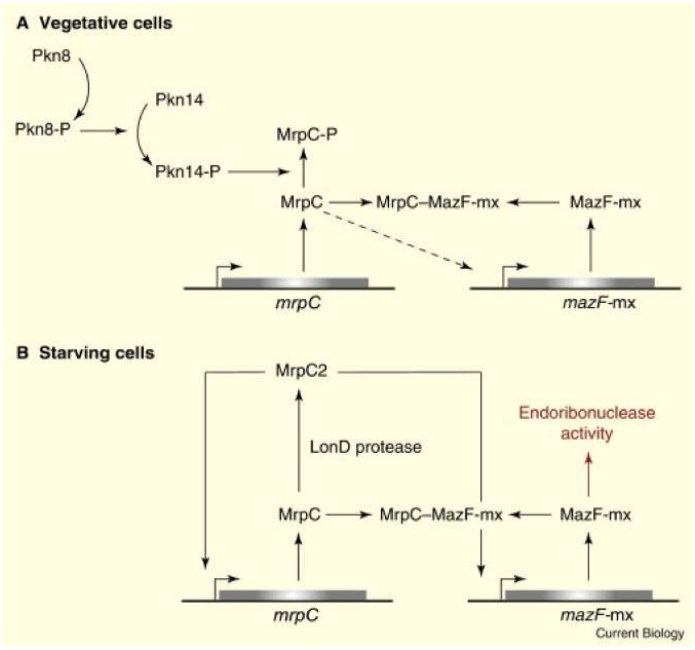

Figure 1.4 Schematic view of the programmed cell death pathway. (A) In vegetative cells, the interaction between MazF and non-phosphorylated MrpC prevent a MazF activity. (B) In response to starvation, the Pkn8–Pkn14 kinase cascade is inactivated and MrpC converted to MrpC2 by LonD protease. In late starving cells (indicated in red), MazF acts as an endoribonuclease. This figure is taken from (Sogaard-Andersen & Yang, 2008).

Peripheral rods are a distinct developmental subpopulation of cells that do not aggregate and remain as rod-shaped cells outside of fruiting bodies. Analysis of the proteins expressed in peripheral rods suggest that these cells are distinct from vegetative rods (O'Connor & Zusman, 1991a). O'Connor and Zusman analyzed the accumulation patterns of several developmentally regulated proteins in the non-aggregating cell and aggregating cell population by immunoblot analysis. This study demonstrated that MbhA (myxobacterial hemagglutinin), Protein S, Protein S1 and Protein C (spore coat protein) are expressed in both cell types but that the expression patterns are different (O'Connor & Zusman, 1991c). It has been hyphothesized that peripheral rods allow *M.xanthus* to utilize low levels of nutirients that would not support spore germination and outgrowth of spores (O'Connor & Zusman, 1991b). Julien *et al*. revealed that aggregating cells express at least two times more CsgA protein than non-aggregating rods cells (Julien *et al.*, 2000).

1.2 Two-component signal transduction systems in *M. xanthus*

In bacteria, two-component signal transduction systems play an important role as a basic stimulus-response coupling mechanism to allow organisms to sense and respond to changes in environmental conditions. The prototypical system consists of a histidine protein kinase (HPK), containing a sensing domain fused to HisKA and HATPase_C signal transmission domains and a reposnse regulator (RR), containing a receiver domain fused to an effector domain. In a simple system, extracellular stimuli are sensed by, and serve to modulate the activities of, the HPK. The HPK transfers a phosphoryl group to the RR which mediates a response (Figure 1. 5A). This paradigm system is termed a 1:1 paired system. However, two component signal systems can also comprise more complex multistep phosphorelays. Typically, a phosphorelay system is composed of HPK which also contains a receiver domain (hybrid). In response to a stimulation, the hybrid HPK autophosphorylates and transfers phosphoryl group to the reciever. Then, this phosphoryl group is transfered to the conserved histidine residue on a histidine phosphotransferase protein (Hpt) and finally to a RR which results in activation of a downstream effector domain to elicit a specific response (Stock *et al.*, 2000) (Figure 1. 5B). Thess more complex signaling systems often involve orphan TCS genes (not encoded with cognate TCS partners) or TCS genes organized in complex arrangments (more than two TCS genes are encoded in the same locos).

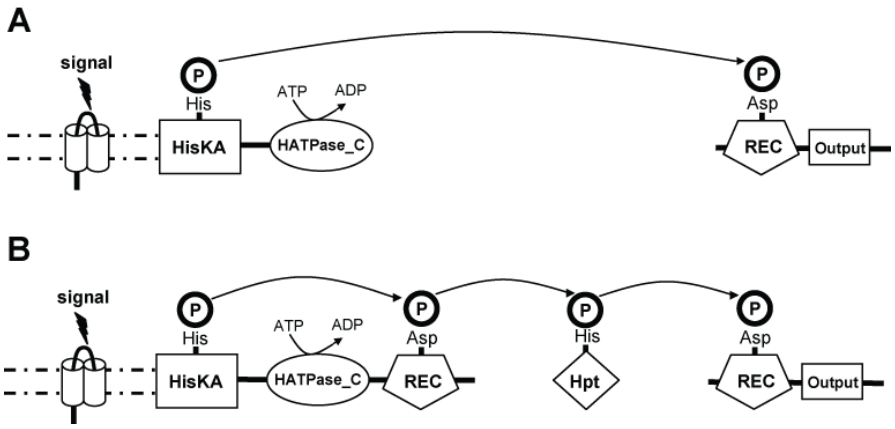

Figure 1.5 Schematic representation of the two-component signal transduction paradigm and the domain structures of each component. (A) A classical system. (B) A multi-component phosphorelay system. HisKA: dimerization domain, HATPase_c: the catalytic and ATPase domain, REC: receiver domain, Output: output domain, HPT: His-containing phosphotransfer domain. See text for details.

The *M. xanthus* genome contains 272 two-component signal transduction (TCS) genes consisting of 118 histidine protein kinases (HPKs), 119 response regulators (RRs) and 14 HPK like genes (Shi *et al.*, 2008). Shi *et al*. classified TCS genes into three groups based on their genetic organization: orphans (not flanked by a cognate TCS partner in the genome), paired (one HPK and one RR) and complex (more than two TCS genes encoded in the same locus) (Figure 1. 6).

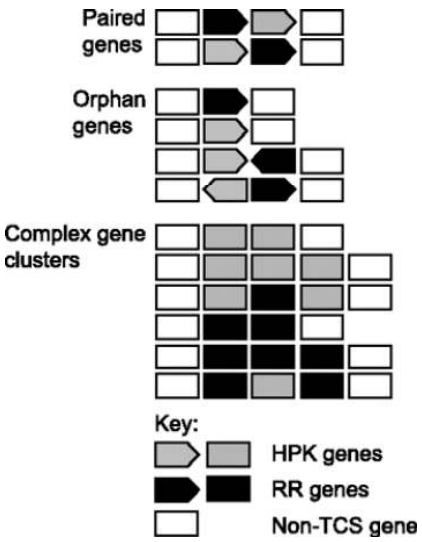

Figure 1.6 Classification scheme of two-component signal trasduction genes. The definition of paired and orphan TCS genes includes information about transcription direction as indicated by the arrow symbols. Complex TCS gene clusters include clusters containing two or more RR genes, clusters containing two or more HPK or HPK-like genes, and clusters with three or more TCS genes irrespective of transcription direction, as indicated by the box symbols. This figure is taken from (Shi et al., 2008).

Of the 272 TCS genes, 71% of the TCS genes are organized either in orphan genes or in complex gene clusters, whereas only 29 % display the standard paired gene organization (Shi *et al.*, 2008).

Interestingly, atypical (cytoplasmic or hybrid) HPKs and atypical RRs (containing non-DNA binding domain or lacking output domain) are overrepresented in orphan or complex gene clusters. These results suggest that the signal transduction pathways encoded by orphan genes and complex gene clusters are involved in complex phosphorelay systems (Shi et al., 2008). Moreover, experimental data through microarray and quantitative real-time PCR analysis have shown that a high proportion of orphan genes and genes encoded in clusters are transcriptionaly regulated during development. These results suggest that a higher proportion of orphan genes is developmentally regulated and may be necessary for contolling development program.

1.3 Negative regulators (NRs) that alter developmental timing in *M. xanthus*

An interesting set of genes (*espA*, *espC*, *red* and *todK*) have been identified that are necessary for negative regulation of developmental progression in *M. xanthus*. Interestingly, *espA, espC, red* and *todK* genes are members of the two component signal transduction family of proteins, but no output proteins have been identified, since all of these genes are encoded as orphans or together with single receiver domain protein.

1.3.1 EspA

The first NR, *espA,* was identified in a screen for abnormal developmenters using random plasmid insertion mutagenesis (Cho & Zusman, 1999). *espA* is cotranscribed with *espB* and transcription is up-regulated during development (Cho & Zusman, 1999). A null mutant in *espA*, a hybrid histidine kinase homolog, causes aggregation and sporulation earlier than wild type. In contrast, mutants in *espB*, encoding a putative transport protein, are delayed for aggregation and sporulation. Moreover, an *espA espB* double mutant also shows the same early development as the *espA* mutant suggesting that that they lie in same signalling pathway and that EspA acts downstream of EspB (Cho & Zusman, 1999).

EspA is hybrid kinase that contains N-terminal forkhead associated (FHA) domain, two PAS/PAC redox sensing domains, and a C-terminal receiver domain (Figure 1. 7). FHA domains are found in many protein kinases and transcription factors in eukaryotes

(Hofmann & Bucher, 1995), and have been proposed to be a basic phosphopeptide recognition motif that plays a important role in phosphor mediated protein interaction processes in eukaryotes (Durocher *et al.*, 1999). PAS/PAC domains are involved in many signaling proteins, where they are used as a sensor domain for energy or oxygen stress (Taylor & Zhulin, 1999).

Based on the early developmental phenotype of an *espA* mutant, it was hypothesized that EspA acts to repress progression through the developmental program until a specific condition or set of conditions is met (Cho & Zusman, 1999). Moreover, it has been demonstrated that two Ser/Thr kinases, PktA5 and PktB8 that are encoded adjacent to the *espAB* locus, regulate developmental program by interacting with EspA and EspB (Stein *et al.*, 2006). This result suggests that regulation of the developmental program by EspA is very complicated. However, signal output of EspA is not clear because it is not genetically organized together with a cognate response regulator gene.

It more recently has been demonstrated that EspA autophosphorylates and transfers a phosphoryl group to its receiver domain. Moreover, point mutations in both the kinase and receiver domains phenocopy the *espA* deletion mutant. These results indicate that kinase activity is required for EspA-mediated control over developmental progression, and that phosphotransfer to the receiver domain is a required step in EspA-mediated control over the developmental program. In this research, Higgs et al. also demonstrated that in the *espA* mutant, *mrpC* expression was similar to that of the wild type, but *espA* mutant induces earlier accumulation of MrpC protein resulting in earlier accumulation of FruA. Earlier accumulation of FruA correlates with earlier aggregation and sporulation development of *espA* mutant (Higgs et al., 2008). These analyses suggest EspA regulates the developmental program by decreasing translational of *mrpC* or stimulating degradation of MrpC.

1.3.2 EspC

In an effort to identify signaling partners (outputs) for EspA, *magellan4 mariner* transposon mutagenesis was used to screen for early developer mutants in *espB* mutant background which shows delayed development (Lee *et al.*, 2005). In this analysis, nine independent insertion mutants were identified. One of the nine insertion mutants was in the *espA* gene, itself. The rest were inserted in new genes: one in *espC*, five in the *red* locus (see below) and two in *Mxan_4465* (Higgs ,Cho, and Zusman, unpublished data).

EspC is an orphan hybrid histidine kinase that contains a receiver domain at the C-terminal and two N-terminal sensing modules: a MASE1 module and, like EspA, a PAS/PAC redox sensing module (Figure 1. 7). MASE1 is a predicted integral membrane sensory domain found in histidine kinases, diguanylate cyclases, and other bacterial signaling proteins (Anantharaman & Aravind, 2003). An *espC* mutant also caused early development phenotype like *espA* mutant and sporulation timing of the *espC* mutant is very similar to that of the *espA* mutant (Lee et al., 2005). EspA and EspC are 49% identical in the kinase domain. *espC* was reported up-regulated during development.

1.3.3 RedCDEF

It has been shown that four additional unusual two-component signal transduction proteins (RedC, RedD, RedE and RedF) also modulate developmental progression (Higgs *et al.*, 2005). A null mutation in *redCDEF* (regulation of early development) displays early developmental phenotype. RedC encodes a membrane-bound histidine kinase, RedD encodes a protein with dual receiver domains, RedE encodes a histidine kinase with no obvious sensing domain, and RedF encodes a single domain receiver protein (Figure 1. 7). Epistasis and yeast two-hybrid interaction analyses suggested that these four proteins are involved in a linear signal transduction system so are treated as one pathway (Higgs et al., 2005).

Recently, in an effort to understand signal flow between the RedCDEF two-component signaling proteins, genetic and biochemical approaches were employed (Jagadeesan *et al.*, 2009). Genetic evidence demonstrated that null mutations of either *redC* or *redF* aggregate and sporulate earlier than wild-type, while *redD* and *redE* mutants are delayed in aggregation and sporulation. Biochemical evidence suggests a novel four component signal transduction mechanism. In this model, early during development, RedC autophosphorylates and transfers its phosphoryl group to RedF which repress the developmental program. Later during development, in response to an unknown signal, RedC transfers its phosphoryl group to the first receiver domain of RedD and the phosphoryl group is then transferred to RedE. Finally, RedE acts as phosphatase on RedF, and dephosphorylated RedF allows development to proceed (Jagadeesan et al., 2009). It is unknown how RedF modulates developmental progression.

1.3.4 TodK

By using mini-Tn5(tet) mutagenesis, the *todK* gene was characterized in the alternative DK1622 wild type strain (Rasmussen & Sogaard-Andersen, 2003). TodK is orphan

histidine kinase homolog that contains a PAS/PAC redox sensing module (Figure 1. 7). A null mutantion in *todK* results in early development and in increased expression of a subset of C-signal-dependent genes. It has been shown that TodK does not interfere with accumulation of CsgA protein suggesting that TodK is not involved in the regulation of C-signal accumulation. In a similar manner, TodK is not involved in the developmentally regulated transcription of *fruA* or in the accumulation of FruA protein suggesting that TodK pathway converges on the C-signal transduction pathway downstream of the accumulation of the FruA protein. It has been shown that the *todK* mutant does not bypass certain known developmental regulators such as *csgA, fruA* and *devR* suggesting that TodK depends on the known components to induce early aggregation and early sporulation. *todK* was reported transcriptionally down regulated during development (Rasmussen & Sogaard-Andersen, 2003). It is not clear what the signal output of TodK is. It has been demonstated that mutant in *dotR* which encodes response regulator located adjacent to TodK had no defect in development. This result suggests that TodK and DotR may not act in the same genetic pathway (Rasmussen & Sogaard-Andersen, 2003)

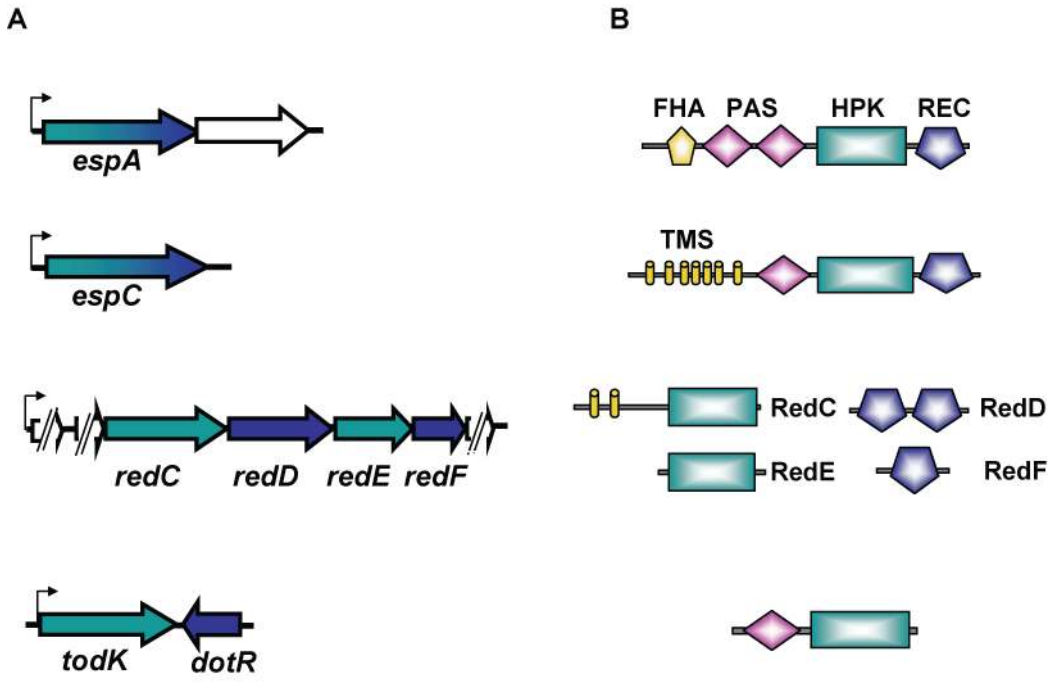

Figure 1.7 A schematic view of genetic organization and domain architecture of *espA*, *espC*, *redCDEF* and *todK*. (A) Genetic organization of *espA*, *espC*, *redCDEF*, and *todK* genes. Hybrid histidine kinases are displayed by green and blue gradation. Histidine kinases are displayed by green. Receivers are displayed by blue. (B) Domain architecture of EspA, EspC, RedCDEF, and TodK. FHA (forkheadassociated domain). PAS (PAS/PAC sensing domain). HPK (histidine protein kinase domain). R EC(receiv-er domain). TMS (transmembrane domain).

1.4 Aim of the project

Based on previous research, it is hyphothesized that the *espA*, *espC, red,* and *todK* gene products are necessary for negative regulation of progression through the developmental program. The aim of this project was 1) to understand whether these NRs function together or in separate pathways to regulate developmetal progression in *M. xanthus*, and 2) to define the point(s) in the developmental program where the NRs signaling pathway(s) exert a function. The results of these analyses will be used to elucidate the advantage for the fuction of NRs in the developmental program.

2 RESULTS

2.1 Genetic analysis of NRs

2.1.1 The *espA*, *espC*, *red* and *todK* genes are regulated during development

We first compared the transcriptional expression level of the *espA*, *espC*, *red* and *todK* genes during development by real-time PCR analysis to enable a direct comparison of the expression patterns in the DZ2 wild type strain during development. Consistent with the literature (Cho & Zusman, 1999, Lee et al., 2005), the real-time PCR results showed that *espA* and *espC* genes are up-regulated after onset of starvation and display nearly indentical expression patterns (Figure 2. 1).

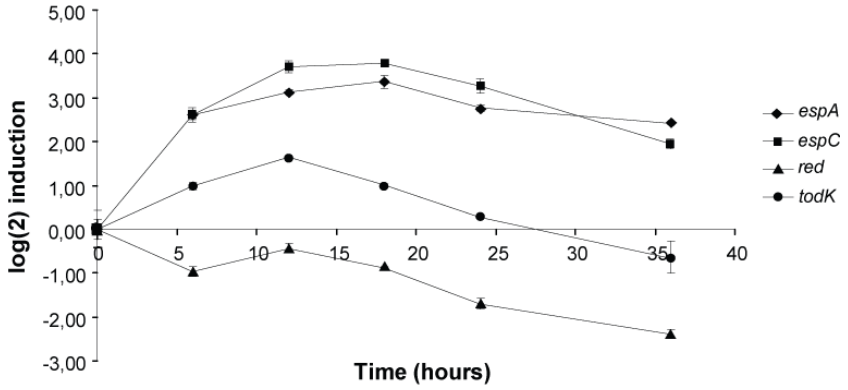

Figure 2.1 Quantitative real-time PCR analysis of NR genes transcription during development.
Wild-type cells were developed in submerged culture and harvested at the indicated time points. RNA was isolated and reverse transcribed into cDNA. Primers specific for *espA, espC, red* and *todK* were used for real-time PCR analysis.

It has been reported in the alternative DK1622 wild type strain that the *todK* mRNA was 10-fold down-regulated after onset of starvation (Rasmussen & Sogaard-Andersen, 2003). However, our result shows that *todK* is slightly up and then down regulated. *red* transcription is approximately 8-fold down regulated over 36 h of development. It has been previously demonstrated that EspA protein patterns follow the transcription patterns (Higgs et al., 2008), and that the Red proteins are expressed in vegetative constion and are down regulated after 36 h of development on CF starvation plates (Jagadeesan et al., 2009). TodK is also expressed during vegetative growth and is down

regulated after 36 h (Figure 2. 36). The protein accumulation pattern of EspC is similar to that of EspA (Schramm & Higgs, unpublished data).

2.1.2 Mutants in the four NRs exhibit three distinct developmental phenotypes

As a first step to determine whether the NR gene products function together or in separate pathways, Δ*espA*, Δ*espC*, Δ*red*, and *todK*::Tn5 insertion mutants were generated in an isogenic background and a rigorous phenotypic comparison was performed. These strains were developed on nutrient-limited starvation medium (CF plates) and heat and sonication resistant spores were counted by hemacytometer (counting chamber) at each developmental time point. It should be noted that in this analysis, we used that *todK* insertion mutants, however we have shown that insertion and deletion mutants of *todK* displayed same phenotype (data not shown) and this result is corresponding to previous reaserch (Rasmussen & Sogaard-Andersen, 2003).

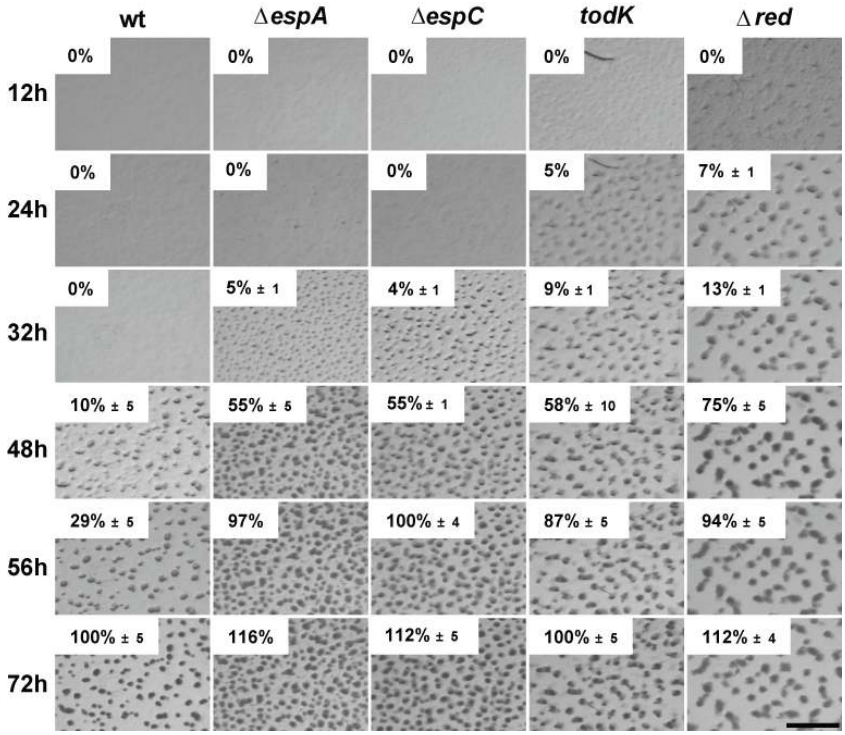

Figure 2.2 Phenotype and sporulation assays for NR mutants used in this study. 10 ul spots (4 X 10^9 cells ml^{-1}) of wild-type (DZ2), *espA* (DZ4227), *espC* (PH1044), *red* (DZ4659) and *todK* (PH1045) mutants were placed on starvation plates and incubated at 32 °C. Pictures were recorded at the indicated time points. Sporulation efficiency was determined as number of heat and sonication resistant spores as a percent of wt spores at 72 h. Scale bar, 1.0 mm.

The wild-type strain initiates aggregation and sporulation between 32 and 48 h, and all NR mutants aggregate and sporulate earlier than the wild type. Development of *espA* and *espC* mutants is approximately 12 h earlier than wild-type, while the *red* mutant is approximately 24 h earlier than wild-type. Development of the *todK* mutant is earlier than the *red* mutant. Interestingly, *espA* and *espC* mutants showed very similar timing of development, while *todK* and *red* mutants are progressively earlier (Figure 2. 1). This result demonstrates that there are at least three distinct NR phenotypes, and suggests that EspA and EspC effect the developmental program differently from TodK and from Red.

2.1.3 EspA and EspC likely lie in the same signaling pathway

The observation that the developmental phenotypes of *espA* and *espC* mutants are very similar each other raised the possibility that EspA and EspC likely act to repress developmental program at a similar point. To further understand whether these two NRs function in one or two distinct signaling pathways, we generated an isogenic *espA espC* double mutant and performed an epistasis analysis. Our analysis demonstrated that developmental phenotype of *espA espC* double mutant is identical to the *espA* and *espC* single mutants (Figure 2. 3). This result suggests that EspA and EspC function together to repress a distinct position in the developmental program.

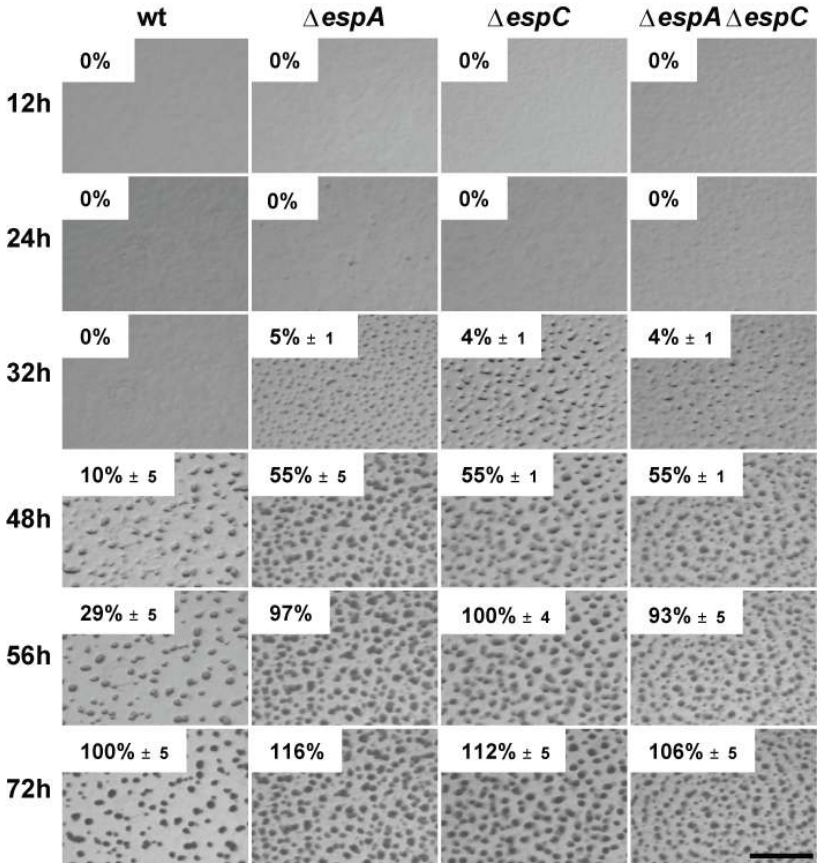

Figure 2.3 Epistatic analysis for *espA* and *espC*. 10 ul spots (4 X 10^9 cells ml^{-1}) of wild-type (DZ2), *espA* (DZ4227), *espC* (PH1044), and *espA espC* (PH1047) mutants were placed on starvation plates and incubated at 32 °C. Pictures were recorded at the indicated time points. Spore efficiency was determined as the number of heat and sonication resistant spores as a percent of wild-type spores at 72 h. Scale bar, 1.0 mm.

2.1.4 The Red TCS system does not lie in the same signaling pathway with EspA/EspC

To understand whether Red functions in the same signaling pathway with EspA and EspC, we next generated *espA red* and *espC red* double mutants in isogenic backgrounds. *red* mutants develop earlier than the *espA* mutant (see Figure 2. 1). Interestingly, the *espA red* double mutant displayed an additive phenotype, it aggregated and sporulated even earlier than the *red* single mutant and formed more disorganized fruiting bodies (Figure 2. 4). The *espC red* double mutant also displayed an additive phenotype similar to *espA red* double mutant (data not shown). These results suggest that Red does not lie in same signaling pathway with EspA/EspC.

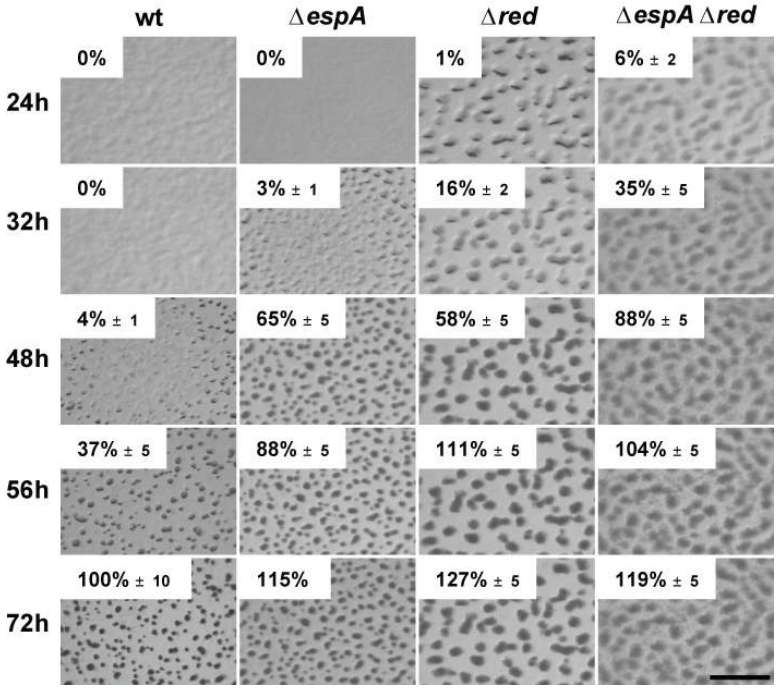

Figure 2.4 Epistatic analysis for *espA* and *red*. 10 ul spots (4 X 10^9 cells ml^{-1}) of wild-type (DZ2), *espA* (DZ4227), *red* (DZ4659), and *espA red* (PH1048) mutants were placed on starvation plates and incubated at 32 °C. Pictures were recorded at the indicated time points. Sporulation efficiency was determined as the number of heat and sonication resistant spores as a percent of wild-type spores at 72 h. Scale bar, 1.0 mm.

2.1.5 TodK does not lie in the same signaling pathway with EspA/EspC

To examine the possibility that TodK is in same singling pathway with EspA and EspC, we next generated *espA todK* and *espC todK* double mutants in an isogenic background. Our analysis revealed that development of *espA todK* is also additively faster than either of the single mutants (Figure 2. 5). The *espC todK* mutant also displayed additive phenotype like *espA todK* double mutants (data not shown). These results suggest that TodK also functions in a different signaling pathway from EspA and EspC.

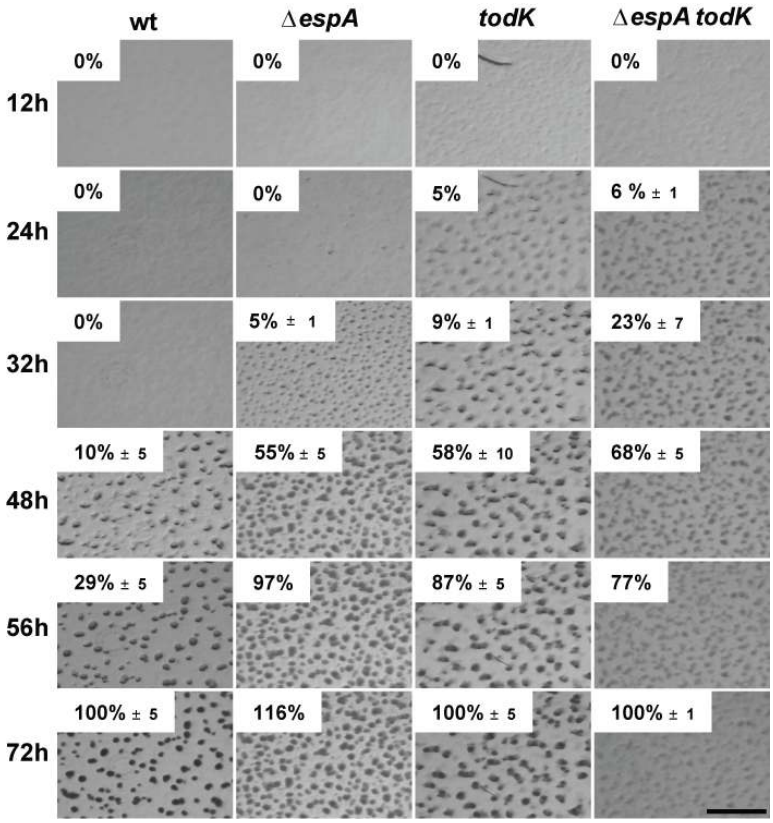

Figure 2.5 Epistatic analysis for *espA* and *todK*. 10ul spots (4 X 10^9 cells ml^{-1}) of wild-type (DZ2), *espA* (DZ4227), *todK* (PH1046), and *espA todK* (PH1049) mutants were placed on starvation plates and incubated at 32 °C. Pictures were recorded at the indicated time points. Sporulation efficiency was determined as the number of heat and sonication resistant spores as a percent of wild-type spores at 72 h. Scale bar, 1.0 mm.

2.1.6 Red and TodK are in different signaling pathways

We next used a similar approach to examine the genetic relationship between *red* and *todK*. A *red todK* double mutant was generated and analyzed. Our analysis revealed that *red todK* double mutant displayed an additive phenotype which develops much earlier than the single mutants (Figure 2. 6). In addition to the additive phenotype, the *red todK* double mutant formed more disorganized fruiting bodies. These results suggest that Red and TodK also do not lie in a single linear signaling pathway. Taken together, all these results suggest that there are at least three distinct signaling pathways in the developmental program: 1) EspA/C, 2) Red, and 3) TodK.

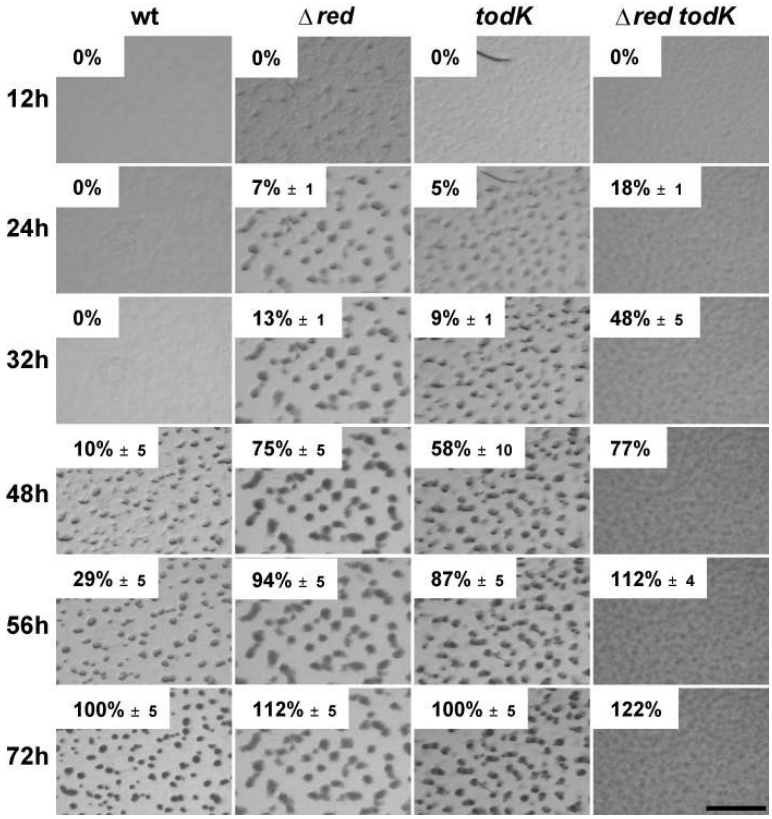

Figure 2.6 Epistatic analysis for *espA* and *todK*. 10 ul spots (4 X 10^9 cells ml^{-1}) of wild-type (DZ2), *red* (DZ4659), *todK* (PH1046), and *red todK* (PH1052) mutants were placed on starvation plates and incubated at 32°C. Pictures were recorded at the indicated time points. Sporulation efficiency was determined as the number of heat and sonication resistant spores as a percent of wild-type spores at 72 h. Scale bar, 1.0 mm.

2.1.7 Coordinated fruiting body formation is destroyed in the absence of the NRs

We next investigated the phenotype of mutants missing two or more of the NRs. Interestingly, our analysis revealed that an *espA espC red todK* quadruple mutant aggregates and sporulates earlier and at higher level than all other combinations of double mutants (Figure 2. 7A). Morover, this quadruple mutant failed to form distinct fruiting bodies. From our genetic analysis of all combinations of kinase mutants, we observed that while DZ2 forms well-rounded and compact fruiting bodies, single, double, and quadruple mutants form progressively more disorganized fruiting bodies (Figure 2. 7A and B) suggesting that there is a negative correlation between rate of development and coordinated fruiting body formation. Moreover, closer examination of the fruiting bodies in the various mutants revealed that the early development mutants formed many spores outside of fruiting bodies (Figure 2. 7C). These results all further suggest that kinases that control the timing of development are required for coordinated fruiting body formation.

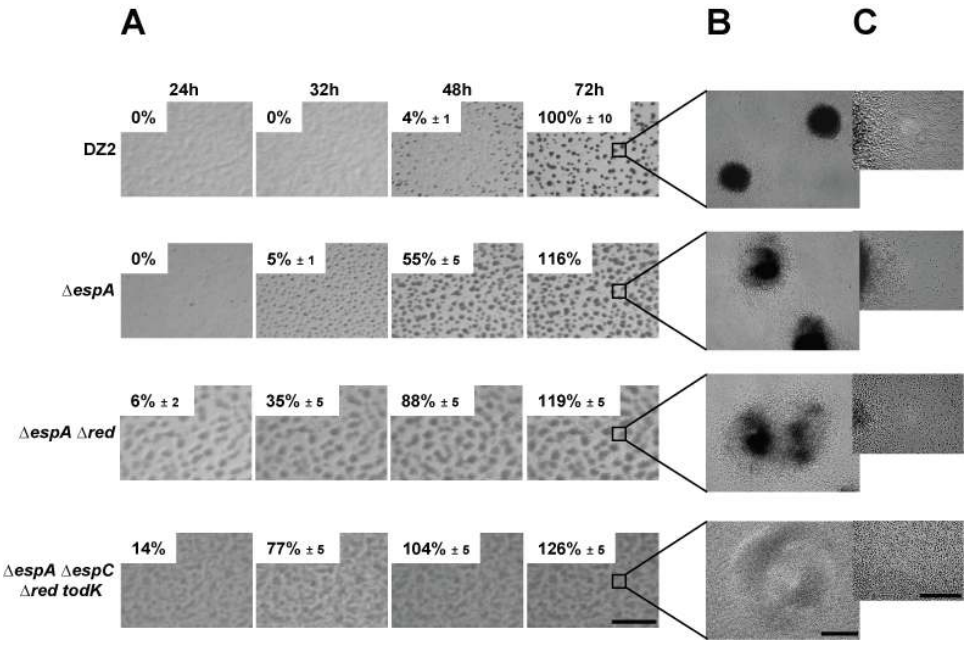

Figure 2.7 Comparative analysis of the NR mutant combinations. (A)10 ul spots (4 X 10^9 cells ml^{-1}) of wild-type (DZ2), *espA* (DZ4227), *espA red* (PH1048), and *espA espC red todK* (PH1054) quadruple mutants were placed on starvation plates and incubated at 32 °C. Pictures were recorded at the indicated time points. Sporulation efficiency was determined as the number of heat and sonication resistant spores as a percent of wild-type spores at 72 hours. Scale bar, 1.0 mm. (B and C) 500 ul of cell culture (2 X 10^7 cells ml^{-1}) of wild-type (DZ2), *espA* (DZ4227), *espA red* (PH1048), or *espA espC red todK* (PH1054) mutants were placed in starvation media (MMC) and incubated at 32°C. Pictures were recorded by inverted microscope at 72 hours development. Scale bar, (B) 100 μm, (C) 50 μm.

2.1.8 Peripheral rods sporulate inappropriately in the NR mutants

As described above, we observed that early development correlates with disorganized fruiting bodies. To further understand this observation, we examined the proportions of lysed cells, spores and peripheral rods. For this, we adapted an assay to separate peripheral rods and fruiting bodies (O'Connor & Zusman, 1991c). Briefly, we first harvested and counted cells at 0 h of development to determine total cell number. We next harvested cells after 5 days of development and separated fruiting bodies from peripheral rods by low speed centrifugation (50 × g) and counted the total remaining number of cells.

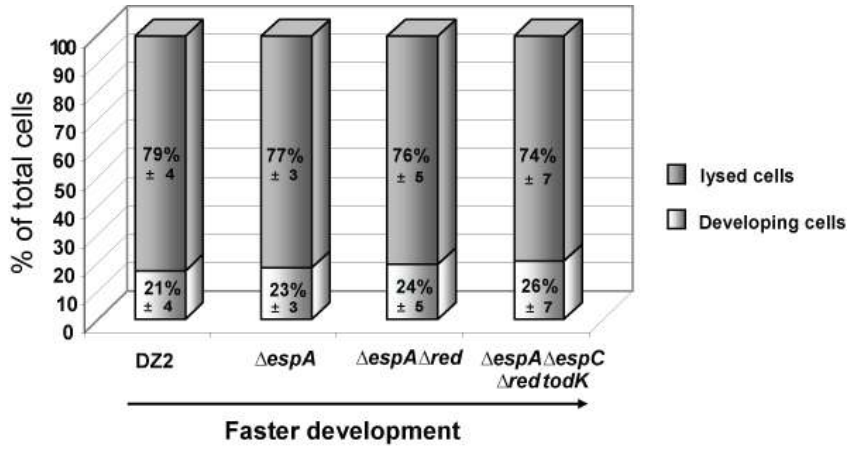

Figure 2.8 Quantification of cell lysis. 500 ul cultures (2 X 10^7 cells ml^{-1}) of wild-type (DZ2), *espA* (DZ4227), *espA red* (PH1048), or *espA espC red todK* (PH1054) mutants were placed in starvation media (MMC) and incubated at 32 °C. Cells were harvested and counted at 0 h of development and after 5 days of development. Lysed cells were calculated by comparing total cells harvested after 5 days of development with the number of cells determined at 0 h of development.

After separation of these two fractions, we counted the number of rods and spores in the supernatant which are expected to be outside of fruiting bodies. In similar manner, we counted spores in the pellet which are expected to be inside of fruiting bodies. In this assay, we first checked the proportion of lysed cells and developing cells (peripheral rods and spores). Our analysis revealed that 79 % of DZ2 cells underwent programmed cell death and this proportion was similar in the NR mutant strains indicating that there is no significant difference in the amount of lysis in each strain (Figure 2. 8).

Next, we focused on the proportion of peripheral rods and spores. Our assay demonstrated that all strains have nearly the same number of spores inside fruiting

bodies even though the fruiting bodies of the quadruple NR mutants are barely distinguishable. In the wild-type, 29 % of cells were peripheral rods and 3 % were loose spores. In contrast, only 18 %, 11 %, 5 % of cells were peripheral rods in *espA*, *espA red*, and *espA espC red todK* quadruple mutants respectively. Conversly, the number of loose spores increased from 3 % in the wild-type, to 11 %, 18 %, and 25 % in the *espA*, *espA red*, and quadruple NR mutants, respectively (Figure 2. 9). These results suggest that peripheral rods are sporulating inappropriately in the early development mutants and that the control mechanisms for peripheral rods are disturbed.

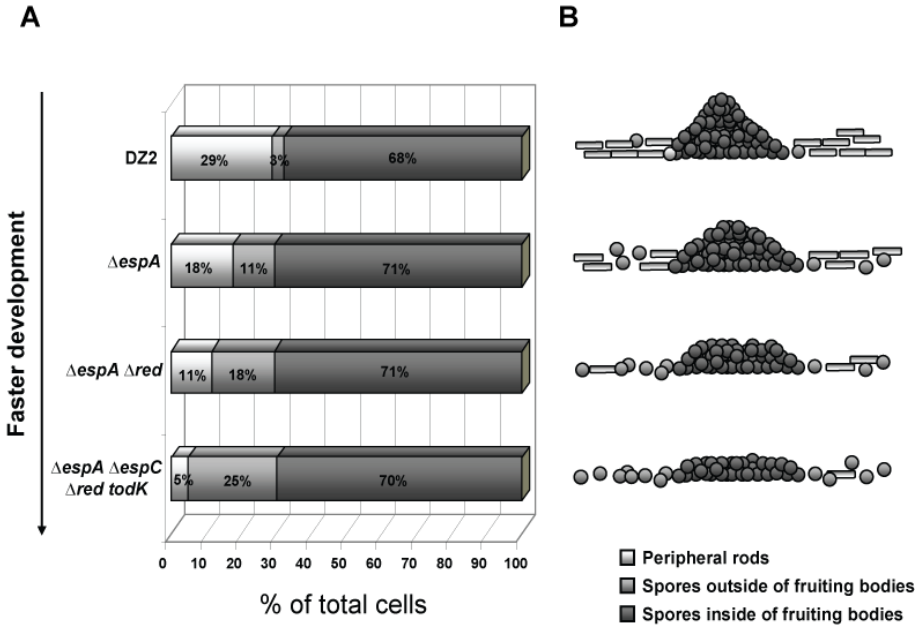

Figure 2.9 Analysis of the developmental subpopulations in the NR mutants. (A) The proportion of peripheral rods and spores in wild-type (DZ2), *espA* (DZ4227), *espA red* (PH1048), and *espA espC red todK* (PH1054) mutants. 500 ul culture (2 X 10^7 cells ml^{-1}) of wild-type (DZ2), *espA* (DZ4227), *espA red* (PH1048), and *espA espC red todK* (PH1054) mutants were placed in starvation media (MMC) and incubated at 32 °C. Cells were harvested after 5 days of development. The number of cells in each population was counted by hemacytometer. (B) Schematic representation of the cell population at 5 days.

2.1.9 The NR depleted mutant follows the ordered developmental program

The observation that almost all cells sporulated in the *espA espC red todK* mutant raised the possibility that these cells were bypassing the ordered cascade of developmental regulator expression. To address this issue, we analyzed expression pattern of developmental marker genes (*fruA, dev, Mxan_3227*) by using real-time PCR in the *espA espC red todK* quadruple mutant. Real-time PCR analysis of *fruA* gene

transcription showed that in the quadruple mutant, *fruA* was highly expressed from between 0 to 6 h and especially *fruA* transcript in the quadruple mutant was approximately 6.5-fold higher than wild type at 6 h of development (Figure 2. 10B). Moreover, real-time PCR analysis of *dev* gene transcription showed that in the quadruple mutant, *dev* was up-regulated between 3 h and 6 h compared to between 12 h and 18 h in the wild type (Figure 2. 10C). In similar manner, expression of *Mxan_3227* (*exo*) was highly up-regulated between 12 h and 15 h in the quadruple mutant compared to between 30 h and 42 h in the wild type (Figure 2. 10D). These results suggest that although *fruA*, *dev* and *exo* are expressed earlier than in the wild-type, they still follow ordered expression patterns and expression of these genes is not bypassed.

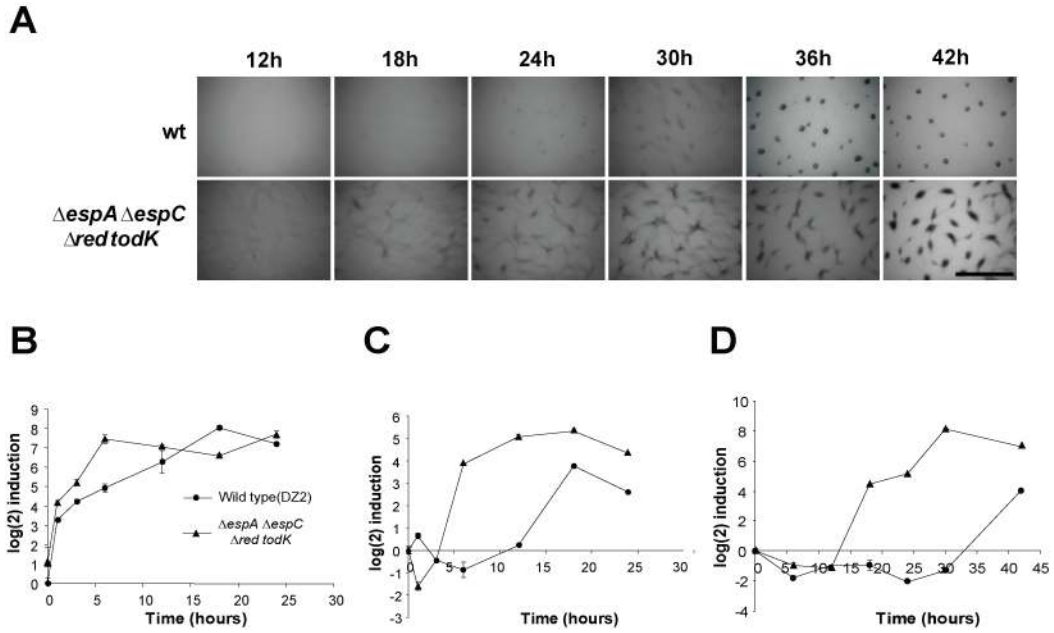

Figure 2.10 Real time PCR analysis of developmetal marker genes. (A) The developmental phenotype of the *espA espC red todK* quadruple mutant compared to the wild type. 16 ml cell culture (2 X 10^7 cells ml^{-1}) of wild-type (DZ2) and *espA espC red todK* (PH1054) mutants were induced to develop under submerged culture and incubated at 32 °C. Pictures were recorded at the indicated times. Scale bar, 1 mm. (B) Primers specific for *fruA* (B), *dev* (C), *Mxan_3227* (D) were used for real-time PCR analysis.

2.1.10 Analysis of NR double mutants with developmental genes

To understand the effect of the NRs on the developmental pathway, we generated double mutants between NRs and certain major developmental regulator genes (*asgA*, *fruA*, *csgA* and *frzCD*). It has been previously shown that in the *espA* mutant, C-signalling can be partially bypassed (Higgs et al., 2008), but that the *todK* mutant cannot bypass C-signaling (Rasmussen & Sogaard-Andersen, 2003).

Mutations in the *asgA* gene can not produce A-signal and the mutants do not develop. Double mutants with *asgA* in all kinase mutant backgrounds displayed same phenotype with the *asgA* mutant suggesting that A-signaling cannot be bypassed in these mutants (Figure 2. 11). Moreover, double mutants with *fruA* also displayed same phenotype as the *fruA* single mutant indicating that these NR mutants cannot bypass the requirement for *fruA* (Figure 2. 11). However, interestingly, *espA csgA* and *espC csgA* double mutants were able to aggregate and sporulate showing almost same level of sporulation efficiency with wild-type (Higgs et al., 2008) (Figure 2. 11). This result indicates that in the *espA* and *espC* mutants, C-signalling can be bypassed. The *red csgA* double mutant was able to aggregate and sporulate in a reduced level compared to *espA csgA* and *espC csgA* mutants indicating that C-signalling can be partially bypassed in the *red* mutant (Figure 2. 11). The *todK csgA* double mutant does not develop which corresponds to what was previously suggested in the alternative wild-type strain, DK1622 (Rasmussen & Sogaard-Andersen, 2003) (Figure 2. 11). Finally, double mutants between *frzCD* and each of the NR mutants displayed a mixed phenotype: cells formed frizzy filaments instead of fruiting bodies, but produced spores in a higher level than the *frzCD* single mutant (Figure 2. 11). This result is consistent with a branched pathway, where the sporulation branch is induced even in the absence of a fully functioning aggregation branch. Taken together, these results are consistent with three distinct mechanisms for control of developmental progression. EspA/EspC can bypass C-signal, Red can partially bypass C-signal, but TodK cannot.

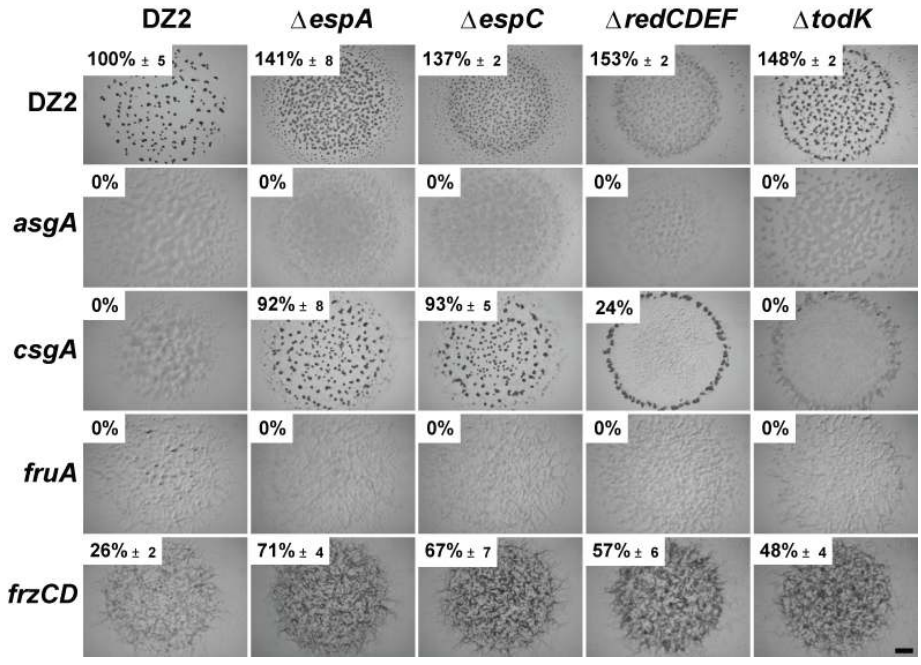

Figure 2.11 The developmental phenotype of key developmental genes in the wild-type, *espA*, *espC*, *red* and *todK* mutant backgrounds. Cells were induced to develop for 72 h on starvation media (CF) plates. Pictures were recorded at the indicated time points. Spore efficiency was determined as number of heat and sonication resistant spores as a percent of wild-type spores at 72 h. Scale bar, 1.0 mm.

2.2 Expression analysis of developmental marker proteins in the NR mutants

To further understand how these kinase mutants modulate the developmental pathway at a molecular level, the accumulation patterns of key developmental marker proteins were examined in NR mutants.

2.2.1 *red* and *todK* mutants behave differently in submerged culture

In order to prepare protein samples for immunoblot analysis, wild-type, *espA*, *espC*, *red* and *todK* mutants were induced for development in submerged starvation cultures, since it allows quick and quantitative recovery of cells. In this analysis, we also examined phenotype and sporulation efficiency of each mutant under these condtions.

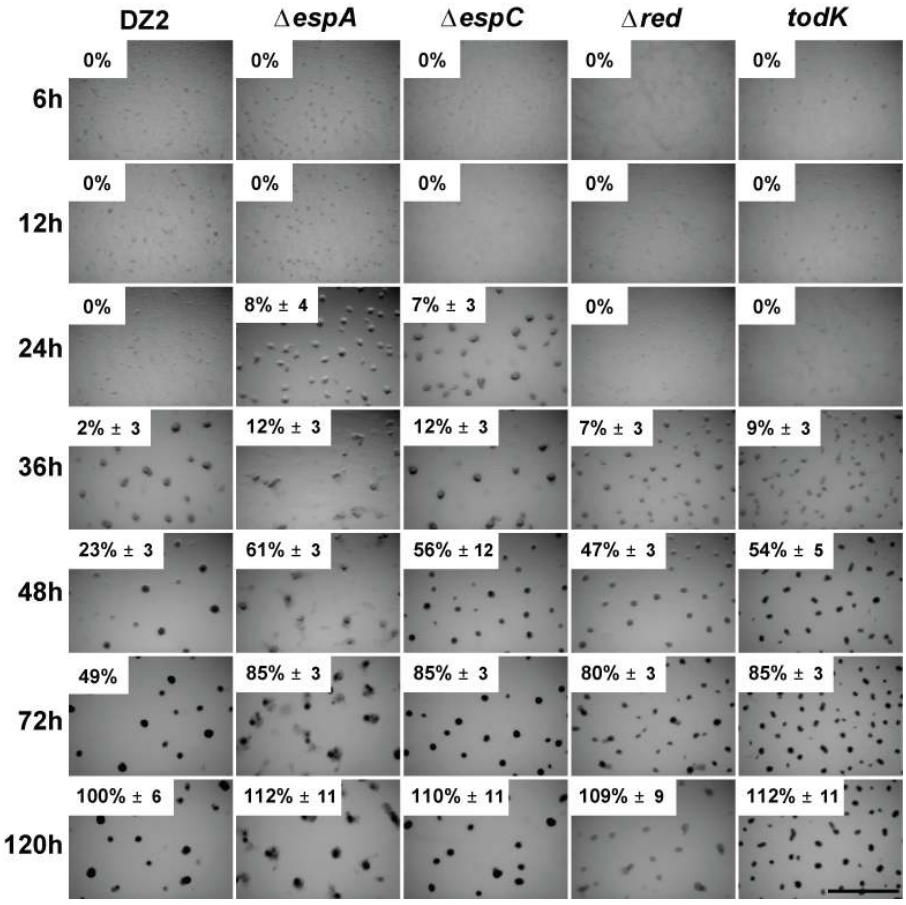

Figure 2.12 The developmental phenotype of NR mutants. 16 ml cell cultures (2 X 10^7 cells ml^{-1}) of wild-type (DZ2) and *espA* (DZ4227), *espC* (PH1044), *red* (DZ4659) and *todK* (PH1045) mutants were induced to develop under submerged culture and incubated at 32 °C. Pictures were recorded at the indicated time. Spore efficiency was determined as number of heat and sonication resistant spores as a percent of wild-type spores at 120 h Scale bar, 1 mm.

Our phenotypic analysis under submerged culture demonstrated that the wild-type strain started aggregation and sporulation between 24 h and 36 h which is slightly faster than during starvation on agar plates. *espA* and *espC* mutants developed earlier than wild-type between 12 h and 24 h. Interestingly however, *red* and *todK* mutants showed an abnormal phenotype compared with the phenotype on starvation agar plates. Both *red* and *todK* mutants still sporulated faster than wild-type, but the timing of aggregation is similar to wild-type. Moreover, development of *red* and *todK* mutants is later than *espA* and *espC* mutants contrary to the phenotype on starvation plates. The *todK* mutant produced spores slightly earlier than the *red* mutant (Figure 2. 12). It is not clear why *red* and *todK* behave differently in submerged culture, but it likely correlates with the different nutrient levels between starvation plates and submerged culture.

2.2.2 EspA and EspC likely act together in the repression of MrpC

In this analysis, we first focused on the expression pattern of developmental marker proteins in *espA* and *espC* mutants, since we preciously demonstrated that EspA and EspC are likely lie in the same signaling pathway. Cells were harvested, resuspended in an equivalent volume of protein sample buffer and subjected to immunoblot analysis. As a control for equal loading of protein samples, we tested the accumulation of PilC protein, a component of the type IV pilus that is not expected to be developmentally regulated (Wu *et al.*, 1997). Our analysis showed that PilC protein was constantly expressed in wild-type and all mutants between 0 h and 24 h (Figure 2.13 A).

We next analyzed the expression pattern of MrpC, a key developmental transcriptional regulator. In the wild-type, MrpC and MrpC2 are expressed at low level from 0 h to 18 h, up-regulated between 18 h and 24 h, and the levels decrease between 24 h and 30 h. The *espA* mutant induces accumulation of MrpC between 0 h and 3 h (Figure 2. 13B). Early accumulation of *espA* mutants was previously observed (Higgs et al., 2008). In a similar manner, the *espC* mutant induces earlier accumulation of MrpC between 0 h and 6 h. We similary examined the expression pattern of FruA. FruA protein is up-regulated in the wild-type between 12 and 18 h. However, *espA* and *espC* mutants induce accumulation of FruA between 3 h and 6 h (Figure 2. 13C). Upregulation of full length CsgA protein (p25) was observed from early onset of starvation in the wild-type and the timing of CsgA accumulation is similar in wild-type, *espA* and *espC* mutants from 0 to 24 h (Fig. 2. 13D). We were unable to detect p17 (C-signal) which is proposed to be necessary for FruA activation in these assays. Current models suggest that activated FruA stimulates methylation of the FrzCD chemosensory protein (Sogaard-Andersen & Kaiser, 1996). We therefore, examined the methylation patterns of FrzCD. In wild type, both

unmethylated and methylated forms were detected and the unmethylated from is lost between 24 h and 30 h. In the *espA* mutant, FrzCD is fully methylated between 18 h and 24 h which correlates with earlier aggregation in the *espA* mutant (Figure 2. 13E). Interestingly, there are differences in the methylation patterns between *espA* and *espC* mutant, despite the similar aggregation phenotypes (see Figure 2. 12). In the *espC* mutant, the FrzCD methylation pattern is slightly faster than wild-type, but later than *espA* mutant (Figure 2.13 E). In this analysis, we also observed that there are significant differences in marker expression patterns at 30 h between the *espA* and *espC* mutants. Interestingly, while *espA* and *espC* mutants produce similar levels of heat and sonication resistant spores during development, *espC* mutant spores do not germinate as efficiently (data not shown) suggesting that EspC may paly an additional role independent of EspA in spore maturation.

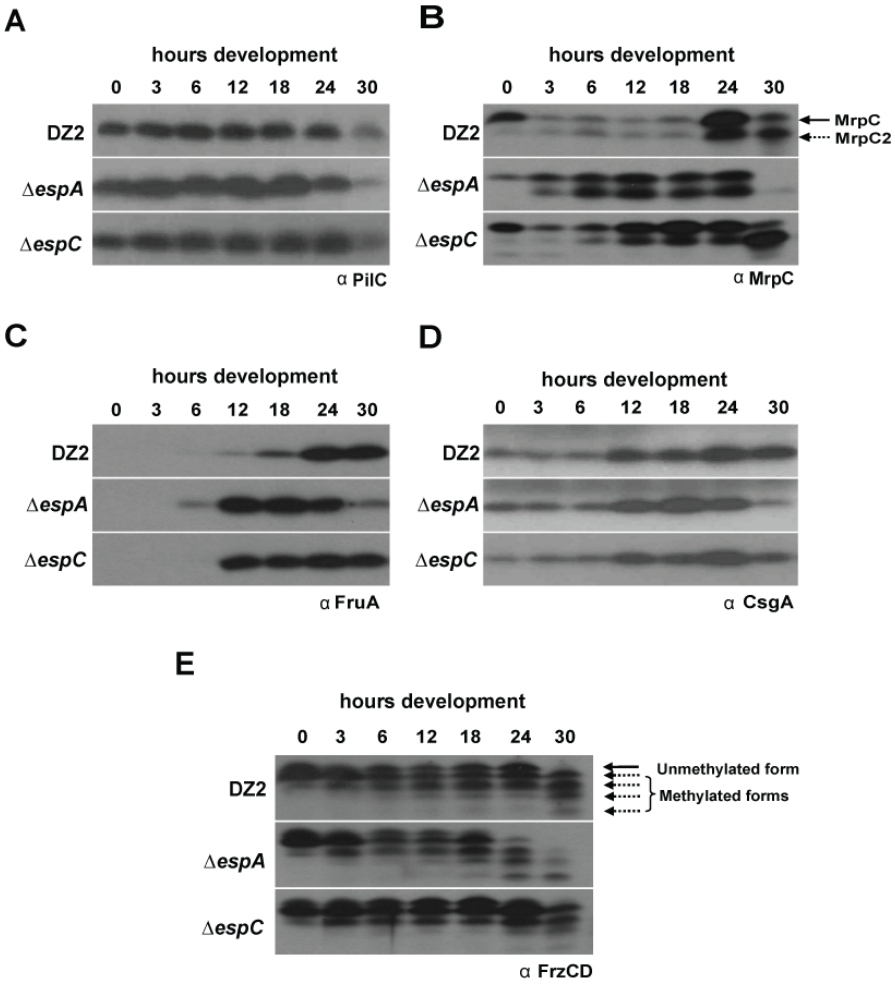

Figure 2.13 Immunoblot analysis of developmental marker protein expression in the wild type, *espA* and *espC* mutants. Cells were grown in submerged culture and harvested at the indicated time points. Samples containing equal proportions of each cell culture was subject to immunoblot analysis and probed with anti-PilA (A), anti-MrpC (B), anti-FruA (C), anti-CsgA (D), or anti-FrzCD (E) polyclonal antisera. (B) Black arrows, MrpC; dotted arrows, MrpC2. (C) CsgA p25. (E) Black arrows, FrzCD unmethylated form; dotted arrows, FrzCD methylated forms.

2.2.3 *red* and *todK* mutants do not appear to induce early accumulation of developmental marker proteins

We took a similar approach to analyze the expression patterns of developmental marker proteins in *red* and *todK* mutants. PilC protein was constantly expressed in wild-type, *red* and *todK* mutants from 0 h to 24 h suggesting that these protein samples were equally loaded. However, unlike in the wild-type and *red* mutant, the expression level of PilC in the *todK* mutants was detected at 30 h (Figure 2. 14A).

Suprisingly, in the *red* mutants, MrpC and FruA accumulated with similar timing, but at lower levels than in the wild-type (Figure 2. 14B and C), while CsgA and FrzCD methylation patterns were only slightly perturbed (Figure 2. 14D and E). These expression patterns suggest an uncoupling of the ordered developmental program. In *todK* mutants, MrpC/MrpC2 were produced approximately 6 h earlier than wild-type, the ratio MrpC to MrpC2 was perturbed, and at 30 h, there was a dramatic accumulation of MrpC/MrpC2 (Figure 2. 14B). FruA and CagA were not significantly perturbed in this mutant (Figure 2. 14C and D), but FrzCD was still detected in the unmethylated form at 30 h (Figure 2. 14E). In summary, MrpC, FruA and FrzCD marker proteins are uncoupled. Taken together, these results confirmed that Red and TodK proteins do not function in one signaling pathway. We hyphothesize that the proportions of the vaious developmental subpopulations is likely perturbed in these mutants.

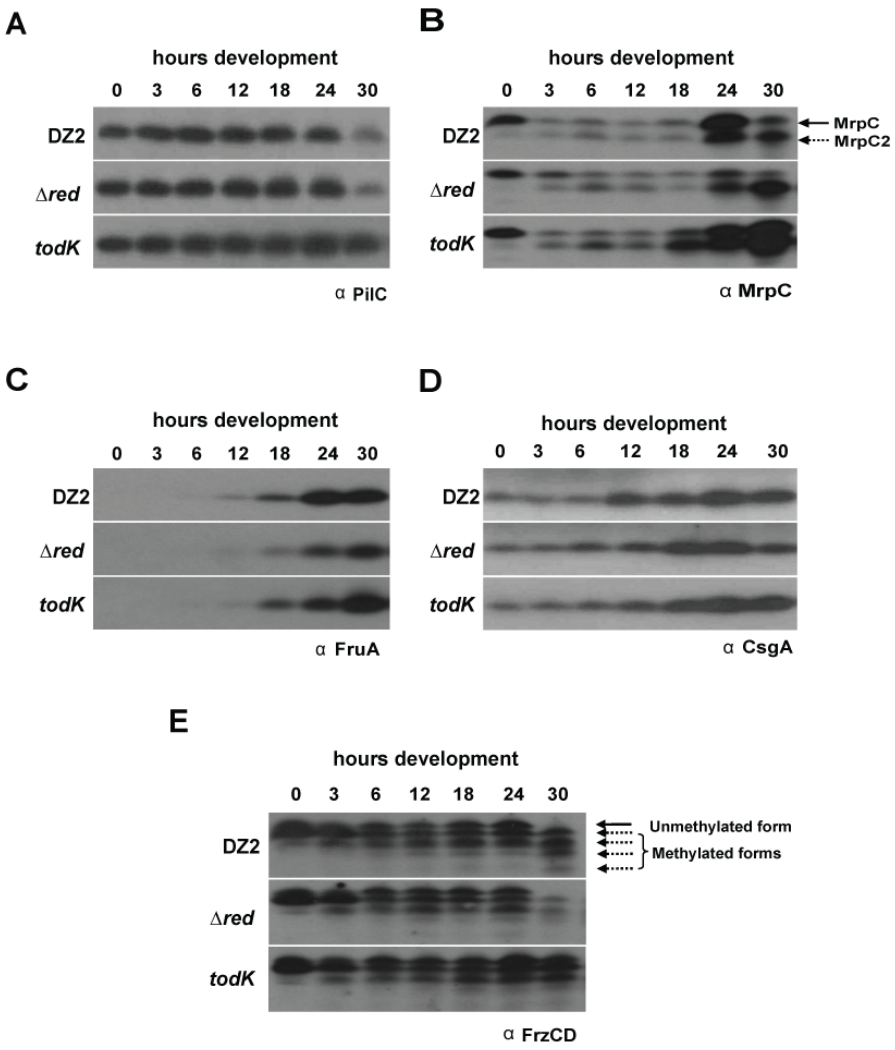

Figure 2.14 Immunoblot analysis of developmental marker protein expression in the wild type, *red* and *todK* mutants. Cells were grown in submerged culture and harvested at the indicated time points. Samples containing equal proportions of cell culture were subject to immunoblot analysis and probed with anti-PilA (A), anti-MrpC (B), anti-FruA (C), anti-CsgA (D), or anti-FrzCD (E) polyclonal antisera. (B) Black arrows, MrpC; dotted arrows, MrpC2. (C) CsgA p25. (E) Black arrows, FrzCD unmethylated form; dotted arrows, FrzCD methylated forms.

2.3 Cell population analysis in the wild-type

Our analysis of developmental maker proteins revealed that *espA* and *espC* mutants induce earlier and coordinated accumulation of MrpC and FruA which can explain the early aggregation and sporulation phenotype. However, although *red* and *todK* mutants aggregate only slightly but sporulate significantly earlier than wild type, they do not appear to induce coordinated accumulation of developmental marker proteins (see Figure 2. 12 and Figure 2. 14). One possible interpretation is that the proportion of the various developmental subpopulations (PCD, sporulation, peripheral rods) is perturbed in *red* and

todK mutant. Moreover, we have shown that peripheral rods are sporulating inappropriately in the NR mutants and that the control mechanisms for peripheral rods are disturbed (see Figure 2. 9). We therefore decided to rigously define the proportions of the different subpopulations during development in the wild-type. We also examined the accumulation of developmental marker proteins in the non-aggregating and aggregating cell populations during developmental program.

2.3.1 Analysis of the total cell number in the developmental subpopulations

To determine the total number of cells and the mumber of cells in each developmental subpopulation, we adapted the peripheral rod/fruiting body separation assay used in section 2.1.8 (O'Connor & Zusman, 1991c). Briefely, low speed centrifugation was used to separate the aggregating cell (pellet) from non-aggregating cell (supernatant) fractions at several times during the developmental program. The number of cells in each fraction was then counted.

The wild-type began to aggregate between 24 h and 30 h (Figure 2. 15A), but did not produce mature spores until 48 h (data not shown). Our cell population analysis revealed that the total cell population of wild-type began to increase after onset of starvation, peaked at 24 h and decreased from 24 h (Figure 2. 15B). The total cell number progressively decreased until 5 days of development such that approximately 80 % cells underwent programmed cell death (data not shown) corresponding to previous research (Wireman & Dworkin, 1977). In a similar manner, the number of non-aggregating cells increased until 24h and then decreased, while the number of aggregating cells increased until 30 h and the decreased. The proportion of non-aggregating and aggregating cell fractions during development is displayed in Figure 2. 15C. Visible fruiting body correlates with approximately 50 % of the cells in each fraction.

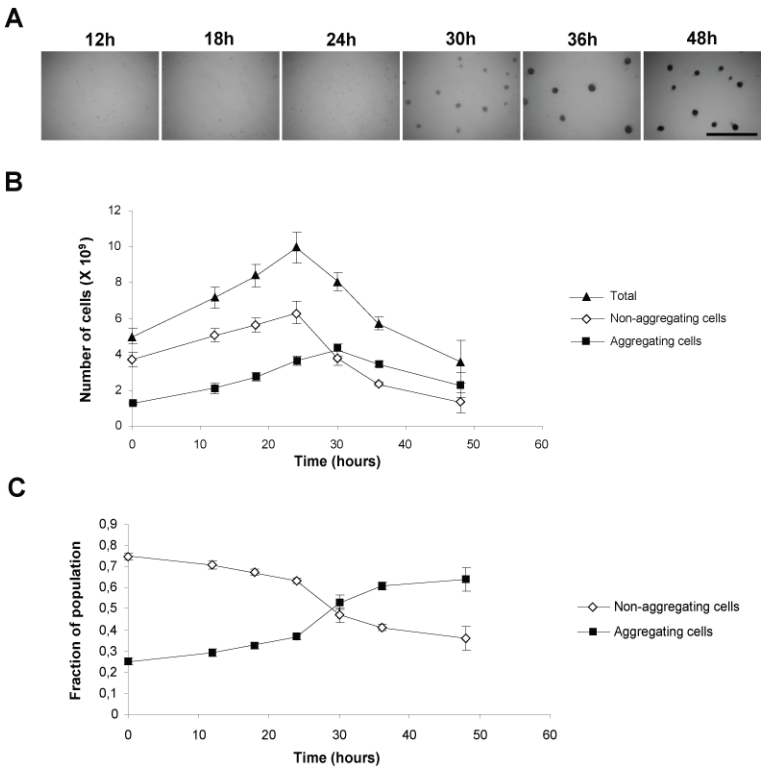

Figure 2.15 Analysis of the developmental subpopulations in wild-type. (A) The developmental phenotype of the wild-type. 16 ml cell culture (2 X 10^7 cells ml^{-1}) of wild-type were induced to develop under submerged culture and incubated at 32 °C. Pictures were recorded at the indicated times. Scale bar, 1 mm. (B) The number of total cells and cells in the supernatant (non-aggregating) and pellet (aggregating) fractions. (C) The proportion of total cells in the non-aggregating and aggregating fractions during development. The average numbers from triplicate independent biological repleicates.

2.3.2 Cells undergo a burst of cell death during development

Our cell population assay in wild-type DZ2 revealed that the total cell number decreased after 24 h suggesting that cells seem to undergo programmed cell death (PCD) around 24 h. To detect cell death during development, the LIVE/DEAD staining technique was applied. Cells for LIVE/DEAD staining were prepared from the same culture from which we performed the cell population assay (Figure 2. 16A upper panel). Our LIVE/DEAD staining analysis revealed that at 24 h of development, 56 % of wild-type DZ2 cells were stained as red (dead cells) (Figure 2. 16A lower panel). This result suggests that big burst of cell death at 24 h leads to a decrease cell population at approximately 24 h in the wild-type (Figure 2. 16B and C). Approximately 15-20 % of the cells are stained red (dead) from 30 h to 48 h. The percent of dead cells was similar in the non-aggregating and aggregating populations during development (data not shown).

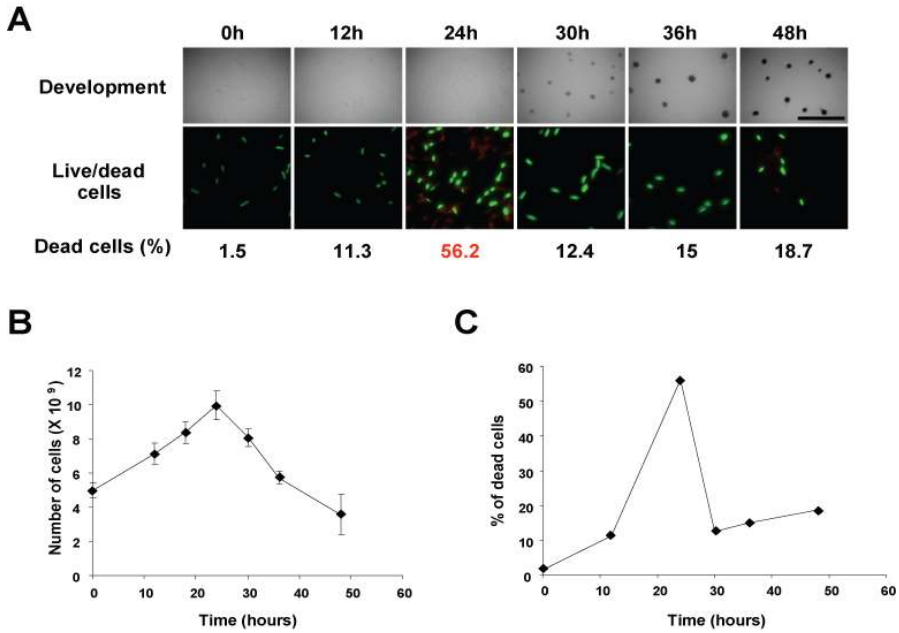

Figure 2.16 LIVE/DEAD staining during development in the wild-type. (A) Developmental phenotype and LIVE/DEAD staining of wild-type. Cells for LIVE/DEAD staining were harvested from submerged culture. Dead cells were displayed as percentage of the total cells counted (n > 100). (B) Total cells counted in the wild-type. (C) Percentage of dead cells during development. Total cells at the indicated time points in (A upper panel) were subjected to LIVE/DEAD staining.

2.3.3 Exopolysaccharide is up-regulated in the aggregating cell fraction

To determine whether the non-aggregating and aggregating cell fractions were distinct, we first analyzed the amount of EPS in each cell fraction using a dye binding assay modified from (Black & Yang, 2004, Black *et al.*, 2006). Our EPS analysis revealed that aggregating cells produce progressively more EPS from 24 h of development, while non-aggregating cells do not upregulate EPS. This result suggests that EPS is regulated in only the aggregating cell population (Figure 2. 17B).

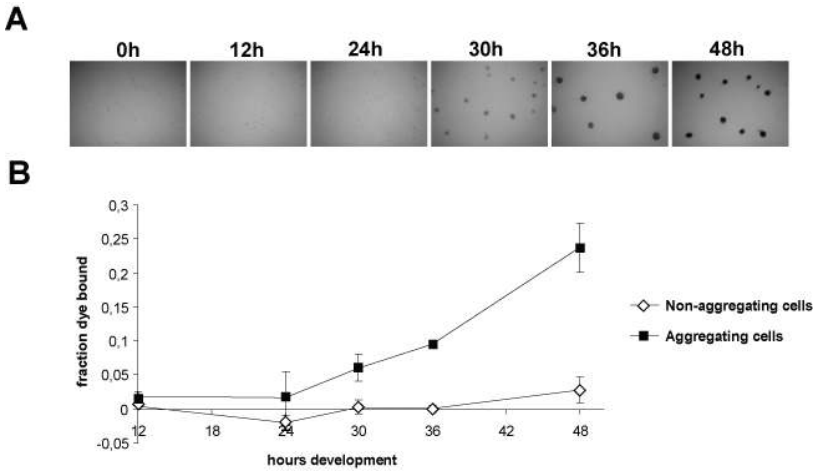

Figure 2.17 Exopolysaccharide assay. (A) Developmental phenotype of cells used for the EPS assay. (B) Relative production of EPS in non-aggregating and aggregating cells at the indicated time points in (A).

2.3.4 Spore coat proteins are regulated in the aggregating cell fraction

It has previously been demonstrated that Protein S is detected at different levels in the non-aggregating and aggregating cell fractions (O'Connor & Zusman, 1991c). Protein S is a spore coat protein that is expressed early during the developmental program (Inouye *et al.*, 1979). Our immunoblot analysis revealed that Protein S is present in both non-aggregating cells and aggregating cells at same level until 24 hours which is the onset of aggregation. However, Protein S was up-regulated in aggregating cells after 24 h, but not in non-aggregating cells (Figure 2. 18A). This result is consistent with accumulation of spore coat protein in the cell population which diferentiates into spores.

Similarly, the expression pattern of Protein C was analyzed in both cell types. It has been proposed that Protein C is a useful marker for development because it is developmentally regulated and spore associated (McCleary et al., 1991). It also has been shown that although Protein C is expressed in cell type specific pattern, it is expressed in all developmental cell types including non-aggregating cells and aggregating cells and spores

from early onset of development (O'Connor & Zusman, 1991c). However, our analysis revealed that Protein C was exclusive to aggregating cells (except for the 48 h time point) and was up-regulated after 30 h when the cells begin to sporulate (Figure 2. 18B). The expression of Protein C exclusively within aggregating cells even at T=0 suggests that certain cells are predestined to be in aggregation centers.

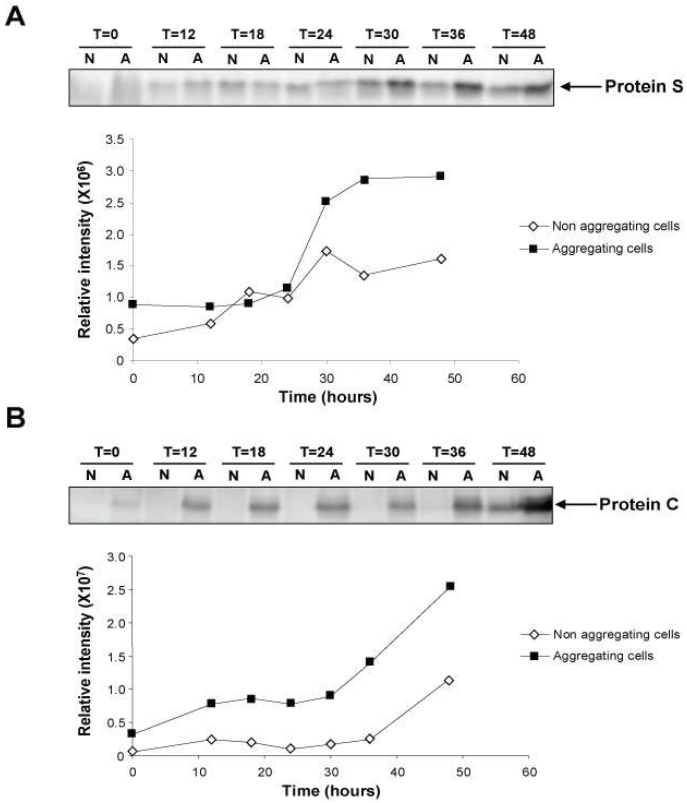

Figure 2.18 Protein S and Protein C expression in non-aggregating and aggregating cell fractions. Cells were grown in submerged culture and harvested at the indicated time points. Protein samples containing equal amount of cells (4.3 X 10^6 cells/μl) were subjected to immunoblot analysis and probed with anti-Protein S (A) or anti-Protein C (B). Upper panels: immunoblots. Lower panels: relative intensity of bands in (A).

2.3.5 Type IV pili subunit proteins, PilA and PilC are differently accumulated in the non-aggregating and aggregating cell fractions

In search of proteins which would be represented equally in both cell types, we next examined the expression pattern of subunit proteins of Type IV pili which are essential for social(S)-motility (Wu & Kaiser, 1995, Wu et al., 1997). PilA is the subunit pilin and PilC is an inner membrane pili biosysthesis protein (Wu & Kaiser, 1997) (Figure 1. 2D). Our analysis revealed that although PilA protein was constantly expressed at low level in non-aggregating cells, it specifically increased in aggregating cells from 0 h to 48 h

of development (Figure 2. 19A). In contrast, the PilC protein level decreased in both cell types. Interestingly, from 0 h to 18 h, PilC protein levels decreased more rapidly in non-aggregating cells than in aggregating cells (Figure 2. 19B). Thus, PilC was constantly more abundant in the non-aggregating cell fraction, while PilA was more abundant in the aggregating fraction.

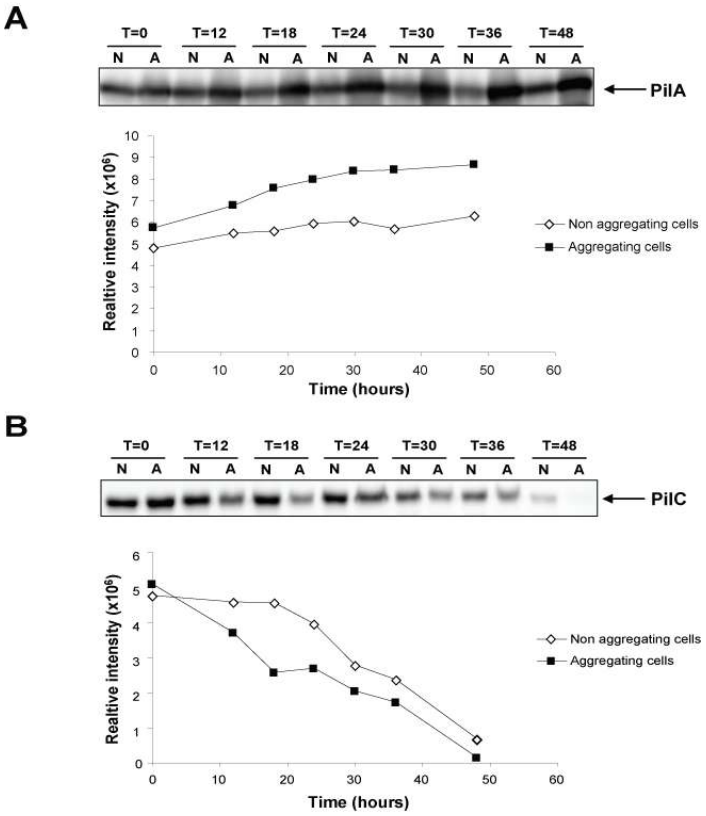

Figure 2.19 PilA and PilC expression in non-aggregating and aggregating cell fractions. Cells were grown in submerged culture and harvested at the indicated time points. Protein samples containing an equal number of cells (4.3 X 10^6 cells/µl) were subjected to immunoblot analysis and probed with anti-PilA (A) and anti-PilC (B) antibodies. Upper panels show the resulting immunoblot. Lower panels show the relative intensity of the bands in (A) .

2.3.6 Key developmetal regulators accumulate to different levels in the non-aggregating and aggregating cell fractions

With the exception of CsgA p25 (Julien et al., 2000), the cell type specific expression of proteins necessary for positively regulating the developmetal program has not been investigated. To investigate if these proteins are influenced by the NRs in a cell specific manner during development, we first analyzed the accumulation patterns of key developmental markers in the wild-type. This analysis revealed that MrpC was present in

equivalent levels in the two cell populations at 0 h of development. However, by 12 h of development, MrpC had decreased in aggregating cells and remained at low levels until between 24 and 30 h. In contrast, in the non-aggregating cell fraction, after the first decrease, MrpC accumulated specifically in these cells until between 24 and 30 h. Between 30 and 48 h, MrpC levels then began to decrese in the non-aggregating cell fraction (Figure 2. 20A and B). We also examined the accumulation of MrpC2 and observed the same general pattern of MrpC2 production. MrpC2 levels increased first in non-aggregating cell fraction up to 24 h and then decreased, while in aggregating cell fraction, MrpC2 accumulated between 24 and 36 h. Interestingly, MrpC2 was cleared from aggregating cells at 48 h (Figure 2. 20 A and C) .

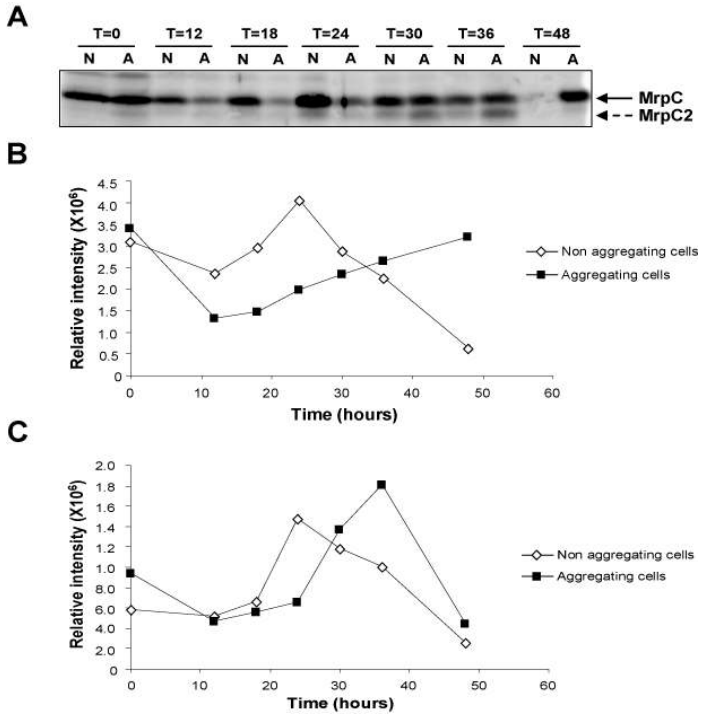

Figure 2.20 MrpC and MrpC2 accumulation in non-aggregating and aggregating cell fractions. Cells were grown in submerged culture and harvested at the indicated time points. Protein samples containing an equal number of cells (4.3 X 10^6 cells/μl) were subjected to immunoblot analysis with anti-MrpC antibody (A) Black arrows, MrpC; dotted arrows, MrpC2. B) Relative intensity of the MrpC bands (C) Relative intensity of the MrpC2 bands.

We next examnined the production of FruA, whose expression is a target of MrpC2. In this analysis, we observed that FruA protein levels increased in both cell types with higher levels in non-aggregating cells until 30 h. However, later during development, FruA protein levels continue to accumulate in the aggregating cell fraction until 48 h of development (Figure 2. 21 A and B). This result corresponds to the timing of aggregation in wild-type and accumulation pattern of the MrpC protein.

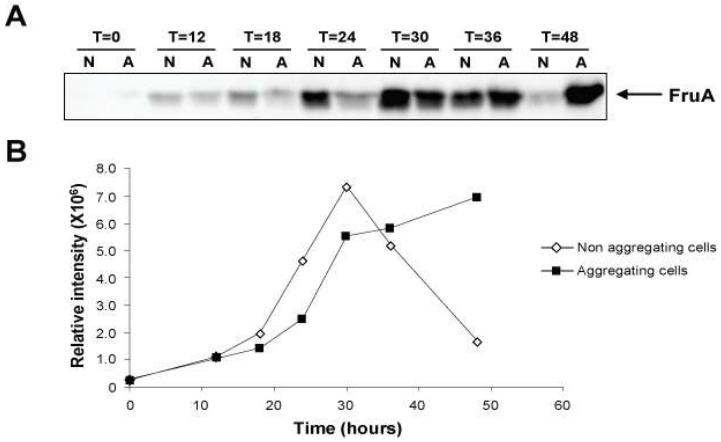

Figure 2.21 FruA expression in non-aggregating and aggregating cell fractions. Cells were grown in submerged culture and harvested at the indicated time points. Protein samples containing equal numbers of cells (4.3 X 10^6 cells/µl) were subjected to immunoblot analysis with anti-FruA antibody (A). (B) Relative intensity of the FruA bands.

Our immunoblot analysis of CsgA p25 revealed that in a similar manner to MrpC and FruA accumulation, CsgA p25 protein first accumulated at higher level in non-aggregating fraction and after 30 h began to accumulate in the aggregating cell fraction (Figure 2. 22A and B). In contrast, CsgA p17 (C-signal) levels increased at an essentially linear rate in the aggregating fraction from 0 h to 48 h. In the non-aggregating fraction CsgA p17 accumulated until 12 h and then decreased (Figure 2. 22 A and C). This result is consistent with current model that C-signal is amplified by increased cell to cell contact within aggregating cells.

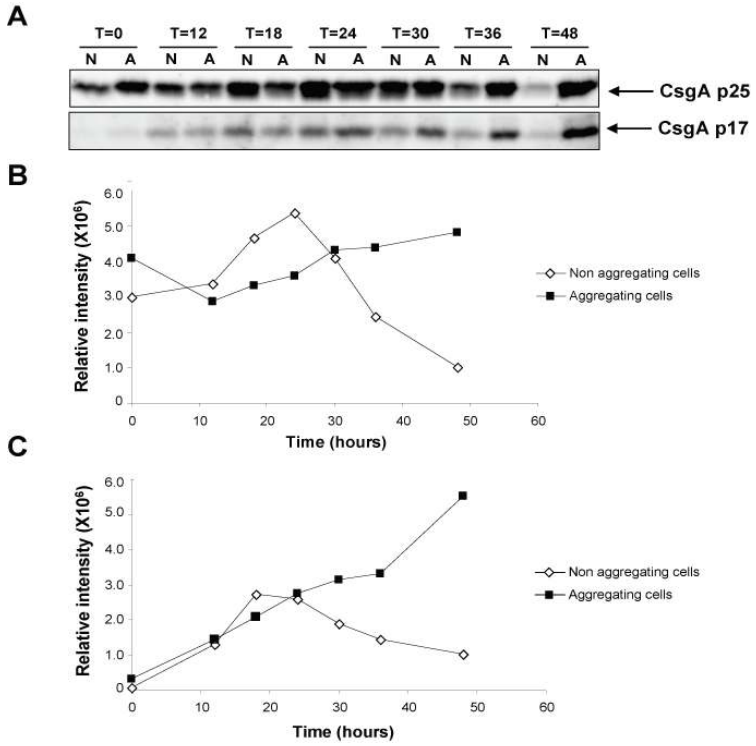

Figure 2.22 CsgA expression in non-aggregating and aggregating cell fractions. Cells were grown in submerged culture and harvested at the indicated time points. Protein samples containing an equal number of cells (4.3 X 10^6 cells/µl) were subjected to immunoblot analysis with anti-CsgA antibody (A). (B) Relative intensity of the CsgA p25 bands. (C) Relative intensity of the CsgA p17 bands.

We next examined the levels and methylation pattern of the FrzCD protein in each fraction. Our analysis revealed that in both cell types, FrzCD levels were dramatically reduced between 12 h and 36 h, and were absent by 48 h. Methylated forms of FrzCD, which migrate more quickly in denaturing electrophoresis, are detected in several lower bands. Increased FrzCD methylation was observed all aggregating cell fractions. Unmethylated FrzCD (highest band) was absent from both fraction after 24 h of development (Figure 2. 23). It should be noted that in this analysis, we could not display relative intensity because there are many bands.

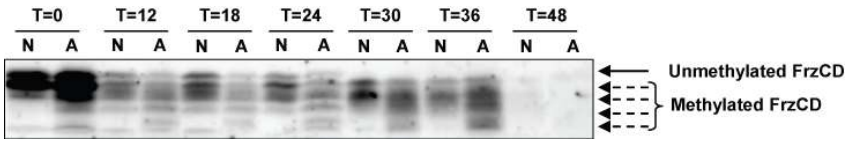

Figure 2.23 FrzCD expression in non-aggregating and aggregating cell fractions. Cells were grown in submerged culture and harvested at the indicated time points. Protein samples containing equal number of cells (4.3 X 10^6 cells/µl) were subjected to immunoblot analysis and probed with anti-FrzCD. Black arrows, FrzCD unmethylated form; dotted arrows, FrzCD methylated forms.

2.4 Analysis of developmental subpopulations in the *red* and *todK* mutants

To determine whether the NR mutants (*red* and *todK*) perturbed the developmental program by alteration of cell type-sepcific accumulation of developmental regulatory proteins, we next analyzed the non-aggregating and aggregating fractions in the *red* and *todK* mutants compared to wild-type.

2.4.1 *red* and *todK* mutants fail to increase cell population during development

To examine the number of cells in total, non-aggregating and aggregating fractions and to prepare protein sample for analysis of developmental marker proteins in the *red* and *todK* mutants versus wild-type, we first induced development in submerged culture and performed a phenotype and sporulation assay. Our analysis showed that while the timing of aggregation in both mutants was only slightly earlier than wild-type, the sporulation rate was much faster than in wild-type (Figure 2. 24).

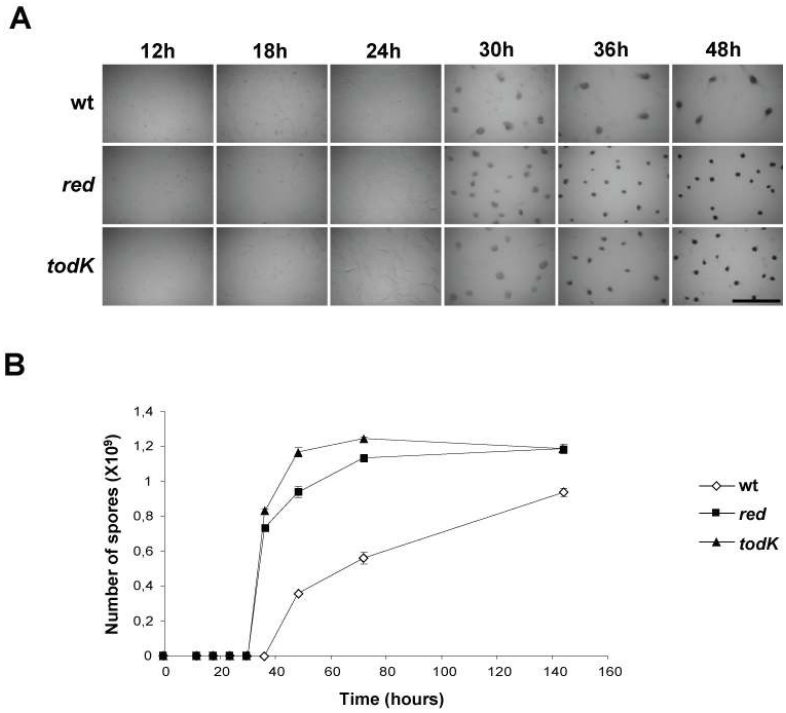

Figure 2.24 The developmental phenotype of *red* and *todK* mutants induced in submerged culture. (A) 16ml cell culture (2 X 10^7 cells ml^{-1}) were induced to develop under submerged culture and incubated at 32°C. Pictures were recorded at the indicated times. Scale bar, 1 mm. (B) Sporulation assay during development. Heat and sonication spores were counted at the indicated time points by a hemacytometer.

Interestingly, our analysis of total cells at several developmental time points demonstrated that while the total cell population of wild-type doubled by 24 h, and then decreased, in both mutants the total cell population increased only 1.2-fold after 18 h (Figure 2. 25A). In the wild-type, the non-aggregating cell fraction increased by 1.8-fold over the first 24 h and then decreased. In both mutants, this fraction remained constant for the first 18 h and then decreased (Figure 2. 25B). Finally, the wild-type aggregating cell fraction more than doubled over 30 h and then decreased, while in both mutants, the aggregating fraction barely doubled over 30 h and then slightly decreased (Figure 2. 25B). Interestingly, the time point at which 50 % of the cells were in each fraction was approximately 2-3 h earlier in both mutants than in wild-type.

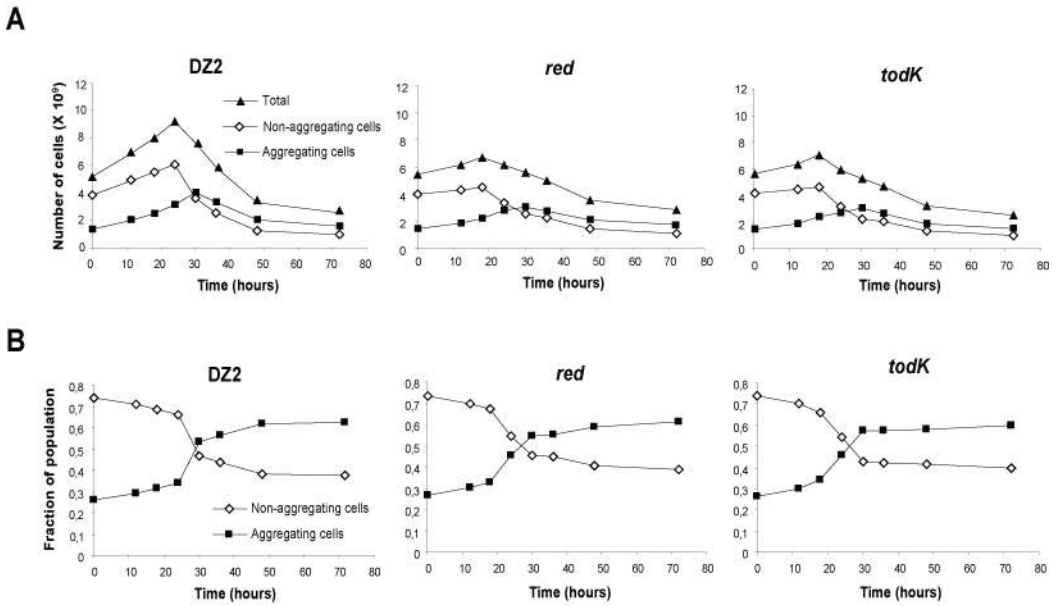

Figure 2.25 Analysis of the number of total cells and the number of cells in the non-aggregating and aggregating cell fractions of wild-type, *red* and *todK* mutants. (A) Number of cells in the total and the subpopulations. Cells were harvested at the indicated time points and counted by hemacytometer. (B) The proportion of the total cells in non-aggregating cells and aggregating cell fractions.

2.4.2 *red* and *todK* mutants seem to undergo a burst of cell death earlier than wild-type

Our analysis of the total cell number during development revealed that both *red* and *todK* mutants failed to increase significantly. To determine whether these mutants lyse prematurely during development, we used the LIVE/DEAD stain technique on *red* and *todK* mutants compared to wild-type. Our analysis revealed that 45 % of *red* and 34 % of *todK* cells stained dead at 24 h, while 32 % of wild-type cells were dead at 27 h suggesting that *red* and *todK* mutants undergo the burst of lysis earlier than wild-type

(Figure 2. 26A). This result suggested that premature PCD could be reason for the failure to increase cell number in both mutants (see Figure 2. 26B and C).

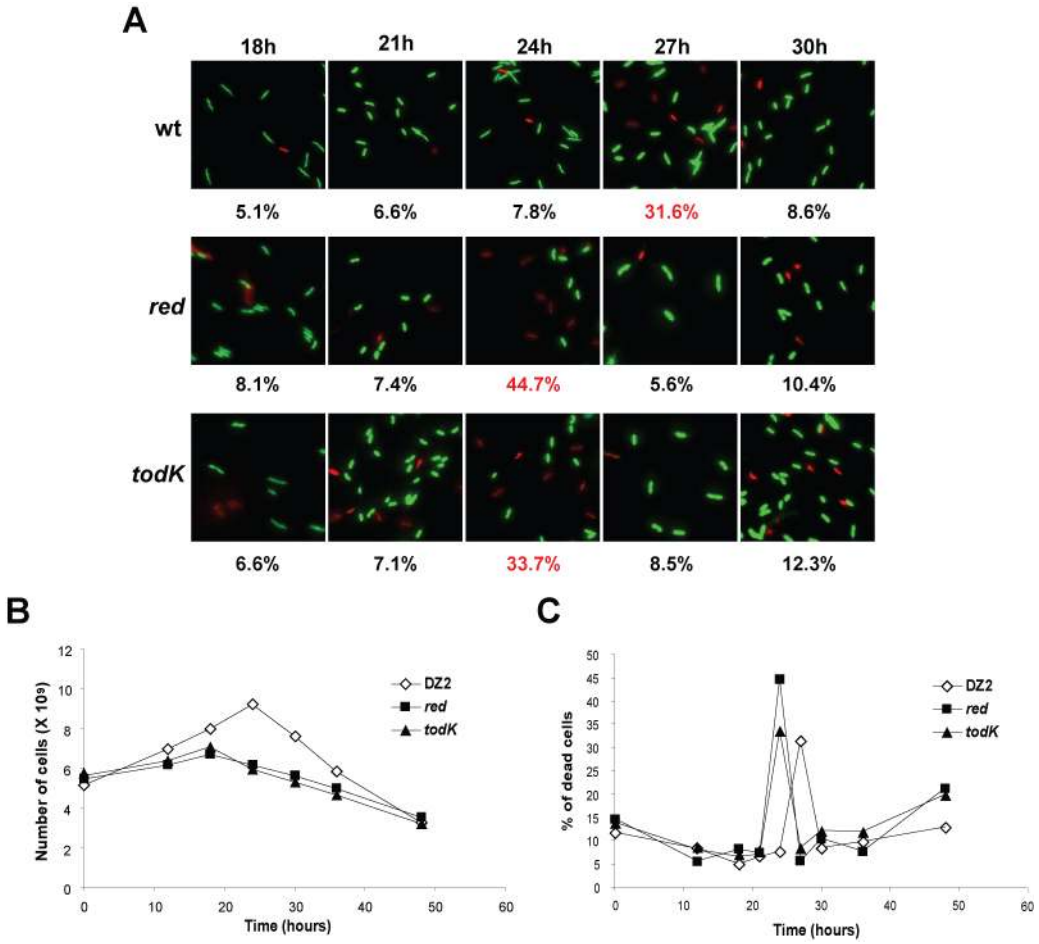

Figure 2.26 LIVE/DEAD staining analysis during development. (A) Fluorescent microscopy images of wild-type (DZ2), *red* (DZ4659) and *todK* (PH1045) mutants at the indicated time points. Cells were harvested from submerged culture, stained and observed by fluorescence microscopy. Red (dead) and green (living) cells were counted (n > 100) and the percent of dead cells is displayed below each image. (B) Total cells of wild-type, *red* and *todK* mutants. (C) Percentage of dead cells during development displayed as a fraction of time.

2.4.3 The accumulation of MrpC and MrpC2 is perturbed in the *red* and *todK* mutants

Our initial analyses demonstrated that *red* and *todK* mutants uncoupled the ordered accumulation of developmental marker proteins that driving the developmental program (see Figure 2. 14). However, since we observed that *red* and *todK* mutants have less total cells than wild-type, it is clear that when we analyzed our protein patterns using equal proportions of the cell culture, the mutants likely contained fewer cells than the

wild-type. To more accurately test the marker patterns, we instead analyzed protein accumulation patterns in equivalent numbers of cells in the developmental non-aggregating and aggregating fractions. To determine the MrpC levels in the total population, we summed the measured intensities of the bands in each fraction. Summed intensities were plotted versus time of development. In the wild-type, MrpC protein accumulated in lower levels compared to *red* and *todK* mutants from 12 h and accumulation of MrpC was continuous until 48 h. Interestingly however, total MrpC was highly accumulated from 12 h to 30 h in both mutants, suddenly disappeared at 36 h and reappeared at 48 h (Figure 2. 27A and B). Moreover, our analysis also revealed that in *red* and *todK* mutants, MrpC2 was highly accumulated at 24 and 30 h compared to wild-type (Figure 2. 27A and C). These results suggest that MrpC and MrpC2, which are essential for development, are overexpressed per cell in *red* and *todK* mutants.

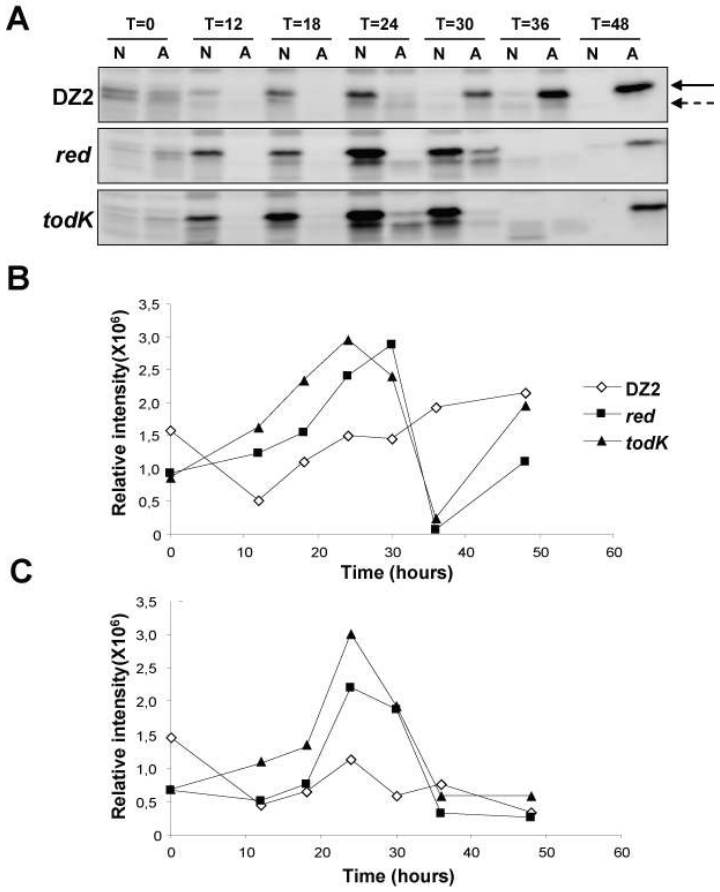

Figure 2.27 MrpC and MrpC2 expression in non-aggregating and aggregating cell fractions of wild-type, *red* and *todK* mutants. Cells were grown in submerged culture and harvested at the indicated time points. Protein samples containing equal amount of cells (4.3 X 10^6 cells/µl) were subjected to immunoblot analysis with anti-MrpC antibody (A) Black arrows, MrpC; dotted arrows, MrpC2. (B) The sum of the MrpC intensity in both cell fractions at each time point. (C) The sum of the MrpC2 intensity in both cell fractions at each time point.

We also examined the MrpC pattern in the different subpopulations. From this analysis, we observed that the proportion of MrpC in the non-aggregating and aggregating cell fractions of *red* and *todK* mutants was perturbed compared to wild-type. As we saw previously, in the wild-type, MrpC first accumulated in the non-aggregating fraction (until 24 h) and then later highly accumulated in the aggregating cell fraction (from 24 h to 48 h) indicating that accumulation pattern of MrpC is switched from non-aggregating to aggregating cell fractions during development (Figure. 2. 28A). However, in both *red* and *todK* mutants, MrpC accumulated in the non-aggregating fraction rapidily and inappropriately highly between 0 h and 30 h. After 30 h, MrpC was absent from the non-aggregating fraction. Interestingly, in the aggregating cell fraction of the *red* and *todK* mutants, MrpC accumulates sharply between 24 h and 30 h, disappeared, and then was detected at 48 h (Figure 2. 28B and C).

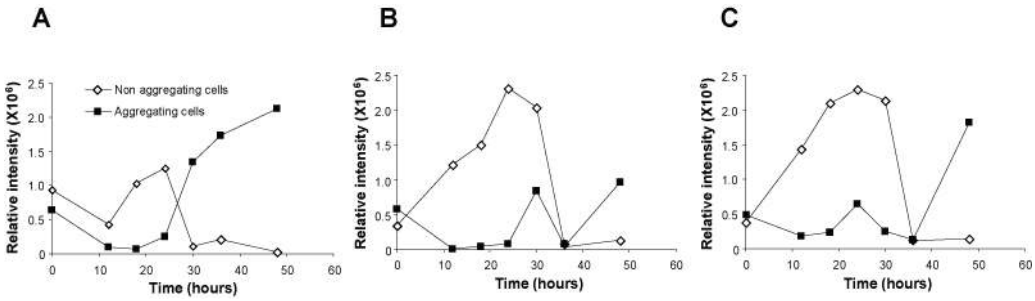

Figure 2.28 The relative intensity of MrpC in non-aggregating and aggregating cell fractions. Relative intensities were measured from immunoblot analysis. (A) wild-type. (B) *red* mutant. (C) *todK* mutant.

On the other hand, in wild-type, MrpC2 accumulated in both non-aggregating and aggregating cell fractions from 12 h and 18 h, respectively, but later MrpC2 highly accumulated in aggregating cells, indicating that accumulation pattern of MrpC2 was switched to aggregating cells later during development (Figure 2. 29A). Similarly, in both mutants, MrpC2 accumulated after the onset of starvation in both non-aggregating cells and aggregating cell fractions, but the level of MrpC2 was much higher than in the wild-type. Furthermore, the accumulation of MrpC2 did not switch to the aggregating cell population later during development. These results indicate that the proportion of MrpC2 as well as MrpC is perturbed in these mutants (Figure 2. 29B and C). The MrpC patterns in the *red* mutants essentially coupled the MrpC patterns in the *todK* mutants in both non-aggregating and aggregating fractions. One important difference is that MrpC2 expression in the aggregating feaction was observed at 24 h in the *todK* mutant, but at 30 h in the *red* mutant.

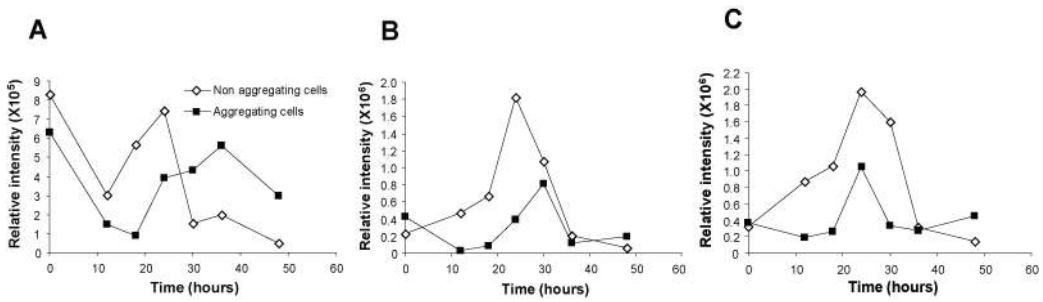

Figure 2.29 The relative intensity of MrpC2 in non-aggregating and aggregating cell fractions. Relative intensities were measured from immunoblot analysis. (A) wild-type. (B) *red* mutant. (C) *todK* mutant.

2.4.4 The accumulation of FruA is perturbed in the *red* and *todK* mutants

We next examined the expression pattern of FruA during the developmental time course in which equal number of cells were analyzed. Cell fractions were separated to analyze the accumulation of FruA in each fraction and FruA in the total population was represented as the sum of both cell types. Our analysis revealed that in the wild-type, FruA gradually accumulated between 12 h and 36 h and then decreased at 48 h. In both mutants, total FruA was rapidly accumulated to inappropriately high levels between 12 h and 36 h and then rapidly decreased between 24 h and 30 h (Figure 2. 30A and B). Thus, when compared in equal numbers of cells, FruA accumulated earlier and at higher levels than in the wild-type. For instance, at 24 h of development, *red* and *todK* mutants expressed 4 times more FruA than in the wild-type. This result corresponds to the MrpC2 accumulation patterns in *red* and *todK* mutants (see Figure 2. 27C).

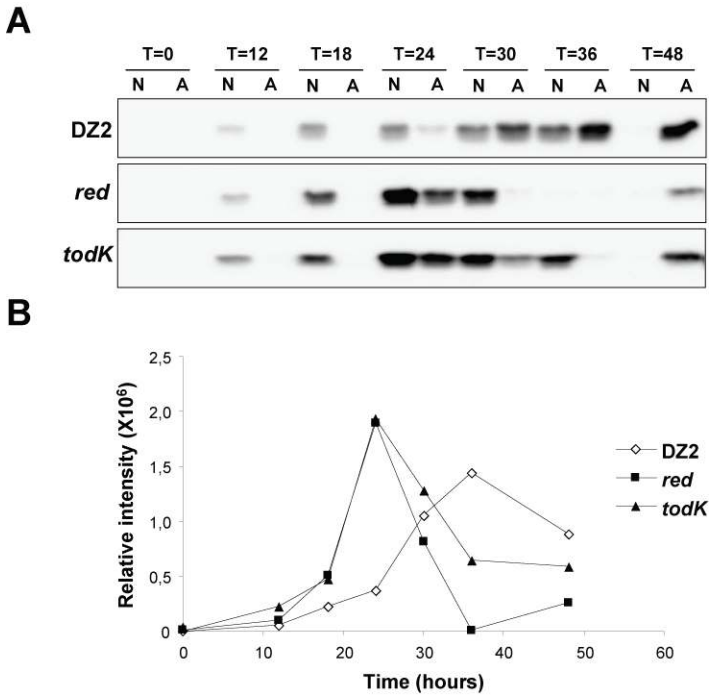

Figure 2.30 FruA accumulation in non-aggregating and aggregating cell fractions of wild-type, *red* and *todK* mutants. Cells were grown in submerged culture and harvested at the indicated time points. Protein samples containing an equal number of cells (4.3 X 10^6 cells/µl) were subjected to immunoblot analysis with anti-FruA antibody (A). (B) The sum of the FruA intensity in both cell fractions at each time point.

Moreover, the accumulation of FruA in the non-aggregating and aggregating cell fraction was perturbed in the *red* and *todK* mutants. In the wild-type, FruA gradually accumulated in the non-aggregating cell fraction fron 12 h to 36 h (Figure 2. 31A). However, in both *red* and *todK* mutants, FruA rapidly accumulated to inappropriately

high levels in the non-aggregating cell fraction from 0 h to 24 h and then began to decrease rapidly (from 24 h to 30 h) in the *red* mutant, and more slowly (from 24 h to 48 h) in the *todK* mutant. Interestingly, in the aggregating cell fraction, FruA was accumulated to a higher level in the *todK* mutant than in *red* mutant (Figure 2. 31B and C). Together, these results suggest that the rapid accumulation of MrpC/MrpC2 (and consequently FruA) in the non-aggregating cells likely causes some cells to begin to sporulate before they have transitioned into the aggregating cell fraction. Thus, fruiting bodies are disorganized and spores are formed outside of the fruiting bodies.

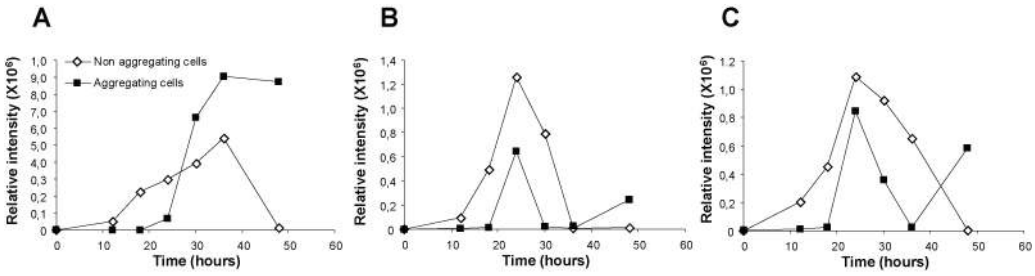

Figure 2.31 The relative intensity of FruA in non-aggregating and aggregating cell fractions. Relative intensities were measured from immunoblot analysis. (A) wild-type. (B) *red* mutant. (C) *todK* mutant.

2.4.5 The accumulation of CsgA p25 and p17 is perturbed in the *red* and *todK* mutants

We also examined the subpopulation specific accumulation patterns of CsgA (p25) and C-signal (p17) in the *red* and *todK* mutants. Our analysis showed that the total CsgA p25 level gradually accumulated approximately 1.5-fold from 0 h to 48 h of development in the wild-type. In contrast, in *red* and *todK* mutants, CsgA p25 protein accumulated approximately 3-fold between 0 h and 30 h, decreased at 36 h and then appeared at 48 h (Figure 2. 32A and B).

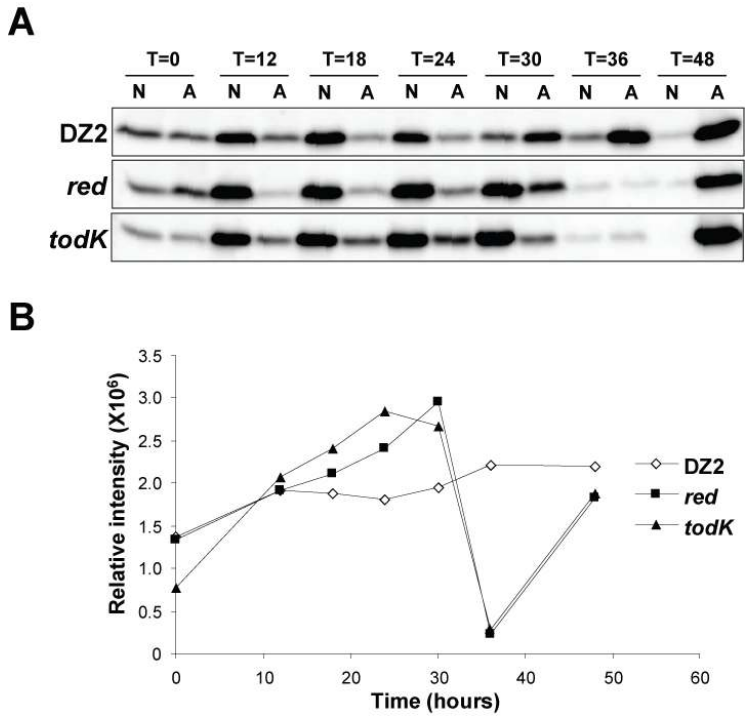

Figure 2.32 CsgA p25 expression in non-aggregating and aggregating cell fractions of wild-type, *red* and *todK* mutants. Cells were grown in submerged culture and harvested at the indicated time points. Protein samples containing equal number of cells (4.3 X 10^6 cells/µl) were subjected to immunoblot analysis with anti-CsgA antibody (A). (B) The sum of the CsgA p25 intensity in both cell fractions at each time point.

Examination of the CsgA p25 levels in the two fractions in the *red* and *todK* mutants revealed that CsgA p25 protein followed the same respective accumulation patterns as seen for MrpC/MrpC2 and FruA (Figure 2. 33A, B and C) suggesting that accumulation of CsgA p25 is also perturbed in both cell types of both mutants.

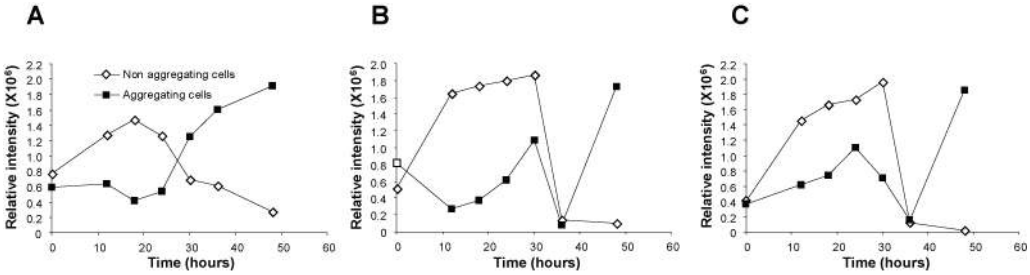

Figure 2.33 The relative intensity of CsgA p25 in non-aggregating and aggregating cell fractions. Relative intensities were measured from immunoblot analysis. (A) wild-type. (B) *red* mutant. (C) *todK* mutant.

We next examined accumulation of p17 (C-signal), the proteolytic product of CsgA that plays an essential role in activation of FruA during development. Our analysis revealed that in the wild-type, p17 gradually accumulated 3.5 times over 0 to 36 h of development and increased again approximatly 3-fold between 36 h and 48 h (Figure 2. 34). In contrast, in both mutants, p17 accumulated more rapidly between 0 h and 30 h, sharply decreased, and then appeared again at a low level at 48 h (Figure 2. 34).

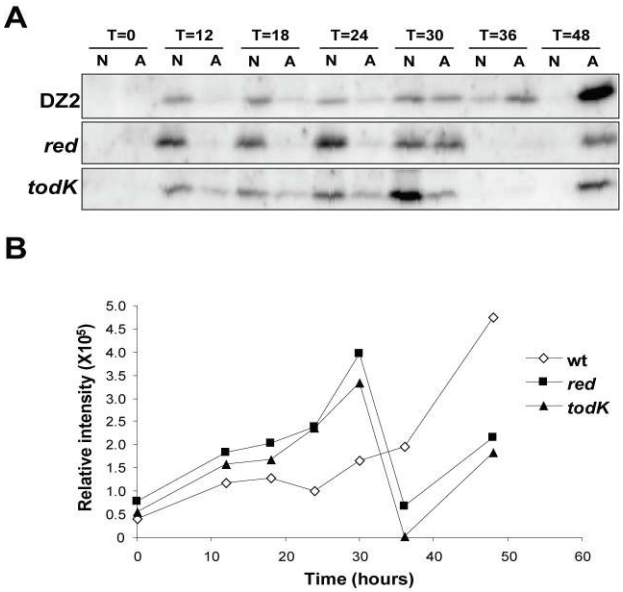

Figure 2.34 CsgA p17 expression in non-aggregating and aggregating cell fractions of wild-type, *red* and *todK* mutants. Cells were grown in submerged culture and harvested at the indicated time points. Protein samples containing equal number of cells (4.3 X 10^6 cells/μl) were subjected to immunoblot analysis with anti-CsgA antibody (A). (B) The sum of the CsgA p17 intensity in both cell fractions at each time point.

Examination of p17 accumulation in the non-aggregating versus aggregating fractions demonstrated that like CsgA, p17 inappropriately accumulated in the non-aggregating fraction, and failed to accumulate properly in the aggregating fraction (Figure 2. 35B and C). Interestingly, the p17 accumulation patterns were different in the *red* versus *todK* mutants (Figure 2. 35B and C).

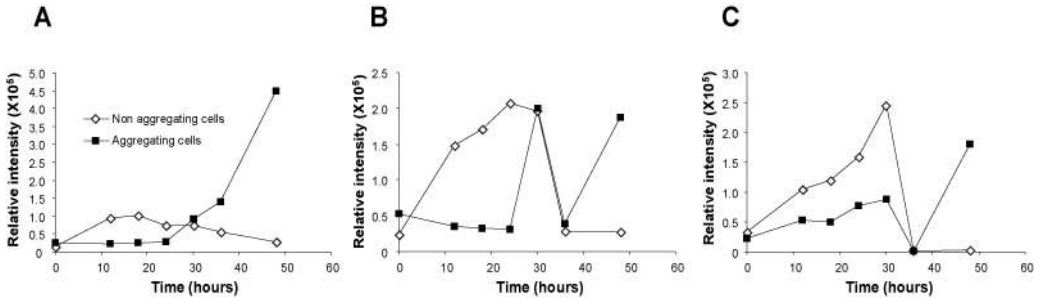

Figure 2.35 The relative intensity of CsgA p17 in non-aggregating and aggregating cell fractions. Relative intensities were measured from immunoblot analysis. (A) wild-type. (B) *red* mutant. (C) *todK* mutant.

Taken together, our expression analysis of developmental marker proteins suggests that most developmental marker proteins are overexpressed per cell in *red* and *todK* mutants and that the cell-specific accumulation of developmental marker proteins is totally perturbed in both *red* and *todK* mutants.

2.5 TodK accumulations differently in non-aggregating and aggregating cell fractions

To determine if the NRs are themselves accumulating in a cell fraction dependent manner, we next examined the expression of TodK in each fraction. As TodK antibodies were not available, we overexpressed and purified TodK (data not shown) and had antibodies generated (Eurogentec). These abtibodies were specific for TodK, since they readily detected approximately 70 kDa proteins in the wild-type, but not in the *todK* mutant (data not shown).

To examine protein accumulation patterns of TodK in the non-aggregating and aggregating cell fractions, we carried out immunoblot analysis in both cell types of wild-type strain. Our immunblot analysis revealed that TodK was highly expressed in vegetative conditions and then down-regulated approximately 16-fold over the course of 48 h of development. TodK was highly expressed in the both the non-aggregating and aggregating cell fraction under vegetative condtions (Figure 2. 36). Interestingly however, after induction of development, TodK was more rapidly depleted in the non-aggregating cell fraction (Figure 2. 36).

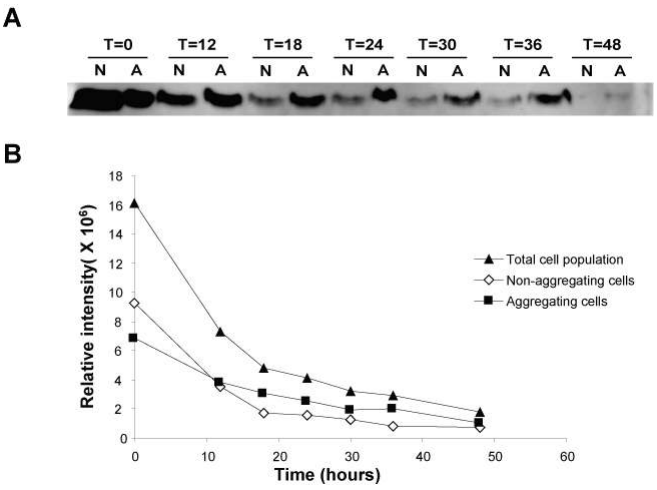

Figure 2.36 Immunoblot analysis of TodK in the wild-type. Cells were grown in submerged culture and harvested at the indicated time points. Protein samples containing equal amount of cells (4.3 X 10^6 cells/μl) were subjected to immunoblot analysis with anti-TodK antibody (A). (B) Relative intensity of TodK expression in total, non-aggregating cell and aggregating cell population.

3 DISCUSSION

M. xanthus has complex developmental program in which there are at least three developmental subpopulations that must be controlled and coordinated temporally and spatially. This developmental program is controlled by a temporally ordered cascade of gene and protein expression coupled to several positive feedback loops (Gronewold & Kaiser, 2001, Boysen *et al.*, 2002, Nariya & Inouye, 2006). Most genes identified to be involved in control of the developmental program are positive regulators: gene disruptions prevent progression past various stages of the developmental program. However, mutants in a small number of genes have previously been described that instead accelerate progression through the developmental program and are thus thought to be negative regulators (NRs) (Cho & Zusman, 1999, Rasmussen & Sogaard-Andersen, 2003, Higgs *et al.*, 2005, Lee *et al.*, 2005, Higgs *et al.*, 2008).

Interestingly, all of the NR genes investigated in this study (*espA*, *espC*, *red*, and *todK*) encode members of the two-component signal transduction (TCS) family. Such TCS systems typically consist of a sensor histidine kinase coupled to a response regulator and function to couple environmental signals to a intracellular response (e.g. change in gene transcription) via phospho-histidine aspartate relays (Stock *et al.*, 2000). However, no outputs to the NR TCS systems have been identified, since these TCS proteins are not organized in paired arrangements with response regulators that contain obvious effector (output) domains. Therefore, it was unknown whether these NRs function in a single or multiple signaling pathways and how they mediate repression of the developmental program. Furthermore, it was not known what advantage the NR genes provide to the *M. xanthus* developmental program, since mutants in these genes do not display a defect in the ability to produce spores. We demonstrate here that these NRs are organized into three distinct signaling pathways that are each necessary to quench the accumulation of several key developmental (positive) regulator proteins. We demonstrate that the NRs play an important role in controlling and coordinating the different developmental subpopulations.

To understand whether these kinases function in one or multiple distinct signaling pathways, we first generated each kinase mutant in an isogenic background and subjected the mutants to a rigorous phenotypic comparison. Our observation that phenotype of *espA* and *espC* mutants is identical, and that *todK* and *red* mutants develop progressively earlier not only indicates that there are three developmental

phenotypes, but also suggests that these signaling pathways effect the developmental program differently. Next, to further understand these distinct phenotypes, we applied epistasis analysis. Epistasis analysis is a foundation in the analysis of genetic networks and is especially used to determine if genes with related mutant phenotypes act in the same or different pathways (Hughes, 2005). Furthermore, genes thought to function in the same pathway can be ordered relative to one another based on the step in the pathway controlled by that gene.

We could expect two results in our epistasis analysis. For example, when we created a double mutant missing two NR genes, if the phenotype of the double mutant displays a non-additive phenotype, these two genes could lie in same signaling pathway. However, if the phenotype of the double mutant displays an additive phenotype, we can say these two genes do not lie in the same signaling pathway. Our epistasis analysis revealed that *espA espC* double mutants are phenotypically identical to each single mutant. This result suggests that EspA and EspC act at the same point in the developmental pathway and may function together. In contrast to the non-additive phenotype of the *espA espC* double mutants, all other combinations of double mutants displayed an additive phenotype. Taken together, our genetic analyses suggested that there are at least three signaling pathways to repress developmental progression: EspA and EspC may act together in the same signaling pathway, but Red and TodK are in distinct signaling pathways with EspA/EspC and each other.

Given the additive phenotypes of the double mutants, we became interested in the phenotypes of a mutant missing multiple or all NRs. Interestingly, our phenotypic analysis revealed that while the wild-type forms well-rounded and compact fruiting bodies, single, double, triple, and quadruple NR mutants form progressively more disorganized fruiting bodies, suggesting a negative correlation between the rate of progression through the developmental program and coordinated fruiting body formation. In particular, the observation that the quadruple mutant (missing all four NRs analyzed in this study) formed apparent lawns of spores raised the possibility that these cells could be bypassing the ordered developmental program in which sporulation is coupled to aggregation. Instead, these mutants could be sporulating as in the chemical-induced sporulation pathway in which additional of certain compounds to vegetatively growing cultures induces rapidly, and synchronous sporulation of all cells in the culture (Dworkin & Gibson, 1964, Komano *et al.*, 1980, O'Connor & Zusman, 1997).

Two observations suggest that the quadruple NR mutant does not sporulate independently of the developmental program. First, although this mutant did not appear to form distinct fruiting bodies, the same number of spores could be isolated in a low speed centrifugation used to isolate fruiting bodies, suggesting that the quadruple NR mutant spores were still primarily generated inside very shallow and disorganized fruiting bodies. Second, quantitative RT-PCR analysis of key developmental regulator gene expression through the developmental program revealed that the ordered expression of *fruA, dev,* and *exo* is still observed although all are expressed significantly earlier than in the wild type.

These analyses instead revealed that the NR mutants are perturbed in the production of peripheral rods (i.e. the peripheral rods are sporulating inappropriately). It has been first proposed that during fruiting body formation, largely two types of cells exist: peripheral rods and sporulating cells. Peripheral rods do not aggregate and remain outside of fruiting bodies, while cells destined to be spores first aggregate into mounds and finally differentiate into spores forming mature fruiting bodies (O'Connor & Zusman, 1991c). O'Connor et al. have demonstrated that several developmentally regulated proteins are expressed in cell type specific patterns suggesting that peripheral rods compose an independent cell type distinct from both fruiting body and vegetative cells (O'Connor & Zusman, 1991a, O'Connor & Zusman, 1991c). It is proposed that peripheral rods play an important role in the life cycle of *M. xanthus* by allowing the exploitation of low amounts of nutrients (O'Connor & Zusman, 1991b).

One of our major questions in this study was how these negative regulators control progression through the development program. To answer this question, we used a similar approach as was previously used for EspA: several gene expression and protein production patterns of key developmental regulators were compared in the *espA* mutant versus the wild type (Higgs et al., 2008). This approach demonstrated that A-signaling is normal in the *espA* mutant, but, while *mrpC* gene expression is not different from wild type, MrpC protein accumulates earlier in the *espA* mutant relative to wild type, suggesting that EspA represses MrpC accumulation in wild type cells. Consistently, developmental regulators that are dependent (directly or indirectly) on MrpC expression were also induced early but in an otherwise ordered pattern, including *fruA*/FruA expression/production, FrzCD methylation, and expression of *dev* and *exo*. These analyses suggest that EspA regulates the developmental program by decreasing translation of *mrpC* or stimulating degradation of MrpC (Higgs et al., 2008). Therefore, this approach is useful to understand where and how these kinases mediate developmental program in case of no clue for signal output.

In this analysis, we first focused on EspC, since EspC likely functions in same signaling pathway with EspA based on our epistasis analysis. Therefore, we could expect that EspC might act to repress the developmental program in similar points with EspA. As expected, the *espC* mutant also induced earlier expression of MrpC which consequently induced earlier accumulation of FruA. FruA induces both aggregation and sporulation and therefore this result corresponds to the early aggregation and early sporulation phenotype of *espC* mutant.

However, we also observed that there are some differences in the accumulation patterns of developmental markers between *espA* and *espC* mutants. First, while the protein level of developmental markers (MrpC, FruA and FrzCD) in the *espA* mutant was decreased at 30 hours of development, the expression of these marker proteins in *espC* mutant was continuous until 30 hours of development. In order to understand this pattern, we performed a germination assay to determine if spores produced by the *espA* and *espC* mutants were equally viable. Our viable spore assays indicated that the *espC* mutant has less viable spores than the *espA* mutant, even though heat and sonication resistant spores between *espA* and *espC* mutant are very similar during development. This result indicates that EspA and EspC likely function together early during development and later EspC seems to have an additional function in spore maturation.

Another difference between the *espA* and *espC* mutants is that although both mutants induce earlier accumulation of developmental marker proteins, accumulation of MrpC and FruA was induced slightly earlier (approximately 6 hours) in the *espA* mutant than in the *espC* mutant. Moreover, the *espC* mutant barely induces earlier methylation of FrzCD compared to the *espA* mutant. These results raised possibility that even though EspA and EspC are in same signaling pathway and likely function together, EspA has dominant function. Recent biochemical observations in our lab support this idea. It has been demonstrated that the receiver domains in both EspA and EspC hybrid histidine kinases must be phosphorylated to repress the developmental program (Higgs et al., 2008) (A. Schramm and P. Higgs, unpublished data). Interestingly, EspC kinase activity is not necessary to repress developmental progression, and EspA phosphorylates both its own receiver and that of EspC (A. Schramm and P. Higgs, unpublished data). Taken together, these results strongly suggest that EspA and EspC are working together in same signaling pathway, but that EspA acts as the core effector for EspAC mediated control. We postulate that in the *espC* mutant, EspA can still transfer a phosphoryl group to its own receiver domain which has a slight repressive effect and therefore, MrpC does not accumulate as rapidly. In the *espA* mutant, however, EspC's receiver cannot be phosphorylated even at low levels, and a stronger derepression of MrpC is observed.

What is the advantage of combining EspA and EspC into a single signaling pathway? One possibility is that diverse signals can be integrated. EspA and EspC contain different signaling input domains: for instance, in EspC the signaling domain spans the membrane while EspA contains a phosphothreonine-specific interaction domain. An additional possibility is that information can be temporally disseminated to either one (EspA) or two (EspA and EspC) receiver domains to fine-tune control the repression of development dependant on environmental conditions not encountered in the laboratory setting. It is still unknown how the phosphorylated receiver domains in EspAC effect the accumulation of MrpC. Possibly, both receiver domains modulate the activity of downstream effector proteins by protein-protein interaction. To identify potential interaction partners, co-immuno-precipitation or a yeast two hybrid screen against a *M. xathus* library could be used.

Our genetic analyses suggested that the Red and TodK NRs do not function in the same signaling pathways with EspA/C or with each other. Interestingly, however, Red and TodK share several similarities. First, unlike the *esp* genes, both *red* and *todK* are vegetatively expressed and are down-regulated during development. Second, under submerged culture conditions, sporulation of both *red* and *todK* mutants is still faster than wild-type, but later than *espA* and *espC* mutants which is contrary to their phenotype on nutrient-limited plates. We think there are two possibilities. One possible interpretation is that the different nutrient availability between starvation plates and submerged culture affects the phenotype of these mutants. The submerged culture is considered strict starvation compared to the nutrient limited plates. It has been proposed that the proportion of peripheral rods in a developing cell population decreases with decreasing levels of nutrients (O'Connor & Zusman, 1991b), so perhaps in these mutants, the relative proportions of the different developmental subpopulations influences the course of development. This may suggest that the Red and TodK systems function to preserve the robustness of the response to starvation.

In order to understand how Red and TodK proteins modulate the developmental program, we analyzed the expression patterns of developmental markers in *red* and *todK* mutants in similar manner as we had done with *espA* and *espC* mutants. Interestingly, our analysis demonstrated that the *red* mutant does not appear to induce earlier accumulation of developmental marker proteins (MrpC, FruA and CsgA) in spite of their early development. Moreover, protein levels of the developmental markers were also lower compared to wild-type. The *todK* mutant induced accumulation of MrpC six hours earlier than wild-type, but, interestingly the accumulation of FruA is similar to wild-type. These observations, together with the perturbation of peripheral rods

observed in the NR mutants, suggested that the proportions of each of these developmental subpopulations could be perturbed in these mutants.

Little is known about the control of the developmental subpopulations throughout the developmental program although it has been demonstrated that MrpC influences PCD through interaction with the toxin MazF (Nariya & Inouye, 2008) and that CsgA (and presumably C-signal) is amplified to higher levels in aggregated cells (Julien *et al.*, 2000). Therefore, to understand the effect of the *red* and *todK* NRs on the developmental subpopulations, we first decided to analyze the three known subpopulation (cells induced for PCD, aggregating leading to sporulation, or pheripheral rods) through development in the wild-type. For this approach, we adapted a previously described assay in which aggregating cells and non-aggregating cells can be separated by a low speed centrifugation step (O'Connor & Zusman, 1991c). Unfortunately, at the early time points of development, this assay will not distinguish between the populations in the supernatant which could consist of cells that never aggregate because they are destined to become peripheral rods, and cells that are being stimulated to aggregate and are in the process of transitioning into the aggregation center (pellet). Nevertheless, this assay provides a good starting point for temporal analysis of the complex subpopulations.

From analysis of the total cell number during development, we observed that the total cells in the developing population doubled up to 24 hours, and then progressively decreased after 24 hours such that by 5 days of development, the surviving cell population is reduced to approximately 20% of the initial population. Our LIVE/DEAD cell stain analysis suggested that cells undergo a massive burst of cell death at 24 hours of development although 5-20% of cells stain dead before and after the massive burst. It has been reported that 80 to 90% of developing cells underwent autolysis during development and massive cell lysis is an integral step in the process of fruiting body formation (Wireman & Dworkin, 1975, Wireman & Dworkin, 1977). More recently, it has been proposed that cells undergo programmed cell death (PCD) mediated by toxin (MazF)-antitoxin (MrpC) mechanism (Nariya & Inouye, 2008). Even though our cell population assay was performed in different wild-type strain, our observation that the cells first double in number and then undergo 80% of PCD during development is consistent with previous research (Nariya & Inouye, 2008). An analysis of the cell number in the non-aggregating and aggregating cell fractions indicates that these two populations increase in number up to 24 hours and 30 hours, respectively. The increase in number of the non-aggregating cell fraction must be due to cell division, but it is not clear if the aggregating cell fraction is increasing due to cell division and/or transition of

the non-aggregating cells into this fraction. The proportion of cells in the two fractions relative to time of development is remarkably robust and the formation of visible aggregates corresponds to approximately 50 % of the cells in the two fractions.

Our analyses confirm that the non-aggregating and aggregating cell populations are distinct cell types. First, exopolysaccharide (EPS) is upregulated only in aggregating cells. This result is not only consistent with the fact that non-aggregating cells have a defect in cohesive cell to cell interaction (O'Connor & Zusman, 1991b), but also consistent with the fact that production of EPS stimulates social (S)-motility by Type IV pilus retraction (Li et al., 2003). Second, the major spore coat proteins, Proteins C and S are expressed much more in aggregating cells, when cells start to form spores. It has been demonstrated that Protein C is expressed in both non-aggregating cells and aggregating cells from early during development in different patterns (O'Connor & Zusman, 1991c). However, our analysis demonstrated that Protein C was present only in the aggregating cell fraction and, interestingly, from the vegetative cell fraction (T = 0 development) indicating that Protein C can be specific marker for the aggregating cell population during development. However, it is unclear which gene encodes for Protein C. Protein C was previously isolated from spores by treatment with 0.1M NaOH or by boiling in 1% SDS and purified Protein C was used to generate polyclonal anti-Protein C antibodies (McCleary et al., 1991). Therefore, it remains to be proved which gene is encoding Protein C and what function of Protein C is. Third, PilA, which is the pilus subunit of Type IV pili (Wu & Kaiser, 1997), is expressed in both cell types, but is more abundant in the aggregating cell population. It is presumed that during development, highly produced pilin is assembled into pili and first offers the opportunity to attach to the EPS of adjacent cells and then EPS triggers pili retraction (Li et al., 2003). Interestingly however, the accumulation of PilC which is required for pilus biosynthesis (Wu & Kaiser, 1997) was overall decreased during the developmental program but was constantly higher in non-aggregating cells. The imbalance of PilA/PilC between the different cell types suggests that pili extension and retraction is limited in the aggregating cells, and hints that the accumulation of PilA in this cell type may serve a different function. For instance, we might speculate that perhaps in the aggregated cells PilA is not retracted and instead serves to anchor cells together.

Even though the non-aggregating cell and aggregating cell fractions were previously defined as distinct cell types by the observation that several developmentally regulated proteins are expressed in a cell type specific manner (O'Connor & Zusman, 1991c), it was unclear how most of the key developmental regulators are expressed in each subpopulation. It has previously have been demonstrated that CsgA accumulates at two

times higher levels in the aggregating cell fraction than in non-aggregating fraction at 24 hours (Julien *et al.*, 2000). However, the relative CsgA, and more importantly C-signal, production patterns over the developmental program were not examined. Therefore, we analyzed the production pattern of developmental markers in both cell types during development. It should be noted that in this analysis, we performed immunoblot analysis on protein samples that each contained an equal number of cells at each time point in order to estimate the per cell levels between both subpopulations. Most importantly, our analysis demonstrated that most of the developmental marker proteins (MrpC, FruA and CsgA) first gradually accumulate in non-aggregating cells and then later rapidly accumulate in the aggregating cell fraction. This result can be explained that the developmental maker proteins in non-aggregating cells stimulate a proportion of the cells in this population to aggregate, and thus these same cells transition into the aggregating cell fraction. Interestingly, however, cells which are already in the aggregating cell population do not accumulate marker proteins between 0 and 24 hours development. One possible interpretation is that programmed cell death takes place more in the aggregating cell population. However, we do not favor this possibility, because analysis of the proportions of dead cells using the LIVE/DEAD stain assay revealed that there was no difference in the proportion of dead cells between non-aggregating and aggregating cells fractions (data not shown). An alternative possibility is that the system is designed so that cells in the aggregating cell population bypass the signaling steps that stimulate aggregation (they are already aggregated) and then, after 24 hours, are stimulated to sporulate in coordination with the cells which are entering the aggregating cell population. This possibility can be explained with current model that distinct low and high threshold levels of activated FruA simulate aggregation and sporulation, respectively (Sogaard-Andersen et al., 1996, Ellehauge et al., 1998, Horiuchi et al., 2002).

Having defined the cell numbers, and developmental regulator accumulation patterns in each developmental subpopulation in the wild type, we next examined whether *red* and *todK* mutants are perturbed in control of these subpopulations. We first quantified the numbers of cells in each subpopulation compared to wild type. Interestingly, this assay revealed that the number of cells in the *red* and *todK* mutants did not increase to the same levels as seen in the wild type. We determined that this is likely due, at least in part, to the burst of cell death occurring earlier than in the wild-type. Importantly, this result suggests that the initial developmental marker profile of the cell cultures in these mutants was likely inaccurate since there were less total cells in the mutants compared to wild type. Therefore, to test marker production patterns in *red* and *todK* mutants, we instead analyzed the marker expression in equivalent numbers of cells at each time point.

Our expression pattern analysis of developmental markers revealed that most of the major developmental maker proteins (MrpC, FruA and CsgA) are significantly over produced per cell in the *red* and *todK* mutants. Furthermore, the accumulation patterns of these marker proteins are perturbed in the aggregating and non-aggregating cell fractions relative to the wild type. These results explain why *red* and *todK* mutants produce spores outside of the fruiting bodies. Normally, *M. xanthus* cells sporulate within fruiting bodies implying that cells are sporulated after completion of aggregation. Our expression analysis revealed that in the wild-type, most developmental marker proteins are first expressed in non-aggregating cells and later highly expressed in aggregating cells. However, in *red* and *todK*, most developmental marker proteins were much earlier and highly expressed in non-aggregating cell and later accumulation of developmental marker proteins are perturbed in aggregating cells compared to wild-type. Therefore, it is presumed that highly accumulated developmental marker proteins in non-aggregating cells of *red* and *todK* mutants induce earlier sporulation outside of fruiting bodies resulting in uncoupled fruiting body formation, before non-aggregating cell finish aggregating. It is interesting to mention here that the timing of accumulation of developmental marker proteins in *todK* mutants is slightly faster than that of *red* mutants. This result corresponds to the early sporulation phenotype of *todK* mutants and supports our idea. However, it is not clear why protein level of most developmental marker proteins were significantly decreased between 30 hours and 36 hours and increased at 48 hours in *red* and *todK* mutants. One possible interpretation is that while *red* and *todK* mutant cells are sporulating, some of cells are also germinating at 48 hours. Alternatively, these cells may be in the very fragile “prespore” stage (O'Connor & Zusman, 1997) such that the cells are lysed during harvest. This stage is likely later than 48 hours in the wild type strain.

It still remains to be identified how TodK and Red specifically repress MrpC (the earliest marker that was examined in our analyses). In the *espA* mutant, it was shown that although MrpC protein accumulates early, *mrpC* expression is not perturbed suggesting that EspA regulates the accumulation of MrpC at the translational or protein degradation level. Therefore, *mrpC* gene expression must be similarly examined in the *red* and *todK* mutants. If *mrpC* expression is earlier in these mutants, *mrpAB* and *spi* gene expression should be tested, since *mrpC* transcription is activated by MrpAB possibly in response to A-signal (Sun & Shi, 2001a, Sun & Shi, 2001b). Production and reception of the A-signal can be monitored by expression of the *spi* gene (Keseler & Kaiser, 1995). Also, our observation that *red* and *todK* mutants fail to increase cell population during development raises the possibility that Red and TodK might influence MrpC interaction with MazF, or with MazF itself.

An additionally interesting question is what is the accumulation pattern of the NRs themselves in the different developmental fractions. To date, we have examined the TodK accumulation profile and our results revealed that TodK protein is vegetatively expressed at high levels and dramatically down-regulated in both subpopulations from an early onset of starvation. However, interestingly TodK is constantly expressed more in aggregating cells suggesting TodK activity may be important in regulation of the developmental subpopulations. Since, in the *todK* mutant, the MrpC and FruA proteins are not significantly differently regulated in the aggregating cell fraction compared to wild type, this result indicates that the function of TodK in the aggregating cell fraction is not to influence accumulation of MrpC and FruA. However, in the non-aggregating cell population, TodK may specifically allow the gradual accumulation of marker proteins since in the *todK* mutant, these proteins are vastly over accumulated in this fraction. Later during development, TodK is degraded and therefore no longer able to represses MrpC/FruA accumulation.

The *M. xanthus* developmental program controlled by several positive feedback loops (e.g. *mrpC* transcrtiption (Nariya & Inouye, 2006), FruA activation through C-signaling (Ellehauge et al., 1998), and *fruA* expression through *devT* (Boysen et al., 2002)) In general, it is known that positive feedback loops induce a biastability known as the property of a determistic system to have two stable steady states. Bistable behaviors have been found both in prokaryotes (Maamar & Dubnau, 2005, Veening *et al.*, 2005, Dubnau & Losick, 2006, Smits *et al.*, 2006) and eukaryotes (Bagowski & Ferrell, 2001, Xiong & Ferrell, 2003, Weinberger *et al.*, 2005). Specifically, it has been proposed that positive feedback loops play important roles in biological bistability to decide cell population heterogeneity of *B. subtilis* (Veening et al., 2005, Dubnau & Losick, 2006, Smits et al., 2006). Only a percentage of cells of a *B. subtilis* population sporulate in response to nutrient limitation. Therefore, initiation of sporulation appears to be a regulatory process with a bistable outcome in *B.subtilis* (Smits et al., 2006, Mitrophanov & Groisman, 2008). The positive autostimulatory loop of *spo0A* is responsible for generating a bistable response resulting in phenotypic variation within the sporulating culture. Commitment to sporulation is modulated by the master regulator Spo0A which directly activates its own expression and participates in a complex phosphorelay that constitutes a multicomponent feedback loop promoting Spo0A activation, suggesting that positive regulation of Spo0A is necessary for coexistence of two (sporulating and nonsporulating) subpopulations (Veening et al., 2005). Bistability is used by eukaryotes as a mechanism of cell fate determination. One example is that in maturation of *Xenopus laevis* oocytes, the Mos-Mek-MAPK multicomponent positive feedback loops induce two subpopulations which consist of maturing subpopulation (high levels of phosphorylated

MAPK) and non-maturing subpopulation (non-phosphorylated MAPK)(Ferrell & Machleder, 1998). Biological regulation systems also contains negative feedback loops which generally serve to stabilize the state of the controlled system (Cinquin & Demongeot, 2002). Moreover, the negative feedback loops repress noise effects in biological systems (Stelling *et al.*, 2004, Loewer & Lahav, 2006). Therefore, well-balanced positive and negative systems can lead to a blend of sensitivity and stability (Stelling et al., 2004).

It has been proposed in *M. xanthus* that ordered cascades of gene expression coupled to several positive feedback loops are required for cell fate decision and/or coupled fruiting body formation between aggregation and sporulation. First, it has been demonstrated that MrpC which activates own gene transcription (Sun & Shi, 2001b) acts as an anti-toxin for MazF which mediate programmed cell death (Nariya & Inouye, 2008) and additionally act as transcriptional regulator for *fruA* which induces both aggregation and sporulation branches of the developmental program (Sogaard-Andersen et al., 1996). Second, C-signal which activates *csgA* transcription (Gronewold & Kaiser, 2001) mediates spatially coordinated fruiting body formation (Kruse *et al.*, 2001). Third, FruA induces *dev* locus transcription (Ellehauge et al., 1998) and one of the products of the *dev* locus (DevT) stimulates FruA synthesis (Boysen et al., 2002). Depending on the C-signal concentration, low levels of phosphorylated FruA activate the aggregation branch (Sogaard-Andersen & Kaiser, 1996) and high levels of phosphorylated FruA induce sporulation (Sogaard-Andersen et al., 1996, Ellehauge et al., 1998, Horiuchi et al., 2002). These results all suggest that positive feedback loops may play role in maintaining biological bistability of subpopulations (survival or death) and coordinated fruiting body formation (aggregation or sporulation). Especially, it has been proposed that perhaps a bistable switch at the level of FruA or another transcription factor that precedes it in the regulatory cascade differentiates peripheral rods from cells that enter fruiting bodies and become spores (Kroos, 2007).

Our results demonstrate that in the *red* and *todK* NR mutants, MrpC (and FruA) protein accumulation dramatically higher than the wild type suggesting premature activation of the positive autoregulatory loops. These results strongly suggest that Red and TodK independently counteract at least the MrpC positive regulatory loop, suggesting that the NRs are necessary to quench this bistable behavior in certain cell populations at certain temporal positions. Thus, the NRs maintain coordination of the developmental subpopulations. What advantage do NR genes provide to the *M. xanthus*? It is presumed that coordinated fruiting body formation that may allow for efficient transfer of large groups of spores to a nutrient rich environment so that spores can germinate in groups and

group feeding of the new population is facilitated. However, in the certain environmental conditions (e.g. nutrient level is rapidly limited or cells are attacked from other microorganisms), *M. xanthus* cells need to produce spores rapidly for their survival by NRs that can control speed of sporulation by quenching or realising key developmental regulators. Therefore, NRs which maintain temporally and spatially organized fruiting body formation could play crucial roles for their long term survival. However, it is still unclear that what the signals sensed by EspA, EspC, Red and TodK are and identification of these signals would clarify some of these questions.

In this thesis work, our interests laid in a unique group of proteins (EspA, EspC, Red, and TodK) that are members of two component signal transduction family and that are thought be negative regulators to repress developmental program. In an effort to understand the role of these negative regulators in developmental program, we revealed that there are at least three signalling pathways to repress developmental program. More importantly, our analysis revealed that these negative regulators control the developmental program by likely quenching (at least) positive feedback loops of MrpC to maintain coordination of the cell population that result in coordinated fruiting body formation. These results strongly suggest well-balanced positive and negative regulators lead well-organized fruiting body formation. Furthermore, these results will contribute to understand specific relationship between positive regulators and negative regulators in complex *M. xanthus* developmental program.

4 MATERIALS AND METHODS

4.1 Reagents and technical equipments

Reagents, enzymes, antibiotics and kits used in this work are listed in Table 4. 1.

Table 4.1 Reagents, enzymes, antibiotics and kits used in this work

Reagents	**Vendor**
Media compound, Agar-Agar	Carl Roth (Karlsruhe) Merck (Darmstadt) Difco (Heidelberg)
Pure chemicals	Carl Roth (Karlsruhe) Merck (Darmstadt)
Page Ruler Prestained Protein Ladder	MIE Fermentas (St. Leon-Rot)
MassRuler DNA Ladder	MIE Fermentas (St. Leon-Rot)
Oligonucleotides	Sigma-Aldrich (Taufkirchen)
Rabbit Antisera	Eurogentec (Seraing, Belgium)
Enzymes	
Platinum® *Pfx* DNA-polymerase	Invitrogen (Karlsruhe)
Taq DNA-polymerase	MIE Fermentas (St. Leon-Rot)
Restriction endonucleases	New England Biolabs (Frankfurt am Main) MBI Fermentas (St. Leon-Rot)
T4 ligase	New England Biolabs (Frankfurt am Main)
Superscript™III reverse transcriptase	Invitrogen (Karlsruhe)
DnaseI (Rnase-free)	Ambion (Huntington, UK)
Proteinase K, Lysozyme	Sigma-Aldrich (Seelze)
Antibiotic	
Kanamycinsulfate, Ampicillin sodiumsalt, Oxytetracycline dehydrate	Carl Roth (Karlsruhe) Sigma-Aldrich (Seelze)
Kits	
PCR purification, gel extraction, plasmid preparation, RNA purification	Quiagen (Hilden) Zymo research (Hiss diagnostics, Freiburg)
BigDye® Terminator v. 3.1 cycle sequencing, Cyber®Green PCR master mix	Applied Biosystems (Darmstadt)
LIVE/DEAD® BacLightTM Bacterial Viability Kit	Invitrogen (Karlsruhe)

Technical equipments and their manufacturers are listed in Table 4.2.

Table 4.2 Technical equipments used in this work

Application	Device	Manufacturer
Centrifugation	RC 5B plus Ultra Pro 80	Sorvall / Thermo Scientific(Dreieich)
	Multifuge 1 S-R Biofuge pico Biofuge fresco	Heraeus / Thermo scientific(Dreieich)
PCR	Mastercycler personal	Eppendorf (Hamburg)
Real time PCR	7300 Real time PCR system	Applied Biosystems (Darmstadt)
Reaction incubation	Thermomixer compact Thermomixer comfort	Eppendorf (Hamburg)
DNA sequencing	3130 Genetic analyzer	Applied Biosystems (Darmstadt)
Cell lyses	FastPrep®24 cell and tissue homogenizer	MP Biomedicals (Illkirch, France)
	Constant cell disruption system	Disruption system(Northants,UK)
Sonification	Branson sonifier 250	Heinemann (Schwäbisch Gmünd)
Protein electrophoresis	Mini-PROTEAN® 3 Cell PROTEAN®II XI Cell	Bio-Rad (München)
Western blotting	TE42 Protein transfer tank TE62 Tank transfer unit	Hoefer (San Francicso, USA)
	TE77 ECL semidry transfer unit	Amersham Bioscience (München)
Chemiluminescence detection	LAS-4000 luminescent image Analyzer Fujifilm FPM-100A	Fujifilm Europe (Düsseldorf)
DNA illumination	UVT_20 LE	Herolab (Wiesloch)
	2 UV Transilluminator LM20E with BioDoc-IT-system and Mitsubishi P93 thermal video printer	UVP (Upland, CA)
Electroporation	Gene pulser	Bio-Rad (München)
DNA concentration	NanoDrop ND 1000	NanoDrop products (Wilmington,USA)
Spctrophotometry	Ultrospec 2100 pro	Amersham Bioscience (München)
Microscopy	Zeiss Axio Imager.M1	Carl Zeiss (Jena)
	DM6000B microscope MZ 8 stereo microscope DME light microscope	Leica Microsystems (Wetzlar)
Incubation of bacteria	Innova 4000® incubator shaker Innova44® incubator shaker	New Brunswick Scientific (Nürtingen)
	B6420 incubator	Heraeus (Langenselbold)
	9020-0075 cooled incubator	Binder (Tuttlingen)
Sterilization	2540E	Tuttnauer (Breda, Netherlands)
	FVS MK 6,5	Fedegari Autoclavi (Albuzzano,Italy)
	MLS-3751L	SANYO (München)

4.2 Microbiological methods

4.2.1 Bacterial strains

The *M.xanthus* and *E.coli* strains used in this work are listed in Table 4. 3 and 4. 4, respectively.

Table 4.3 *M. xanthus* strains used in this work

Strain	Genotype or characteristics	Reference or source
DZ2	Wild type	(Campos & Zusman, 1975)
DZ4227	DZ2 Δ*espA*	(Cho & Zusman, 1999)
PH1044	DZ2 Δ*espC*	This study
DZ4659	DZ2 Δ*redCDEF*	(Higgs et al., 2005)
SA1681	DK 1622 Δ*todK*	(Rasmussen & Sogaard-Andersen, 2003)
PH1045	DZ2 Δ*todK*	This study
SA1634	DK1622 *todK*::mini-Tn*5* (*tet*) 8846	(Rasmussen & Sogaard-Andersen, 2003)
PH1046	DZ2 *todK*::mini-Tn*5* (*tet*) 8846	This study
PH1047	DZ2 Δ*espA* Δ*espC*	This study
PH1048	DZ2 Δ*espA* Δ*redCDEF*	This study
PH1049	DZ2 Δ*espA todK*::mini-Tn*5* (*tet*) 8846	This study
PH1050	DZ2 Δ*espC* Δ*redCDEF*	This study
PH1051	DZ2 Δ*espC todK*::mini-Tn*5* (*tet*) 8846	This study
PH1052	DZ2 Δ*redCDEF todK*::mini-Tn*5* (*tet*) 8846	This study
PH1053	DZ2 Δ*espA* Δ*espC* Δ*redCDEF*	This study
PH1054	DZ2 Δ*espA* Δ*espC* Δ*redCDEF todK*::miniΩTn*5* (*tet*) 8846	This study
PH1010	DZ2 :: asgA km^R	(Higgs et al., 2008)
DK9035	DK1622 *csgA*::*Tn5-132*ΩLS205 Δ*frz*(´*CD-F*)::Kan´	(Sogaard-Andersen et al., 1996)
PH1014	DZ2 *csgA*::*Tn5-132*ΩLS205	(Higgs et al., 2008)
PH1013	DZ2 :: *fruA* km^R	(Higgs et al., 2008)
DZ4169	DZ2 :: *frzCD* km^R	(Shi *et al.*, 1993)
PH1011	DZ2 Δ*espA* :: asgA km^R	(Higgs et al., 2008)
PH1015	DZ2 Δ*espA csgA*::*Tn5-132*ΩLS205	(Higgs et al., 2008)
PH1012	DZ2 Δ*espA* :: *fruA* km^R	(Higgs et al., 2008)
PH1016	DZ2 Δ*espA* :: *frzCD* km^R	(Higgs et al., 2008)
PH1055	DZ2 Δ*espC* :: asgA km^R	This study
PH1056	DZ2 Δ*espC csgA*::*Tn5-132*ΩLS205	This study
PH1057	DZ2 Δ*espC* :: *fruA* km^R	This study
PH1058	DZ2 Δ*espC* :: *frzCD* km^R	This study
PH1059	DZ2 Δ*redCDEF* :: asgA km^R	This study
PH1060	DZ2 Δ*redCDEF csgA*::*Tn5-132*ΩLS205	This study
PH1061	DZ2 Δ*redCDEF* :: *fruA* km^R	This study
PH1062	DZ2 Δ*redCDEF* :: *frzCD* km^R	This study
PH1063	DZ2 Δ *todK* :: asgA km^R	This study
PH1064	DZ2 Δ *todK csgA*::*Tn5-132*ΩLS205	This study
PH1065	DZ2 Δ *todK* :: *fruA* km^R	This study
PH1066	DZ2 Δ *todK* :: *frzCD* km^R	This study

Table 4.4 *E.coli* strains used in this work

Strain	Genotype or characteristics	Reference or source
Top10	Host for cloning F¯ *endA1 recA1 galE15 galK16 nupG rpsL* ∆*lacX74* Φ80*lacZ* ∆M15 *araD*139 ∆(*ara, leu*)7697 *mcrA* ∆(*mrr-hsdRMSmcrBC*) λ-	Invitrogen
BL21λDE3	F– ompT gal dcm lon hsdSB(rB- mB-) λ(DE3) [lacI lacUV5-T7 gene 1 ind1 sam7 nin5]	Novagen
BL21λDE3/pLysS	F- ompT gal dcm lon hsdSB(rB- mB-) λ(DE3) pLysS(cmR)	Novagen

4.2.2 Media and cultivation of bacteria

Media and solutions were autoclaved for 20 min at 121 °C and 1 bar over pressure. Heat sensitive liquids solutions were filtered using 0.22 µm pore size filters (Millipore, Schwalbach) and added after media was cooled to 60 °C.

E.coli cells were aerobically grown on Luria-Bertani (LB) media containing antibiotics, when necessary. To prepare broth culture, *E.coli* cells were inoculated and aerobically grown in Luria-Bertani (LB) broth supplemented with 100 µg ml^{-1} of ampicillin or 50 µg ml^{-1} of kanamycin, when necessary (Table 4. 5) (Bertani, 1951). Antibiotics and X-Gal were added if selection for antibiotics resistance or blue-white screening was intended. The *E. coli* cultures were incubated at 37 °C until the cultures reached the necessary cell density. The optical density of *E. coli* culture was measured at 550 nm with a spectrophotometer using a 1 cm path length cuvette.

Table 4.5 Growth media for *E. coli*

Medium	Composition
Luria-Bertani (LB) broth **(Bertani, 1951)**	1% (w/v) tryptone, 0.5% (w/v) yeast extract, 1% (w/v) NaCl If needed, 100 µg/ml Ampicillin-Sodiumsalt or 50 µg/ml kanamycin was added.
LB agar **(Bertani, 1951)**	LB-Medium, 1% (w/v) Agar-Agar If needed, after autoclaving and cooling to 60 °C, 100 µg/ml Ampicillin-Sodiumsalt, kanamycin or 40 µg/ml X-gal was added.

The *M. xanthus* cells were cultivated on Casitone yeast extract (CYE) agar in the dark. To carry out subsequent assays for *M. xanthus*, cells were inoculated by using a sterile wooden stick and incubated in Casitone yeast extract (CYE) broth at 32 °C for overnight. The optical density of *M. xanthus* culture was measured at 550 nm with a spectrophotometer using a 1 cm path length cuvette. [-1]

Table 4.6 Growth media for *M. xanthus*

Medium	Composition
Casitone yeast extract (CYE) broth (Campos & Zusman, 1975)	daH_2O, 1 % Bacto™ Casitone, 0.5 % yeast extract, 10 mM morpho-linepropanesulphonic acid (MOPS) pH 7.6, 8 mM magnesium sulphate (MgSO4) If needed, 100 µg/ml kanamycin was added.
Casitone yeast extract (CYE) agar (Campos & Zusman, 1975)	CYE broth, 1.5 % Difco™ agar If needed, after autoclaving and cooling to 60 °C, 100 µg/ml kanamycin was added.
Casitone yeast extract (CYE) top agar	CYE broth, 1.0 % Difco™ agar

4.2.3 Storage of *M. xanthus* and *E. coli*

E. coli cells grown on LB agar plates were stored up to four weeks at 4 °C. For long term storage, 680 µl of *E. coli* cell suspension was mixed with 320 µl of 50 % glycerol in a 2 ml sterile screw cap tube. Tubes were directly stored at -80 °C freezer.
M. xanthus cells grown on CYE agar plates were stored up to four week at 18 °C in the dark. For long term storage, *M. xanthus* cells culture were grown to 4×10^8 cells ml^{-1} (0.7 A_{550}) in 20 ml of CYE broth at 32 °C , 750 µl of DMSO (final concentration 0.5 M) was added to induce spores with continued incubation overnight at 32 °C. Cells were harvested and concentrated at 4,620 ×g at room temperature for 10 min. Cell pellets were resupended with 2 ml of CYE broth and 1ml of suspension was transferred to 2 ml sterile screw cap tube containing 250 µl of DMSO. Tubes were directly stored at -80 °C freezer.

4.2.4 Analysis of *M. xanthus* developmental phenotypes

To induce development of *M. xanthus* on agar plates, clone fruiting (CF) agar plates were used (Table 4. 7). *M. xanthus* cells were grown to approximately 4×10^8 cells ml^{-1} (0.7 A_{550}) at 32 °C with shaking at 240 rpm in the dark, overnight and the cell density was measured. Cells were harvested by centrifugation at 7.800 x g for 2 min at room

temperature. The cell pellet was washed with MMC starvation buffer, centrifuged again for 2 min and resuspended to 4×10^9 cells ml^{-1} in starvation buffer. 10 µl or 20 µl of the cell suspensions were spotted on the surface of a CF agar plate (Hagen *et al.*, 1978). After drying, agar plates were incubated at 32°C in the dark. Development was examined with a stereomicroscope and recorded every 6 to 12 h for 5 days.

For development in submerged culture, cells were grown to approximately 4×10^8 cells ml^{-1} (0.7 A_{550}) at 32 °C with shaking at 240 rpm in dark overnight and directly diluted to 2×10^7 cells ml^{-1} in fresh CYE rich medium. 500 µl of cell suspensions were placed in 24-well tissue culture plates and incubated at 32 °C in the dark for 24 h. Rich media was gently and completely removed by aspiration and added equal volume of MMC starvation buffer (Table 4. 7). Development was induced at 32 °C in the dark and recorded by taking pictures every 6 to 12 h for 5 days. For large scale submerged cultures, 16 ml of 2×10^7 cells ml^{-1} was placed in 85 mm cell culture plates.

Table 4.7 Starvation media for *M.xanthus* development

Medium	Composition
Clone fruiting (CF) agar (Bretscher & Kaiser, 1978, Campos *et al.*, 1978, Hagen *et al.*, 1978) Prepared at least 24h before use	daH_2O, 0.015 % Bacto™ Casitone, 10 mM Morpholine-propanesulphonicacid (MOPS) pH 7.6, 8 mM magnesium-sulphate ($MgSO_2$), 1 mM potassium dihydrogen phosphate (KH_2PO_4), 0.2 % tri-sodium citrate 2-hydrate ($C_6H_5Na_3O_7$*$2H_2O$), 0.02 % ammonium sulphat ($H_8N_2O_4S$), 1.5 % Difco™ agar After autoclaving and cooling to 60 °C or before using the medium 0.1 % sodium pyruvate ($C_3H_3NaO_3$) was added.
MMC-buffer for submerged culture	10 mM MOPS, pH 7.0, 4 mM $MgSO_4$, 2 mM $CaCl_2$

To determine the timing and efficiency of sporulation, sporulation assay was applied. From agar plates, cells were scarped fro agar plates and resupended in 0.5 ml water. For submerged culture, cells were harvested and transferred to new 1.5 ml tubes. Cells were placed in heating block at 50 °C for 1 h and sonicated at output 3, 30% power and 30 pulses. 10 µl of cells were placed onto a counting chamber suitable for bacteria (Hawksley, Lancing, UK) and aspherical spores were counted under light microscope. Three biological experiments were performed for each strain to determine the sporulation efficiency as number of spores as a percent of wt spores at 72 h. Spore viability was determined by germination assays. 100-fold serial dilutions of heat and sonication-treated cells were plated in CYE soft agar and incubated for 7 days. Colonies were counted after 5 days. Colony numbers were calculated as percent of wild-type.

4.2.5 Cell population analysis of *M. xanthus*

To quantify the number of cells in each subpopulation the method of O´Connor and Zusman was modified (O'Connor & Zusman, 1991c). Procedures of cell population assay used in this work are described in Figure 4. 1.

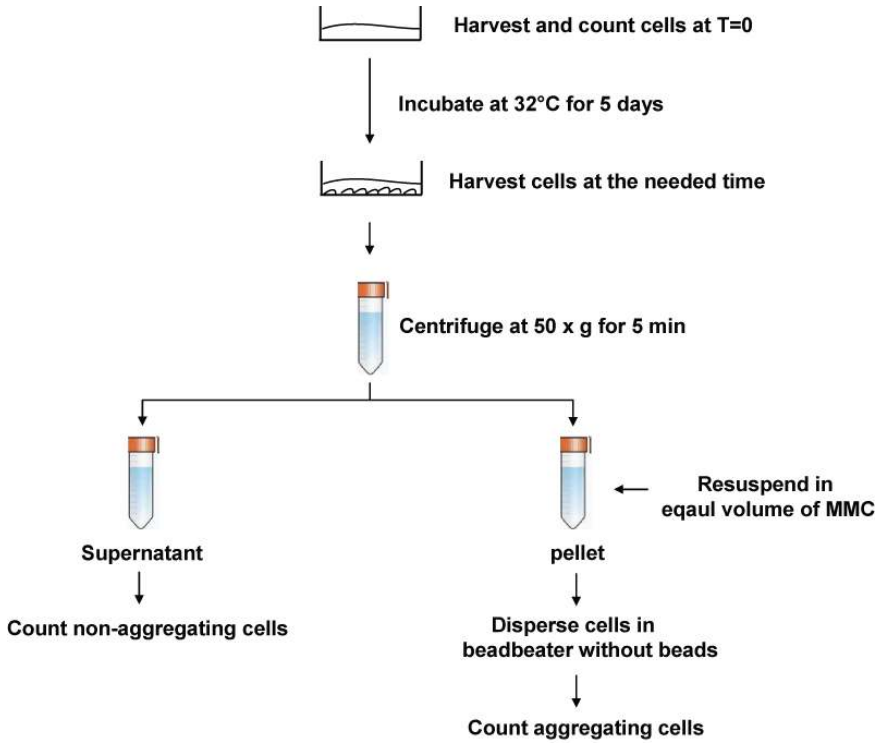

Figure 4.1 Procedure of cell population assay. This figure was adapted from (O'Connor & Zusman, 1991c). See details above description. See text for details.

Cells were developed under submerged culture conditions and harvested with a 20 ml glass pipette and transferred to a 50 ml sterile conical tube. Then, non-aggregating cells and aggregating cells were separated by centrifugation at 50 × g for 5 min. The supernatant (non-aggregating cells) was transferred to a 50 ml sterile tube, and the pellet (aggregating cells) was resuspended with an equal volume (~16ml) of MMC starvation buffer. Resuspended pellet cells were dispersed by a beadbeater (Fastprep MP24) without beads at 5 m/s for 45 sec. From 24 h, beadbeating was increased to 4 times, repectively. Each number of cells in each fraction was counted under microscope with counting chamber.

4.3 Molecular biological methods

4.3.1 Oligonucleotides and plasmids

Oligonucleotides used as primers to amplify gDNA and cDNA templates are listed in Table 4. 8.

Table 4.8 Oligonucleotides used in this work

Name	Sequence (5'-3') [a]	Description
M13 f [b]	cacgacgttgtaaaacgacggccag	Sequencing primer
oPH344 (M13 r) [b]	gcggataacaatttcacac	Sequencing primer
T7 f [c]	taatacgactcactataggg	Sequencing primer
T7 r [c]	gctagttattgctcagcgg	Sequencing primer
oPH355	gacgaattcgtcggttacctgacacgc	Froward primer used for Δ*espC* screening
oPH352	gacctcgagggctacagcatggggcggc	Reverse primer used for Δ*espC* screening
oPH438	cacctgtccgtgcgcagcgaagcggagc	Forward primer used for Δ*redCDEF* screening
oPH329	agtcacgtcctggaggtctctgcctgc	Reverse primer used for Δ*redCDEF* screening
oPH471	ccttccaggcaacgggggcg	Forward primer used for Δ*todK* screening
oPH472	ctgcagtgcgcgcgccgag	Reverse primer used for Δ*todK* screening
oPH369	cgacgttggatgaactcacg	Forward primer used for *espA* real time PCR
oPH370	gcacggtgacgtcggaac	Reverse primer used for *espA* real time PCR
oPH371	gggctggtcgtcgtgtacc	Forward primer used for *espC* real time PCR
oPH372	gacgcgcccacgaagacg	Reverse primer used for *espC* real time PCR
oPH242	gtcccacgctggtgatgtt	Forward primer used for *redB* real time PCR
oPH243	ggcttgaggaagagcacgaa	Reverse primer used for *redB* real time PCR
todK qPCR f	ctcccggacgccttcttc	Forward primer used for *todK* real time PCR
todK qPCR r	ggccatgtctggattacagta	Reverse primer used for *todK* real time PCR
oPH252	cgtcacggaaggcatcaatc	Forward primer used for *fruA* real time PCR
oPH253	cgagatgatttccggtgtgc	Reverse primer used for *fruA* real time PCR
exo qPCR f	atgaacctctatccggacatcgt	Forward primer used for *exo* real time PCR
exo qPCR r	agctcgaaggccgtctca	Reverse primer used for *exo* real time PCR
devR qPCR f	aaacatcaccagcctccagaa	Forward primer used for *exo* real time PCR
devR qPCR r	tgcatggctcctgctcatt	Reverse primer used for *exo* real time PCR
oPH601 [d]	gacgaattcatgccccccaccccgcc	Forward primer used for todK overexpression palsmid
oPH604 [d]	gcggtcgacttagtcgcgcgggttcc	Reverse primer used for todK overexpression palsmid

[a] Underlined sequences indicate restriction sites used for cloning.

[b] M13-for and oPH344 are primers for sequencing of the in-frame deletion fragments in pBJ114 and for checking the insertion after first homologous recombination.

[c] T7 f and T7 r primers for sequencing of wild type gene fragment in pET 24, 28, 32 system.

[d] Primers used to generate todK protein over-expression constructs.

The Plasmids used in this study are listed in Table 4. 9.

Table 4.9 Plasmids used in this work

Plasmids	Description	Reference/Source
pBJ114	pUC119 with Kmr and galK; derived from pKG2	(Julien et al., 2000)
pBS109	pKY480 Δ*espC*	(Lee et al., 2005)
pBS131	pBJ114 Δ*espC*	This study
pKY573	pBJ114 Δ*espA*	(Cho & Zusman, 1999, Higgs et al., 2008)
pPH127	pBJ114 :: *asgA*	(Higgs et al., 2008)
pPH128	pBJ114 :: *fruA*	(Higgs et al., 2008)
pAAR138	pBJ113 Δ*todK*	(Rasmussen & Sogaard-Andersen, 2003)
pET32+	Expression plasmid, T7-Promotor, His6-Tag (N- andC-terminal), Thioredoxin-Tag and S-tag (Nterminal), Amp^R	Novagen
pBS134	pET32+ *todK*	This study

4.3.2 Construction of plasmids

For DNA fragment amplification, purified chromosomal DNA from *M. xanthus* wild-type strain DZ2 was used as a template.

pBS 131

This plasmid is a pBJ114 derivative and was generated for regenerating *espC* deletion mutants in an isogenic background. *espC* DNA fragments were digested from pBS109 with EcoRI and BamHI and cloned into EcoRI and BamHI sites of pBJ114.

pBS134

This plasmid was constructed to overexpress full length TodK protein under control of T7 promoter of pET32+ plasmids. *todK* gene was amplified by PCR using oPH601 and oPH604 primers and cloned into EcoRI and SalI sites of pET32+ plasmids. This construction was transformed into *E, coli* top 10 strains and selected on LB agar containing Ampicilin and Kanamycin. Plasmids were sequenced to confirm the error and error-free plasmids were transformed into *E.coil* BL21λDE3 and BL21λDE3/pLysS, respectively to induce overexpression of TodK protein.

4.3.3 Generation of *M. xanthus* insertion mutants

To generate double mutants between histidine kinases and *asgA*, pPH127 plasmid was introdued into *espC* (PH1044), *red* (DZ4659) and *todK* (PH1045) deletion mutants, respectively and plasmids integration was selected by Kanamycin resistance. In similar manner, *fruA* mutant was generated by producing pPH128 (Higgs et al., 2008) into *espC*, *red* and *todK* deletion mutants, respectively (Figure 4. 2). To generate mutants in *csgA*, genomic DNA isolated from strain PH1014 (DZ2::*csgA*) was electroporated into *espC* (PH1044), *red* (DZ4659) and *todK* (PH1045), and the resulting double homologous recombination events were selected by oxytetracycline resistance. In a similar manner, genomic DNA isolated from strain DZ4169 (DZ2::*frzCD*) was electroporated into *espC* (PH1044), *red* (DZ4659) and *todK* (PH1045) and double homologous events were selected by Kanamycin resistance.

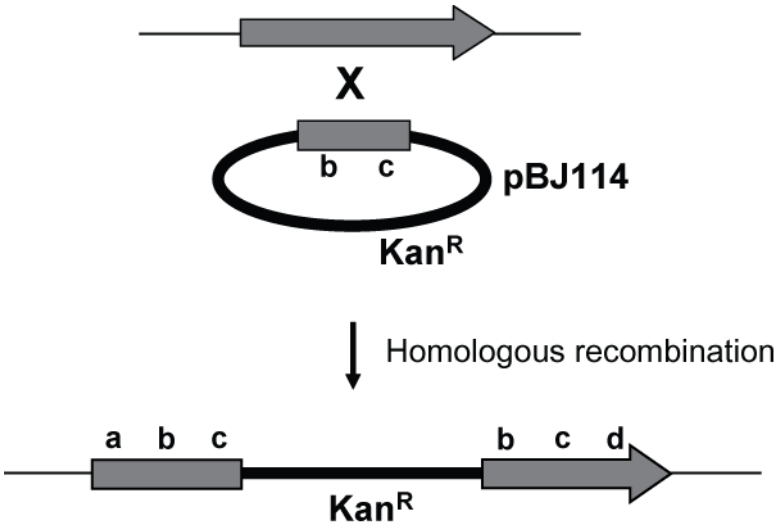

Figure 4.2 Generation of insertion mutants. Target gene of approximately 500 bp length was amplified by PCR. The purified PCR product was cloned into the pBJ114 plasmid. The plasmid was electroporated into *M. xanthus* where homologous recombination leads to disruption of the target gene.

4.3.4 Generation of *M. xanthus* in-frame deletion mutants

In-frame deletion mutants of specific genomic regions were generated by two-step homologous recombination modified from a previously reported method (Ueki *et al.*, 1996). Approximately 500 bp upstream and downstream of the target gene were amplified by PCR and fused together by overlap extension PCR. The fused PCR fragments were then cloned into pBJ114 which contains the Kanamycin resistance gene and the *galK* gene for counter selection. These plasmids were sequenced to confirm

error. The plasmids were introduced into *M. xanthus* cells by electroportation and integrated into either upstream or downstream of the target region by homologous recombination.

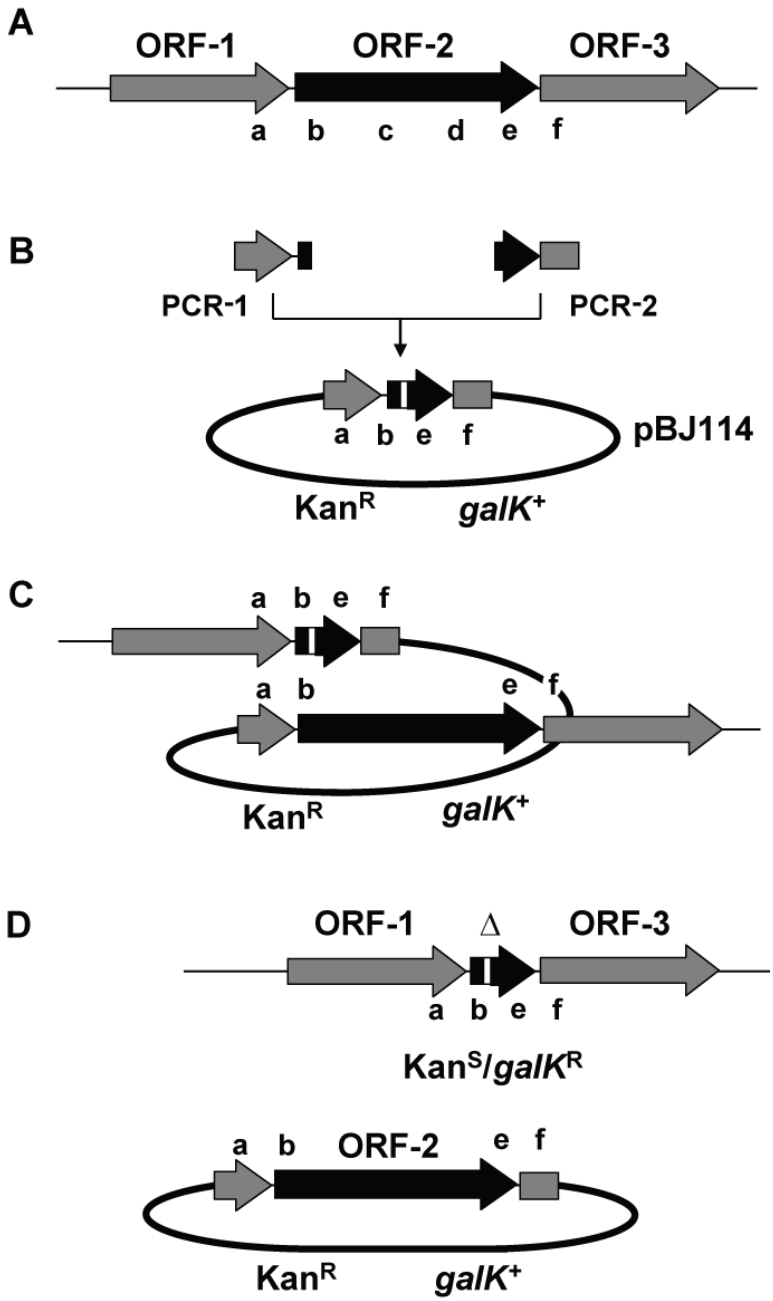

Figure 4.3 Scheme of in-frame deletion mutagenesis. (A) a and b regions and e and f regions are amplified by PCR and fused together by overlap extension PCR. (B and C) plasmids are cloned into pBJ114 and the first homologous recombination leads to plasmid integration up- or downstream of the genomic region to be deleted. (D) The second recombination event eliminates either only the vector (reconstitution) or the vector with the target region (in-frame deletion).

Recombination was selected for by resistance to kanamycin, since pBJ114 cannot replicate in *M. xanthus* but provides for kanamycin resistance. Each 5' integration and 3' integration were checked by PCR using either M13 forward primer and upstream primer of target gene or M13 reverse primer (oPH344) and downstream primer of target gene. To select for plasmid loss, the insertion mutants were grown in CYE medium to $0.5A_{550}$ and 100 µl of this culture were added to 3 ml CYE 50°C prewarmed soft agar and plated on CYE agar containing 2.5 % galactose. Loss of the integrated plasmid (excision) via a second homologous recombination event was screened by *galK*-mediated counterselection on CYE plates containing 2.5 % galactose for 7 days, since excision of plasmids containing deleted target gene result in kanamycin-sensitive (Kan^S) and galactose-resistant (Gal^R). Finally, Kan^S and Gal^R colonies were checked by PCR using up- and downstream primers of the target genes.

4.3.5 Isolation of genomic DNA from *M. xanthus*

The *M. xanthus* cells were grown to 0.7 A_{550} in 20 ml of CYE broth at 32 °C overnight. The cells were harvested by centrifugation at 4,620 × g for 10 min. The cell pellet was resuspended to 7 A_{550} in TE buffer (10 mM Tris, 1 mM EDTA, pH 8.0) and transferred to fresh 2 ml tubes. 5 % (w/v) sodium dodecyl sulfate (SDS), 100 µg ml^{-1} proteinase K and 50 µg ml^{-1} DNAse-free RNase A were directly added to cell suspension and incubated at 37 °C for 1 h. Subsequently, 5M NaCl and 12.15 % (w/v) CTAB/NaCl solution (50 ml ddH_2O, 5 gcetyl trimethylammonium bromide, 2.05 g NaCl) were added to solution and incubated at 65 °C for 10 min. Then the solution was mixed with 975 µl of a phenol: chloroform: isoamyl alcohol mixture (25:24:1 ratio). Each tube was centrifuged at maximum speed using a micro centrifuge for 3 min. The top aqueous layer was transferred to a fresh 2 ml tube and directly mixed with equal volume of chloroform: Isoamyl alcohol mixture (24:1 ratio). The mixture was centrifuged at maximum speed in micro centrifuge for 3 min and the top aqueous layer was transferred into a fresh tube. Then 0.6 volume of isopropanol were added to tube containing aqueous and solution was mixed by inverting until genomic DNA was visible and precipitated. Precipitated genomic DNA was picked by sterile tip, transferred into fresh tube containing 70 % ethanol (EtOH), and centrifuged at maximum speed for 5 min. The supernatant was discarded and 1 ml of 70 % ethanol (EtOH) was added to wash. The solution containing genomic DNA was centrifuged and the supernatant was discarded. Finally, the genomic DNA was resuspended in 50 µl elution buffer (10 mM Tris pH 8.0). Concentration of the genomic was measured by using a Nano-drop and diluted to100 ng/µl. This genomic DNA was used either as template for PCR or genomic DNA for transformation of insertion mutagenesis.

4.3.6 Isolation of plasmid DNA from *E. coli*

Plasmid DNA for transformation was isolated by using the QIAprep Spin Miniprep-Kit (Qiagen) from *E. coli.* Concentration of the plasmid was measured by using Nano-drop. Plasmid DNA for checking transformants was isolated by using alkaline lysis method (Birnboim & Doly, 1979).

4.3.7 Polymerase chain reaction (PCR)

Amplification of specific DNA for cloning was performed by polymerase chain reaction (PCR) using Platinum® *Pfx* DNA polymerase (Invitrogen) in an Eppendorf ® MasterMix cycler (Eppendorf). A standard PCR reaction mix is shown in Table 4. 10. DNA amplifications for confirming plasmid integration or deletion mutants was carried out using *Taq* DNA polymerase.

Table 4. 10 PCR reaction mix

Component	Amount
genomic DNA	100 ng
Forward primer (50 µM stock)	0.25 µl
Reverse primer (50 µM stock)	0.25 µl
2 x FailSafe™ PCR PreMix J	12.5 µl
Platinum® Pfx (0.625 units)	0.25 µl
daH2O	add to 25 µl

A standard PCR program is shown in Table 4.11. The reaction conditions were modified based on predicted primer annealing temperature, expected product sizes and DNA polymerase (see Table 4.11). The PCR products were purified using a QIAquick® PCR Purification Kit (Qiagen) or extracted from agarose gels using QIAquick® Gel Extraction Kit.

Table 4.11 Standard PCR program

Step	Temperature	Time
Initial denaturation	95°C	3 min
Denaturation*	95°C	30 s
Primer annealing*	62°C (5 to 8°C below predicted melting temperature)	15 s
Polymerization*	68°C	2 min per kb
Final elongation	68°C	5 min
Hold	4°C	Keep at 4°C

* = 25 cycles

4.3.8 Determination of nucleic acid concentration

The concentration and purity of DNA/RNA was determined by Nano drop ND-1000 spectrophotometer.

4.3.9 Agarose gel electrophoresis

DNA fragments and plasmid DNA were separated by size with agarose gel electrophoresis in 0.5 X TAE (40 mM Tris, 1 mM EDTA, pH 8.0 with acetic acid) buffer. To detect nucleic acid, ethidiumbromide was added to agarose in a final concentration of 0.01 % (v/v). 6 × sample loading buffer (0.2 % Bromophenolblue, 0.2 % Xylencyanol, dissolved in 50 % glycerol) was mix with samples to 1 x final concentration. The samples were loaded in 0.8 % to 1 % gels and the gels were run for 30 min at 120V. After electrophoresis, agarose gel images were visualized using a 2UV-Transilluminator (UVP-Bio-Doc-IT-System, UniEquip) at 365 nm wavelength and documented with an electronic P93E thermoprinter (Mitsubishi). DNA fragments were isolated from agarose gels by cutting out and purification with the QIAquick® Gel Extraction Kit.

4.3.10 Digestion and ligation of DNA fragments

Endonucleases were used for DNA digestion. 0.5 to 1 µg of purified PCR product and plasmid DNA were mixed with appropriate buffers and concentration of the endonucleases and the mixture was incubated as recommended by the supplier (New England biolabs). Restriction enzyme treated DNA samples were cleaned up and

purified with the QIAquick® PCR Purification Kit (Qiagen) and the fragment size was determined by agarose gel electrophoresis.

T4 DNA ligase was used to ligate inserts into vectors. Inserts and vectors were mixed in a 1:3 ratio and T4 ligase buffer was added. The mixture was incubated for 2 h at room temperature. Alternatively, the mixture was incubated overnight at 16 °C. Ligation products were purified with the QIAquick® PCR Purification Kit (Qiagen) and used for transformation.

4.3.11 Preparation and transformation of electro competent *E. coli* cells

To prepare electro competent *E.coli* cells (*E.coli* Top10), an overnight *E.coli* cell culture was used to subculture. 2 ml of a overnight culture was inoculated to 200 ml LB-medium. Cells were grown to log phase (approximately 0.6 A_{550}) at 37 °C shaking at 240 rpm and directly harvested by centrifugation at 5.000 × g for 20 min at 4 °C. To remove media components and salts, the cell pellet was resuspended in 400 ml ice cold sterile 10% (v/v) glycerol and centrifuged again. The washing steps were repeated with 200 ml, 100 ml, 50 ml and 10 ml volume of 10 % glycerol. Finally, the pellet was resuspended in 1 ml ice cold sterile 10 % (v/v) glycerol and 50 µl aliquots were stored at -80°C.

For *E, coli* transformation, 1-5 µl purified ligation reaction or plasmids were gently mixed with ice-cold 50 µl electrocompetent *E. coli* cells. The suspension was immediately transferred into a 0.1 cm ice cold electroporation cuvettes and pulsed with 1.5 kV, 25 µF and 200 Ω. 1 ml LB medium were immediately added to the cuvettes and the suspension was gently mixed and transferred into fresh 2 ml tube. The samples were incubated for 1 h at 37 °C shaking at 240 rpm. 100 µl and 200 µl aliquots were then plated on LB agar containing appropriate antibiotics. The plates were incubated at 37 °C over night, colonies transferred onto fresh agar plates and screened for the presence of the plasmid and insert by PCR or enzyme digestion.

4.3.12 Preparation and transformation of chemical competent *E. coli* cells

To prepare chemical competent cells, *E. coli* strains were grown in 5 ml LB-medium. 1/100 overnight culture was inoculated into 5 ml ml LB-medium and grown to log phase (0.6 A_{550}) at 37°C shaking at 240 rpm. The cell culture was immediately cooled on ice and harvested by centrifugation at 5,000 x g for 10 min at 4°C. The cell pellet was resuspended in 500 µl ice cold sterile TSS (1% tryptone, 0.5% yeast extract, 1 % NaCl, 10 % PEG (MW 3350 or 8000), 5 % DMSO, and 50 mM $MgCl_2$ or $MgSO_4$, pH

6.5) (Chung *et al.*, 1989). 100 µl aliquots were stored at -80°C.

For transformation of *E. coli*, 1-5 µl purified plasmids were gently mixed with 100 µl of ice-cold chemical competent *E. coli* cells and incubated on ice for 30 min. The cells were then heat shocked at 37 °C for 2 min. After addition of 0.5 ml LB, the cells were incubated at 37 °C shaking at 240 rpm for 1 h. After incubation, 100 µl and 200 µl were plated on LB plates containing appropriate antibiotic and incubated overnight at 37°C. Colonies were transferred onto a fresh LB agar plate and screened for the presence of the plasmid by PCR.

4.3.13 Transformation of *M. xanthus* cells

To prepare electro competent *M. xanthus*, cells were grown to approximately 0.4 A_{550} in 100 ml CYE at 32 °C shaking at 240 rpm. The cell culture was harvested in two 50 ml sterile tubes by centrifugation at 4.620 × g for 10 min at room temperature. Each cell pellet was resuspended in 50 ml of ddH_2O and centrifuged as above. The washing steps were repeated with 25 ml, 15 ml, and 10 ml volume of ddH_2O. Finally, each cell pellet was resuspended in 100 µl of ddH_2O and two tubes were combined in a fresh tube. The suspension was divided into 50 µl aliquots and used directly for electroporation.

For the transformation, 1 µg plasmid DNA or 5 µg genomic DNA was gently mixed with 50 µl electro competent *M. xanthus* cells. The suspension was immediately transferred into 0.1 cm ice cold electroporation cuvettes and pulsed with 650 V, 25 µF and 400 Ω. Then, 1 ml CYE medium were immediately added to the cuvettes and the suspension was gently mixed and transferred into fresh 2 ml tube. The samples were incubated for 1 h at 32 °C shaking at 240 rpm. After incubation, 50 µl, 100 µl, 200 µl, 650 µl cells were added to 3 ml molten CYE top agar, vortexed brifely and plated on CYE agar plates containing appropriate antibiotics. The plates were incubated in sealed plastic container at 32°C for 5 to 7 days and colonies were transferred to fresh CYE agar plates. These colonies were subjected for confirmation of plasmid integration by PCR.

4.3.14 DNA sequencing

After generation of recombinant plasmids, DNA sequencing was performed to check internal error in DNA fragments. Recombinant plasmid DNA was used as template for the chain termination method. For sequencing reactions, Big Dye® Terminator™ Cycle Sequencing Kit (Applied Biosystems, Darmstadt) was applied according to the instructions of the manufacturer and reaction was carried out as shown in Table 4.12.

The reaction products were purified by DNA precipitation. 10 µl 125 mM EDTA, 9 µl 3 M sodium acetate (pH 4,6), 80 µl HPLC-H_2O and 400 µl 96% ethanol were directly added to the reaction solution and incubated for 30 min at room temperature. The reaction solution was centrifuged at 15,000 x g for 30 min at 20 °C and the supernatant was discarded. The pellet was washed twice with 1ml fresh 70 % EtOH. Finally, the supernatant was removed and the pellet was air dried. For sequencing, the pellet was resupended in 20 µl formamide. DNA sequencing was performed using 3130 Genetic Analyser (Applied Biosystems, Darmstadt) and DNA sequences were analysed with the Vector NTI software.

Table 4.12 Incubation times and temperatures for DNA sequencing reactions

Step	Temperature	Time
Initial denaturation	96°C	1 min
Denaturation*	96°C	10 s
Primer annealing and elongation*	60°C	4 min
Hold	4°C	Keep at 4°C
* = 25 cycles		

4.3.15 Quantitative real time polymerase chain reaction (RT-PCR)

To isolate total RNA, the hot-phenol method was applied (Sambrook, 1989). *M. xanthus* cells were developed in 16 ml of submerged culture as described above. Developed cells from submerged culture were harvested by centrifugation at 4.620 × g for 10 min according to desired time points. The cell pellet was directly resuspended in 1ml solution 1 (0.3M sucrose; 0.01M NaAc, pH 4.5) and transfer into a 15 ml conical centrifugation tube containing 1ml of 65 °C solution 2 (2% SDS; 0.01M NaAc, pH 4.5). The samples were mixed gently by inversion 5 times. 2 ml of 65 °C hot phenol was added to the sample tubes, mixed gently by inversion and the sample was incubated at 65°C for 5 min. After incubation, the bottom of the sample tubes was chilled by liquid nitrogen for 5 s and centrifuged at 4.620 ×g for 5min at 4 °C. The aqueous top layer was transferred to a fresh 15 ml centrifugation tube containing 2 ml of hot phenol and sample tubes were chilled and centrifuged as described above. The cell extraction step was peformed by Phenol:chloroform:isoamyl alcohol (25:24:1, pH 6.6) and chloroform: isoa-myl alcohol (24:1). After centrifugation, the aqueous top layer was subsequently transferred to a fresh 15ml centrifugation tube containing 2 ml of Phenol:chloroform:iso -amyl alcohol (25:24:1, pH 6.6) and 2 ml of chloroform:isoamyl alcohol (24:1). To

precipitate RNA, the aqueous top layer (approximately 1 ml) was transferred to a fresh 15ml centrifugation tube containing 100 µl of 3M NaAc (pH 4.5) and 2.5 ml of 96 % EtOH. Samples were incubated at -80°C for 30 min. or at -20°C overnight. After incubation, sample tubes were centifuged at 4.620 ×g for 30 min at 4 °C and the supernatant was carefully removed. To wash RNA solution, 5 ml of ice-cold 75% EtOH was added and centrifuged at 4.620 ×g for 5 min at 4 °C. The washing step was repeated. Finally, supernatant was removed and pellet was air dried and dissolved in 100 ul of RNase-free water. Concentarion and purity of RNA was measured by Nano-drop.

Purified 10 µg of total RNA was incubated in the presence of RNase-free DNase I and incubated at 37 °C for 1 h. DNase I treatment mix is shown in Table 4. 13. After incubation, 4 ul of 25 mM EDTA was added and incubated at 65 °C for 10 min. RNA was cleaned up and purified using Qiagen RNeasy Mini Kit according to the manufacturer´s instruction. 1.0 µg of DNA-free total RNA was used as the template to synthesize cDNA using the Superscript 3 kit (Invitrogen). The reccommended reverse transcription protocol is shown in Table 4. 14.

Table 4. 13 DNase I treatment mix

Component	Amount
RNA	10 µg
Reaction buffer	10 µl
RNase free water	add to 90 µl
DNase I	10 µl

Table 4. 14 Reverse transcription reaction mix and steps

Component	Amount
1 ug of total RNA	10 µl
100 ng of random primer	2 µl
10 mM dNTP	1 µl
Incubate at 65 °C for 5 min. and snap cool on ice	
5 × reverse transcription buffer	4 µl
RNase inhibitor	1 µl
Reverse transcriptase	1 µl
0.1M DTT	1 µl
Incubate the reaction mix at	
25 °C for 5min,	
55 °C for 50min	
70℃ for 15min	

The qauntitative real time PCR (RT-PCR) was performed by applying SYBR GREEN PCR Master Mix kit (Applied Biosystem) in total 26 µl. Reactions was performed in triplicate and with 1:50 diluted cDNA. Control reactions contained no cDNA (no reverse transcriptase) and H_2O (no template) as negative controls and gDNA as positive control. Real time PCR reaction mix and program used in this work are shown in Table 4. 15 and 4. 16, respectively. Data were analyzed by the average of the C_t values of each triplecate sample. Then, the ΔC_t values were determined by subtraction of the C_t value for each time point from the C_t value of the t = 0 h sample.

Table 4.15 Real time PCR reaction mix (26 µl)

Component	Volume	Final concentration
SYBR® Green PCR Master Mix	13 µl	1 X
5 µM oligonucleotide f	1 µl	0.2 µM
5 µM oligonucleotide r	1 µl	0.2 µM
Template (cDNA or gDNA)	2 µl	0,4 ng – 0,4 pg
daH_2O	9 µl	-

Table 4.16 Real time PCR program

Step	Temperature	Time
Initial denaturation	95 °C	10 min
Denaturation	95 °C	15 s
Primer annealing and elongation*	60 °C	1 min
Denaturation*	95 °C	15 s
Recording of dissociation curve	60 °C 95 °C	30 s 15 s
Hold	10 °C	Keep at 4 °C
= 40 cycles		

4.4 Biochemical methods

4.4.1 Heterologous overexpression and purification of TodK in *E. coli*

To express and purify TodK protein, pET32a+ which are optimized for inducible overexpression protein in *E. coli* and provides fusion tags to facilitate for protein purification were used. Full length gene encoding TodK protein was amplified by PCR and cloned into pET32a+, repectively. The plasmids were comfirmed by sequencing and error free plasmids were transformed into *E. coli* BL21λDE3 and *E. coli* BL21λDE3/pLysS strains by chemical transformation method. Tranformants were

selected by antibiotics and various conditions were tested to optimize the yield in soluble protein. Overnight *E.coli* cells culture was used as first culture and 10 ml of overnight culture was inoculated to 1 litter LB-medium supplemented with either ampicillin (100 µg ml^{-1} for BL21λDE3) or ampicillin and chloramphenicol (100 µg ml^{-1} for BL21λDE3/pLysS) and incubated at 37 °C shaking at 240 rpm. Cells were grown to 0.8 A_{550} and 1 ml of cell culture was harvested by centrifugation and resuspended in 2 x LSB. TodK protein overespression was induced by adding 0.5 mM isopropyl-1-thio-Dgalactopyranoside (IPTG) and incubation at 18°C for overnight shaking at 240 rpm. After incubation, 1 ml of cell culture was harvested by centrifugation and resuspended in 2 x LSB. The remaining cell culture was harvested by centrifugation at 5.000 × g for 20 min at 4°C. 1 ml of cell culture prepared before induction and after induction was used for solubility test of TodK proteins.

4.4.2 Protein purification

Overexpressed TodK protein was purified by affinity chromatography. Cell pellets were resuspended in 50 ml binding buffer (10 mM HEPES, 150 mM NaCl, 10 mM imidazole, pH 7.4) on ice and disrupted by Constant cell disruption system (Northants, UK). The cell debris and membranes were removed by ultracentrifugation at 100.000 × g for 1 h at 4°C and supernatant fraction containing the soluble protein was purified by affinity chromatography via FPLC equipment (Amersham Biosciences, Munchen) using a 1 ml of Amersham HisFF1 trap nickel affinity column (Amersham Bioscience, Munchen). The column was washed, equilibrated with 5ml of binding buffer and supernatant fraction was loaded to allow binding of proteins to through nickel affinity column at 4 °C for with flow rate of 1 ml min^{-1}. The column was washed with 25 ml of binding buffer and the target fusion protein was eluted gradiently using 20 to 500 mM imidazole in 30 ml of elution buffer (10 mM HEPES, 0.5 M NaCl, pH 7.4). The elution was collected in 1 ml fraction and subjected to SDS-PAGE for monitoring the purity of proteins. The concentration of purified fusion proteins was measured and dialyzed against 10 mM HEPES, 150 mM NaCl, pH 7.4.

4.4.3 SDS Polyacrylamide Gel Electrophoresis (SDS-PAGE)

To examine heterologous protein expression under denaturing conditions, SDS-PAGE (Laemmli, 1970, Schagger & von Jagow, 1987) was applied. Protein samples were mixed with equal volumes of 2 x Laemmli sample buffer (LSB; 0.125 M Tris-HCl pH 6.8, 20 % glycerol, 4 % SDS, 10 % 2 β-mercaptoethanol, 0.02 % bromophenol blue) and heated at 96°C for 5 min. PageRuler™ prestained protein ladder (Fermentas) was used to estimate the molecular weight of proteins. Electrophoresis was performed in Bio-Rad

electrophoresis chambers (Bio-Rad, München) at 150 V in 1 X Tris-glycine-SDS running buffer (25 mM Tris; 190 mM Glycine; 0, 1% SDS). Proteins were visualized by soaking the gel in staining solution (70 % methanol, 7 % acetic acid, 0.25 % Coomassie brilliant blue R250) for 30 min and in destaining solution (70 % methanol, 7 % acetic acid) until protein bands became clearly visible.

Table 4.17 Composition of a 8% resolving and a 5 % stacking gel

	Resolving gel (10 ml)		**Stacking gel (5 ml)**	
	Volume	Final concentration	Volume	Final concentration
daH2O	4.8 ml	-	2.8 ml	
4X resolving buffer [a]	2.5 ml	375 mM	-	-
4X stacking buffer [b]	-	-	1.25 ml	125 mM
30 % acrylamide	2.6 ml	8 %	825 µl	5 %
TEMED	6 µl	0.06 %	3.75 µl	0.75 %
10% (w/v) APS	80 µl	0.08 %	50 µl	0.1 %

[a] 4X resolving buffer (1.5 M Tris-HCl pH 8.8, 0.4 % SDS)

[b] 4X stacking buffer (0.5 M Tris-HCl pH 6.8, 0.4 % SDS)

4.5 Immunoblot analysis

4.5.1 TodK antibody generation

Purified TodK protein was divided into 50 µg aliquots and lyophilised. 1.6 mg of Lyophilised TodK protein sent to Eurogentec (Seraing, Belgium) for the generation of polyclonal antibodies in rabbit based on super speedy program.

4.5.2 Preparation of protein samples for immunoblot analysis

To perform immunoblot analysis, protein samples were prepared with three different methods such as equal protein concentration, equal proportion of cell culture or equal cell number. Cells were developed in 16 ml of submerged culture and harvested by centrigution at 4.620 ×g for 10 min at the desired time points.

Protein sample as equal protein concentraion

Cell pellets were resuspended in 500 µl starvation buffer (MMC) containing 1:20 protease inhibitor and transferred to 1 ml microcentrifuge tube. Samples were sonicated at 3 x output,

30 % power and 15 pulses and put on ice. This step was repeated. Alternatively, samples were transferred into 2 ml screw cap tubes filled with 0.5 g 0.1 mm zirconia/silica beads (BioSpec, Bartlesville). Cells were mechanically disintegrated using a FastPrep®-24 tissue and cell homogenizer (MP Biomedicals, Illkirch, France) six times for 45 s each at 6.5 m/s speed. Protein samples were prepared to 0.5 µg μl^{-1} by adding appropriate Lamelli sample buffer and boiled at 99 °C for 5 min.

Protein sample as equal proportion of cell culture

After cell lysis as decribed above, the cell lysates were mixed with an equivalent volume of 2 x Laemmli sample buffer and the mixture was boiled at 99 °C for 5 min.

Protein sample as equal cell number

Cells were harvested from 16 ml of submerged culture by using a 20 ml glass pippet and transferred to fresh 50 ml cuntifuge tubes. To determine the cell number, the cells were dispersed by bead beater without bead at 5 m/s speed for 45 s. Cell numbers were counted by using counting chamber under light microscop and directly resuspended to 4.3×10^6 cells ul^{-1} in Lamelli sample buffer containing 1:20 mammalian protease inhibitor cocktail. Samples were boiled at 99 °C for 10 min. To lyse remaining cells, 200 µl of samples were transferred into 2 ml screw cap tubes filled with 0.2 g, 0.1 mm zirconia/silica beads. Cells were mechanically disintegrated using a FastPrep®-24 tissue and cell homogenizer (MP Biomedicals, Illkirch, France) six times for 45 s each at 6.5 m/s speed. Samples were boiled at 99°C for 5 min before use.

4.5.3 Determination of protein concentration

Protein concentrations were determined based on Bradford assay (Bradford, 1976) using the Bio-Rad protein assay kit (Bio-Rad, Munchen) according to the instructions of the manufacturer. Standard curves were obtained using series of dilutions of a protein standard (bovine serum albumin). The absorbance was measured at 595 nm with an Ultrospec 2100 pro spectrophotometer (Amersham). The protein concentrations were calculated based on the slope value of the standard curve. Alternatively, protein concentrations were determined by BCA™ Protein Assay Kit (Pierce, Rockford) according to the instructions of the manufacturer. Absorbance was measured at 562 nm.

4.5.4 Immunoblot analysis

Protein samples were prepared as described in section 4.5.2. 4.3×10^7 to 8.6×10^7 cells μl^{-1} of cell lysates were loaded on SDS-PAGE gels. Depending on the molecular mass, 8 to 13 % gels were prepared. To detect protein modification such as phosphorylation or methylation, large electrophoresis chambers (Bio-Rad, München) were used. After electrophoresis, proteins present in gels were blotted into polyvinylidene fluoride (PVDF) membranes using a tank transfer system (Hoeffer) in transfer buffer (25 mM Tris, 192 mM glycine, 10 % methanol, 0.1% SDS, pH 8.3). Alternatively, proteins were transferred into PVDF membrane using semi-dry system (Amersham Bioscience). After blotting, membrane was briefly soaked in methanol, washed with ddH2O and incubated in blocking buffer (PBS, 137 mM NaCl, 10 mM phosphate, 2.7 mM KCl, 5% non-fat milk powder, 0.1% tween-20, pH 7.4) for 1 h at room temperature. Primary antibodies were added to membrane in blocking buffer according to appropriate dilution and incubated for 1 h at room temperature. Primary antibodies were transferred to fresh bottle and membrane was washed 3 times with skim milk buffer for 10 min. Then, 1:20.000 diluted secondary anti-rabbit IgG was added to membatane in blocking buffer and incubated for 1 h at room temperature. After incubation, secondary antibodies were removed and membrane was washed 3 times with PBS buffer (137 mM NaCl, 10 mM phosphate, 2.7 mM KCl pH 7.4) for 10 min. After washing step in PBS buffer, chemiluminescence substrate (Pierce) was added to membrane and signals were detected by exposure to CL-Xposure Film (Pierce) or using the LAS-4000 luminescent image analyzer (Fuji). The relative intensity of proteins was quantified by MultiGauge software (Fuji).

Table 4.18 Dilutions of primary antibodies used for immunoblotting.

Antibody	MrpC	FruA	CsgA	FrzCD	Protein C	Protein S	PilA	PilC	EspA	TodK
Dilultion	1:1,000	1:5,000	1:5,000	1:5,000	1:5,000	1:5,000	1:10,000	1:5,000	1:1,000	1:2,000

4.6 LIVE/DEAD staining analysis

The timing and proportion of cell death was determined by employing a live dead stain kit (LIVE/DEAD® BacLightTM Bacterial Viability Kit, Invitrogen) according to instructions of the manufacturer. The cells were developed in 16 ml of submerged culture and harvested at the desired time points. Cell numbers were counted by counting chamber under light microscope and cells were centrifuged at 4.620 ×g for 10 min. The pellets were resuspended in 1ml MMC buffer and transferred to 2 ml bead beating tubes.

The cells were dispersed by bead beating without bead at 5 m/s speed for 45 s and diluted to approximately 1.5 X 10^8 cells ml^{-1} in MMC buffer. Equal volumes of component A (SYTO® 9, green-fluorescent nucleic acid stain) and component B (propidium iodide, red-fluorescent nucleic acid stain) in a 1.5ml tubes were combined and 3 µl of the dye mixture were added to 1 ml of cell suspension. After mixing thoroughly, the samples were incubated at room temperature in the dark for 15min. For fluorescence microscopy, 5 µl of cells were spotted on Agar pads [(1% agarose in A50 starvation buffer (10 mM MOPS, pH 7.2, 1 mM CaCl2, 1 mM MgCl2, 50 mM NaCl)] and covered with a cover slip. Live and dead cells were observed under fluorescence microscope equipped with green (at 500 nm) and red (at 550 nm) channel. After recording pricture, images were analyzed by Metamorph ver 7.5 and relative dead cells were calculated.

4.7 Exopolysaccharide (EPS) analysis

To verify difference between non-aggregating cells and aggregating cell, Exopolysaccharide (EPS) assay was applied (Black & Yang, 2004, Black et al., 2006). Cell samples were prepared as described in section 4.2.5. Each cell population was centrifuged at at 4.620 ×g for 10 min. The pellets were resuspended in 1ml MMC buffer and transferred to 2ml bead beating tubes. The cells were dispersed by bead beating without bead at 5 m/s speed for 45 s and diluted to approximately 2.0 X 10^8 cells ml^{-1} in 3.5 ml of MMC buffer. 10 µl of trypan blue buffer (10 mM MPOS, 1mM NaCl, 1 mg ml^{-1} trypan blue) were added to triplicate 990 ul of cell suspension and control containing buffer to make final concentration 10 µg ml^{-1} of trypan blue. The samples were mixed briefly and incubated in the dark for 30 min. After incubation, the samples were centrifuged at 16.200 ×g for 5 min at room temperature. Then, absorbance of supernatants was measured at 585 nm for trypan blue and fraction of dye bound per relative proportion of cells was calculated in non-aggregating cells and aggregating cells.

REFERENCES

Anantharaman, V. & L. Aravind, (2003) Application of comparative genomics in the identification and analysis of novel families of membrane-associated receptors in bacteria. *BMC Genomics* 4: 34.

Arnold, J. W. & L. J. Shimkets, (1988) Cell surface properties correlated with cohesion in Myxococcus xanthus. *J Bacteriol* 170: 5771-5777.

Bagowski, C. P. & J. E. Ferrell, Jr., (2001) Bistability in the JNK cascade. *Curr Biol* 11: 1176-1182.

Banerjee, S. & I. Bose, (2008) Functional characteristics of a double positive feedback loop coupled with autorepression. *Phys Biol* 5: 46008.

Behmlander, R. M. & M. Dworkin, (1991) Extracellular fibrils and contact-mediated cell interactions in Myxococcus xanthus. *J Bacteriol* 173: 7810-7820.

Bertani, G., (1951) Studies on lysogenesis. I. The mode of phage liberation by lysogenic Escherichia coli. *J Bacteriol* 62: 293-300.

Birnboim, H. C. & J. Doly, (1979) A rapid alkaline extraction procedure for screening recombinant plasmid DNA. *Nucleic Acids Res* 7: 1513-1523.

Black, W. P., Q. Xu & Z. Yang, (2006) Type IV pili function upstream of the Dif chemotaxis pathway in Myxococcus xanthus EPS regulation. *Mol Microbiol* 61: 447-456.

Black, W. P. & Z. Yang, (2004) Myxococcus xanthus chemotaxis homologs DifD and DifG negatively regulate fibril polysaccharide production. *J Bacteriol* 186: 1001-1008.

Blackhart, B. D. & D. R. Zusman, (1985) "Frizzy" genes of Myxococcus xanthus are involved in control of frequency of reversal of gliding motility. *Proc Natl Acad Sci U S A* 82: 8767-8770.

Bonner, P. J., W. P. Black, Z. Yang & L. J. Shimkets, (2006) FibA and PilA act cooperatively during fruiting body formation of Myxococcus xanthus. *Mol Microbiol* 61: 1283-1293.

Boysen, A., E. Ellehauge, B. Julien & L. Sogaard-Andersen, (2002) The DevT protein stimulates synthesis of FruA, a signal transduction protein required for fruiting body morphogenesis in Myxococcus xanthus. *J Bacteriol* 184: 1540-1546.

Bradford, M. M., (1976) A rapid and sensitive method for the quantitation of microgram quantities of protein utilizing the principle of protein-dye binding. *Anal Biochem* 72: 248-254.

Bretscher, A. P. & D. Kaiser, (1978) Nutrition of Myxococcus xanthus, a fruiting myxobacterium. *J Bacteriol* 133: 763-768.

Campos, J. M., J. Geisselsoder & D. R. Zusman, (1978) Isolation of bacteriophage MX4, a generalized transducing phage for Myxococcus xanthus. *J Mol Biol* 119: 167-178.

Campos, J. M. & D. R. Zusman, (1975) Regulation of development in Myxococcus xanthus: effect of 3':5'-cyclic AMP, ADP, and nutrition. *Proc Natl Acad Sci U S A* 72: 518-522.

Cho, K. & D. R. Zusman, (1999) Sporulation timing in Myxococcus xanthus is controlled by the espAB locus. *Mol Microbiol* 34: 714-725.

Chung, C. T., S. L. Niemela & R. H. Miller, (1989) One-step preparation of competent Escherichia coli: transformation and storage of bacterial cells in the same solution. *Proc Natl Acad Sci U S A* 86: 2172-2175.

Cinquin, O. & J. Demongeot, (2002) Positive and negative feedback: striking a balance between necessary antagonists. *J Theor Biol* 216: 229-241.

Cochran, J. W. & R. W. Byrne, (1974) Isolation and properties of a ribosome-bound factor required for ppGpp and ppGpp synthesis in Escherichia coli. *J Biol Chem* 249: 353-360.

Dana, J. R. & L. J. Shimkets, (1993) Regulation of cohesion-dependent cell interactions in Myxococcus xanthus. *J Bacteriol* 175: 3636-3647.

Dubnau, D. & R. Losick, (2006) Bistability in bacteria. *Mol Microbiol* 61: 564-572.

Durocher, D., J. Henckel, A. R. Fersht & S. P. Jackson, (1999) The FHA domain is a modular phosphopeptide recognition motif. *Mol Cell* 4: 387-394.

Dworkin, M., (1962) Nutritional requirements for vegetative growth of Myxococcus xanthus. *J Bacteriol* 84: 250-257.

Dworkin, M. & S. M. Gibson, (1964) A System for Studying Microbial Morphogenesis: Rapid Formation of Microcysts in Myxococcus Xanthus. *Science* 146: 243-244.

Dworkin, M. & D. Kaiser, (1993) *Myxobacteria II*. American Society for Microbiology, Washington, DC.

Ellehauge, E., M. Norregaard-Madsen & L. Sogaard-Andersen, (1998) The FruA signal transduction protein provides a checkpoint for the temporal co-ordination of intercellular signals in Myxococcus xanthus development. *Mol Microbiol* 30: 807-817.

Ferrell, J. E., Jr., (2002) Self-perpetuating states in signal transduction: positive feedback, double-negative feedback and bistability. *Curr Opin Cell Biol* 14: 140-148.

Ferrell, J. E., Jr. & E. M. Machleder, (1998) The biochemical basis of an all-or-none cell fate switch in Xenopus oocytes. *Science* 280: 895-898.

Gronewold, T. M. & D. Kaiser, (2001) The act operon controls the level and time of C-signal production for Myxococcus xanthus development. *Mol Microbiol* 40: 744-756.

Hagen, D. C., A. P. Bretscher & D. Kaiser, (1978) Synergism between morphogenetic mutants of Myxococcus xanthus. *Dev Biol* 64: 284-296.

Harris, B. Z., D. Kaiser & M. Singer, (1998) The guanosine nucleotide (p)ppGpp initiates development and A-factor production in myxococcus xanthus. *Genes Dev* 12: 1022-1035.

Haseltine, W. A. & R. Block, (1973) Synthesis of guanosine tetra- and pentaphosphate requires the presence of a codon-specific, uncharged transfer ribonucleic acid in the acceptor site of ribosomes. *Proc Natl Acad Sci U S A* 70: 1564-1568.

Higgs, P. I., K. Cho, D. E. Whitworth, L. S. Evans & D. R. Zusman, (2005) Four unusual two-component signal transduction homologs, RedC to RedF, are necessary for timely development in Myxococcus xanthus. *J Bacteriol* 187: 8191-8195.

Higgs, P. I., S. Jagadeesan, P. Mann & D. R. Zusman, (2008) EspA, an orphan hybrid histidine protein kinase, regulates the timing of expression of key developmental proteins of Myxococcus xanthus. *J Bacteriol* 190: 4416-4426.

Hofmann, K. & P. Bucher, (1995) The FHA domain: a putative nuclear signalling domain found in protein kinases and transcription factors. *Trends Biochem Sci* 20: 347-349.

Horiuchi, T., M. Taoka, T. Isobe, T. Komano & S. Inouye, (2002) Role of fruA and csgA genes in gene expression during development of Myxococcus xanthus. Analysis by two-dimensional gel electrophoresis. *J Biol Chem* 277: 26753-26760.

Hughes, T. R., (2005) Universal epistasis analysis. *Nat Genet* 37: 457-458.

Inouye, M., S. Inouye & D. R. Zusman, (1979) Biosynthesis and self-assembly of protein S, a development-specific protein of Myxococcus xanthus. *Proc Natl Acad Sci U S A* 76: 209-213.

Jagadeesan, S., P. Mann, C. W. Schink & P. I. Higgs, (2009) A novel "four-component" two-component signal transduction mechanism regulates developmental progression in Myxococcus xanthus. *J Biol Chem* 284: 21435-21445.

Julien, B., A. D. Kaiser & A. Garza, (2000) Spatial control of cell differentiation in Myxococcus xanthus. *Proc Natl Acad Sci U S A* 97: 9098-9103.

Kaiser, D., (1979) Social gliding is correlated with the presence of pili in Myxococcus xanthus. *Proc Natl Acad Sci U S A* 76: 5952-5956.

Kaiser, D., (2004) Signaling in myxobacteria. *Annu Rev Microbiol* 58: 75-98.

Kearns, D. B., P. J. Bonner, D. R. Smith & L. J. Shimkets, (2002) An extracellular matrix-associated zinc metalloprotease is required for dilauroyl phosphatidylethanolamine chemotactic excitation in Myxococcus xanthus. *J Bacteriol* 184: 1678-1684.

Keseler, I. M. & D. Kaiser, (1995) An early A-signal-dependent gene in Myxococcus xanthus has a sigma 54-like promoter. *J Bacteriol* 177: 4638-4644.

Kim, D., Y. K. Kwon & K. H. Cho, (2007) Coupled positive and negative feedback circuits form an essential building block of cellular signaling pathways. *Bioessays* 29: 85-90.

Kim, S. H., S. Ramaswamy & J. Downard, (1999) Regulated exopolysaccharide production in Myxococcus xanthus. *J Bacteriol* 181: 1496-1507.

Kim, S. K. & D. Kaiser, (1990) Cell alignment required in differentiation of Myxococcus xanthus. *Science* 249: 926-928.

Kim, S. K. & D. Kaiser, (1991) C-factor has distinct aggregation and sporulation thresholds during Myxococcus development. *J Bacteriol* 173: 1722-1728.

Komano, T., S. Inouye & M. Inouye, (1980) Patterns of protein production in Myxococcus xanthus during spore formation induced by glycerol, dimethyl sulfoxide, and phenethyl alcohol. *J Bacteriol* 144: 1076-1082.

Kroos, L., (2007) The Bacillus and Myxococcus developmental networks and their transcriptional regulators. *Annu Rev Genet* 41: 13-39.

Kruse, T., S. Lobedanz, N. M. Berthelsen & L. Sogaard-Andersen, (2001) C-signal: a cell surface-associated morphogen that induces and co-ordinates multicellular fruiting body morphogenesis and sporulation in Myxococcus xanthus. *Mol Microbiol* 40: 156-168.

Laemmli, U. K., (1970) Cleavage of structural proteins during the assembly of the head of bacteriophage T4. *Nature* 227: 680-685.

Lee, B., P. I. Higgs, D. R. Zusman & K. Cho, (2005) EspC is involved in controlling the timing of development in Myxococcus xanthus. *J Bacteriol* 187: 5029-5031.

Li, S. F. & L. J. Shimkets, (1993) Effect of dsp mutations on the cell-to-cell transmission of CsgA in Myxococcus xanthus. *J Bacteriol* 175: 3648-3652.

Li, Y., H. Sun, X. Ma, A. Lu, R. Lux, D. Zusman & W. Shi, (2003) Extracellular polysaccharides mediate pilus retraction during social motility of Myxococcus xanthus. *Proc Natl Acad Sci U S A* 100: 5443-5448.

Licking, E., L. Gorski & D. Kaiser, (2000) A common step for changing cell shape in fruiting body and starvation-independent sporulation of Myxococcus xanthus. *J Bacteriol* 182: 3553-3558.

Loewer, A. & G. Lahav, (2006) Cellular conference call: external feedback affects cell-fate decisions. *Cell* 124: 1128-1130.

Maamar, H. & D. Dubnau, (2005) Bistability in the Bacillus subtilis K-state (competence) system requires a positive feedback loop. *Mol Microbiol* 56: 615-624.

Manoil, C. & D. Kaiser, (1980a) Accumulation of guanosine tetraphosphate and guanosine pentaphosphate in Myxococcus xanthus during starvation and myxospore formation. *J Bacteriol* 141: 297-304.

Manoil, C. & D. Kaiser, (1980b) Guanosine pentaphosphate and guanosine tetraphosphate accumulation and induction of Myxococcus xanthus fruiting body development. *J Bacteriol* 141: 305-315.

Mattick, J. S., C. B. Whitchurch & R. A. Alm, (1996) The molecular genetics of type-4 fimbriae in Pseudomonas aeruginosa--a review. *Gene* 179: 147-155.

McBride, M. J., T. Kohler & D. R. Zusman, (1992) Methylation of FrzCD, a methyl-accepting taxis protein of Myxococcus xanthus, is correlated with factors affecting cell behavior. *J Bacteriol* 174: 4246-4257.

McBride, M. J. & D. R. Zusman, (1993) FrzCD, a methyl-accepting taxis protein from Myxococcus xanthus, shows modulated methylation during fruiting body formation. *J Bacteriol* 175: 4936-4940.

McCleary, W. R., B. Esmon & D. R. Zusman, (1991) Myxococcus xanthus protein C is a major spore surface protein. *J Bacteriol* 173: 2141-2145.

Merroun, M. L., K. Ben Chekroun, J. M. Arias & M. T. Gonzalez-Munoz, (2003) Lanthanum fixation by Myxococcus xanthus: cellular location and extracellular polysaccharide observation. *Chemosphere* 52: 113-120.

Mignot, T., (2007) The elusive engine in Myxococcus xanthus gliding motility. *Cell Mol Life Sci* 64: 2733-2745.

Mitrophanov, A. Y. & E. A. Groisman, (2008) Positive feedback in cellular control systems. *Bioessays* 30: 542-555.

Mittal, S. & L. Kroos, (2009a) A combination of unusual transcription factors binds cooperatively to control Myxococcus xanthus developmental gene expression. *Proc Natl Acad Sci U S A* 106: 1965-1970.

Mittal, S. & L. Kroos, (2009b) Combinatorial regulation by a novel arrangement of FruA and MrpC2 transcription factors during Myxococcus xanthus development. *J Bacteriol* 191: 2753-2763.

Nariya, H. & M. Inouye, (2008) MazF, an mRNA interferase, mediates programmed cell death during multicellular Myxococcus development. *Cell* 132: 55-66.

Nariya, H. & S. Inouye, (2005) Identification of a protein Ser/Thr kinase cascade that regulates essential transcriptional activators in Myxococcus xanthus development. *Mol Microbiol* 58: 367-379.

Nariya, H. & S. Inouye, (2006) A protein Ser/Thr kinase cascade negatively regulates the DNA-binding activity of MrpC, a smaller form of which may be necessary for the Myxococcus xanthus development. *Mol Microbiol* 60: 1205-1217.

Nudleman, E. & D. Kaiser, (2004) Pulling together with type IV pili. *J Mol Microbiol Biotechnol* 7: 52-62.

O'Connor, K. A. & D. R. Zusman, (1991a) Analysis of Myxococcus xanthus cell types by two-dimensional polyacrylamide gel electrophoresis. *J Bacteriol* 173: 3334-3341.

O'Connor, K. A. & D. R. Zusman, (1991b) Behavior of peripheral rods and their role in the life cycle of Myxococcus xanthus. *J Bacteriol* 173: 3342-3355.

O'Connor, K. A. & D. R. Zusman, (1991c) Development in Myxococcus xanthus involves differentiation into two cell types, peripheral rods and spores. *J Bacteriol* 173: 3318-3333.

O'Connor, K. A. & D. R. Zusman, (1997) Starvation-independent sporulation in Myxococcus xanthus involves the pathway for beta-lactamase induction and provides a mechanism for competitive cell survival. *Mol Microbiol* 24: 839-850.

Ogawa, M., S. Fujitani, X. Mao, S. Inouye & T. Komano, (1996) FruA, a putative transcription factor essential for the development of Myxococcus xanthus. *Mol Microbiol* 22: 757-767.

Pedersen, F. S., E. Lund & N. O. Kjeldgaard, (1973) Codon specific, tRNA dependent in vitro synthesis of ppGpp and pppGpp. *Nat New Biol* 243: 13-15.

Rasmussen, A. A. & L. Sogaard-Andersen, (2003) TodK, a putative histidine protein kinase, regulates timing of fruiting body morphogenesis in Myxococcus xanthus. *J Bacteriol* 185: 5452-5464.

Reichenbach, H., (1999) The ecology of the myxobacteria. *Env. Microbiol.* 1: 15-21.

Reichenbach, H., (2001) Myxobacteria, producers of novel bioactive substances. *J Ind Microbiol Biotechnol* 27: 149-156.

Rolbetzki, A., M. Ammon, V. Jakovljevic, A. Konovalova & L. Sogaard-Andersen, (2008) Regulated secretion of a protease activates intercellular signaling during fruiting body formation in M. xanthus. *Dev Cell* 15: 627-634.

Rosenberg, E., K. H. Keller & M. Dworkin, (1977) Cell density-dependent growth of Myxococcus xanthus on casein. *J Bacteriol* 129: 770-777.

Rosenbluh, A. & M. Eisenbach, (1992) Effect of mechanical removal of pili on gliding motility of Myxococcus xanthus. *J Bacteriol* 174: 5406-5413.

Sambrook, J., E. F. Fritsch, and T. Maniatis., (1989) *Molecular cloning:a laboratory manual, 2nd ed.* Cold Spring Harbor Laboratory Press, Cold Spring Harbor, N.Y.

Schagger, H. & G. von Jagow, (1987) Tricine-sodium dodecyl sulfate-polyacrylamide gel electrophoresis for the separation of proteins in the range from 1 to 100 kDa. *Anal Biochem* 166: 368-379.

Shi, W., T. Kohler & D. R. Zusman, (1993) Chemotaxis plays a role in the social behaviour of Myxococcus xanthus. *Mol Microbiol* 9: 601-611.

Shi, W., F. K. Ngok & D. R. Zusman, (1996) Cell density regulates cellular reversal frequency in Myxococcus xanthus. *Proc Natl Acad Sci U S A* 93: 4142-4146.

Shi, X., S. Wegener-Feldbrugge, S. Huntley, N. Hamann, R. Hedderich & L. Sogaard-Andersen, (2008) Bioinformatics and experimental analysis of proteins of two-component systems in Myxococcus xanthus. *J Bacteriol* 190: 613-624.

Shimkets, L. & C. R. Woese, (1992) A phylogenetic analysis of the myxobacteria: basis for their classification. *Proc Natl Acad Sci U S A* 89: 9459-9463.

Shimkets, L. J., (1986a) Correlation of energy-dependent cell cohesion with social motility in Myxococcus xanthus. *J Bacteriol* 166: 837-841.

Shimkets, L. J., (1986b) Role of cell cohesion in Myxococcus xanthus fruiting body formation. *J Bacteriol* 166: 842-848.

Shimkets, L. J., (1987) Control of morphogenesis in myxobacteria. *Crit Rev Microbiol* 14: 195-227.

Shimkets, L. J., (1990a) Social and developmental biology of the myxobacteria. *Microbiol Rev* 54: 473-501.

Shimkets, L. J., (1990b) Social and developmental biology of the myxobacteria. *Microbiol. Rev.* 54: 473-501.

Singer, M. & D. Kaiser, (1995) Ectopic production of guanosine penta- and tetraphosphate can initiate early developmental gene expression in Myxococcus xanthus. *Genes Dev* 9: 1633-1644.

Smits, W. K., O. P. Kuipers & J. W. Veening, (2006) Phenotypic variation in bacteria: the role of feedback regulation. *Nat Rev Microbiol* 4: 259-271.

Sogaard-Andersen, L. & D. Kaiser, (1996) C factor, a cell-surface-associated intercellular signaling protein, stimulates the cytoplasmic Frz signal transduction system in Myxococcus xanthus. *Proc Natl Acad Sci U S A* 93: 2675-2679.

Sogaard-Andersen, L., F. J. Slack, H. Kimsey & D. Kaiser, (1996) Intercellular C-signaling in Myxococcus xanthus involves a branched signal transduction pathway. *Genes Dev* 10: 740-754.

Sogaard-Andersen, L. & Z. Yang, (2008) Programmed cell death: role for MazF and MrpC in Myxococcus multicellular development. *Curr Biol* 18: R337-339.

Stein, E. A., K. Cho, P. I. Higgs & D. R. Zusman, (2006) Two Ser/Thr protein kinases essential for efficient aggregation and spore morphogenesis in Myxococcus xanthus. *Mol Microbiol* 60: 1414-1431.

Stelling, J., U. Sauer, Z. Szallasi, F. J. Doyle & J. Doyle, (2004) Robustness of cellular functions. *Cell* 118: 675-685.

Stock, A. M., V. L. Robinson & P. N. Goudreau, (2000) Two-component signal transduction. *Annu Rev Biochem* 69: 183-215.

Sun, H. & W. Shi, (2001a) Analyses of mrp genes during Myxococcus xanthus development. *J Bacteriol* 183: 6733-6739.

Sun, H. & W. Shi, (2001b) Genetic studies of mrp, a locus essential for cellular aggregation and sporulation of Myxococcus xanthus. *J Bacteriol* 183: 4786-4795.

Taylor, B. L. & I. B. Zhulin, (1999) PAS domains: internal sensors of oxygen, redox potential, and light. *Microbiol Mol Biol Rev* 63: 479-506.

Thony-Meyer, L. & D. Kaiser, (1993) devRS, an autoregulated and essential genetic locus for fruiting body development in Myxococcus xanthus. *J Bacteriol* 175: 7450-7462.

Tyson, J. J., K. C. Chen & B. Novak, (2003) Sniffers, buzzers, toggles and blinkers: dynamics of regulatory and signaling pathways in the cell. *Curr Opin Cell Biol* 15: 221-231.

Ueki, T. & S. Inouye, (2003) Identification of an activator protein required for the induction of fruA, a gene essential for fruiting body development in Myxococcus xanthus. *Proc Natl Acad Sci U S A* 100: 8782-8787.

Ueki, T., S. Inouye & M. Inouye, (1996) Positive-negative KG cassettes for construction of multi-gene deletions using a single drug marker. *Gene* 183: 153-157.

Veening, J. W., L. W. Hamoen & O. P. Kuipers, (2005) Phosphatases modulate the bistable sporulation gene expression pattern in Bacillus subtilis. *Mol Microbiol* 56: 1481-1494.

Viswanathan, P., K. Murphy, B. Julien, A. G. Garza & L. Kroos, (2007) Regulation of dev, an operon that includes genes essential for Myxococcus xanthus development and CRISPR-associated genes and repeats. *J Bacteriol* 189: 3738-3750.

Wall, D. & D. Kaiser, (1999) Type IV pili and cell motility. *Mol Microbiol* 32: 1-10.

Wall, D., P. E. Kolenbrander & D. Kaiser, (1999) The Myxococcus xanthus pilQ (sglA) gene encodes a secretin homolog required for type IV pilus biogenesis, social motility, and development. *J Bacteriol* 181: 24-33.

Weinberger, L. S., J. C. Burnett, J. E. Toettcher, A. P. Arkin & D. V. Schaffer, (2005) Stochastic gene expression in a lentiviral positive-feedback loop: HIV-1 Tat fluctuations drive phenotypic diversity. *Cell* 122: 169-182.

Whitworth, D. E., (2008) Myxobacteria. In.: American Society for Microbiology.

Wireman, J. W. & M. Dworkin, (1975) Morphogenesis and developmental interactions in myxobacteria. *Science* 189: 516-523.

Wireman, J. W. & M. Dworkin, (1977) Developmentally induced autolysis during fruiting body formation by Myxococcus xanthus. *J Bacteriol* 129: 798-802.

Wolgemuth, C., E. Hoiczyk, D. Kaiser & G. Oster, (2002) How myxobacteria glide. *Curr Biol* 12: 369-377.

Wu, S. S. & D. Kaiser, (1995) Genetic and functional evidence that Type IV pili are required for social gliding motility in Myxococcus xanthus. *Mol Microbiol* 18: 547-558.

Wu, S. S. & D. Kaiser, (1997) Regulation of expression of the pilA gene in Myxococcus xanthus. *J Bacteriol* 179: 7748-7758.

Wu, S. S., J. Wu & D. Kaiser, (1997) The Myxococcus xanthus pilT locus is required for social gliding motility although pili are still produced. *Mol Microbiol* 23: 109-121.

Xiong, W. & J. E. Ferrell, Jr., (2003) A positive-feedback-based bistable 'memory module' that governs a cell fate decision. *Nature* 426: 460-465.

Yang, Z., X. Ma, L. Tong, H. B. Kaplan, L. J. Shimkets & W. Shi, (2000) Myxococcus xanthus dif genes are required for biogenesis of cell surface fibrils essential for social gliding motility. *J Bacteriol* 182: 5793-5798.

CURRICULUM VITAE

Personal Information

Name	Bongsoo Lee
Date/Place of birth	1977-06-09, Paju, Republic of Korea

Education

2009	PhD (Dr. rer. Nat) candidate. Thesis Advisor: Dr. Penelope I. Higgs Phillips University and Max Planck Institute for Terrestrial Microbiology, Marburg, Germay Department of Ecophysiology
2004	M.Sc. (Molecular Microbiology), Thesis Advisor: Dr. Kyungyun Cho Hoseo University, Republic of Korea Department of Biochemistry
2002	B.Sc. (Life Science) Hoseo University, Republic of Korea Section of Life Science

ACKNOWLEDGEMENTS

I would like to acknowledge and extend my heartfelt gratitude to the following persons who have made the completion of this thesis possible.

First of all, I am deeply indebted to my supervisor Dr. Penelope I. Higgs for her guidance, suggestions and encouragement throughout my research and thesis.

I wish to express my sincere gratitude and appreciationto my these committee members, Prof. Dr. MD Lotte Søgaard-Andersen, Prof. Dr. Erhard Bremer, Prof. Dr. Hans-Ulrich Mösch and Prof. Dr. Uwe Maier and my IMPRS thesis committee for their invaluable time for ideas, and comments.

A special thanks to Petra Mann for her excellent technical assistance and for her kind mind and care throughout my stay in Marburg. I would like to extend my thanks to IMPRS coordinators Dr. Juliane Dörr (former), Dr. Ronald Brudler (present) and Susanne Rommel for their help in official issues.

I would like to gratefully acknowledge past and present members of the Higgs group for helpful discussions and their help. I would like to extend my thanks to all colleagues from Department of Ecophysiology, for providing a friendly working environment.

In a special way, I would like to express my deepest gratitude to my parents, sister and brother, for their encouragement and unconditional support throughout my life and in particular during my thesis.

ERKLÄRUNG

Ich erkläre, dass ich meine Dissertation

„ The role of negative regulators in coordination of the *Myxococcus xanthus* developmental program “

selbstständig, ohne unerlaubte Hilfe angefertigt und mich dabei keiner anderen als der von mir ausdrücklich bezeichneten Quellen und Hilfen bedient habe.

Die Dissertationwurde in der jetzigen oder einer ähnlichen Form noch keiner anderen Hochschuleeingereicht und hat noch keinen sonstigen Prüfungszwecken gedient.

Marburg, _____

Bongsoo Lee